SOME ASPECTS OF TERNARY FISSION OF ^{235}U, ^{239}Pu AND ^{252}Cf

by

B. KRISHNARAJULU NAIDU

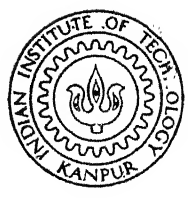

DEPARTMENT OF PHYSICS

INDIAN INSTITUTE OF TECHNOLOGY KANPUR

SEPTEMBER 1977

SOME ASPECTS OF TERNARY FISSION OF ^{235}U, ^{239}Pu AND ^{252}Cf

A Thesis Submitted
In Partial Fulfilment of the Requirements
for the Degree of
DOCTOR OF PHILOSOPHY

by
B. KRISHNARAJULU NAIDU

to the

DEPARTMENT OF PHYSICS
INDIAN INSTITUTE OF TECHNOLOGY KANPUR
SEPTEMBER 1977

PHY-1977-D-NAI-SOM

The history of mankind is one of continuous development from the realm of necessity to the realm of freedom. This process is never-ending. In any society in which classes exist class struggle will never end. In classless society the struggle between the new and the old and between truth and falsehood will never end. In the fields of the struggle for production and scientific experiment, mankind makes constant progress and nature undergoes constant change; they never remain at the same level. Therefore, man has constantly to sum up experience and go on discovering, inventing, creating and advancing. Ideas of stagnation, pessimism, inertia and complacency are all wrong. They are wrong because they agree neither with the historical facts of social development over the past million years, nor with the historical facts of nature so far known to us (i.e. nature as revealed in the history of celestial bodies, the earth, life, and other natural phenomena).

MAO TSE-TUNG

as quoted by Chou En-lai

TO

MY PARENTS

whose affection and enthusiasm

has always been inspiring

CERTIFICATE

Certified that the work presented in this thesis entitled " Some Aspects of Ternary Fission of ^{235}U, ^{239}Pu and ^{252}Cf" by Mr. B. Krishnarajulu Naidu, has been done under my supervision and that it has not been submitted elsewhere for a degree.

G. K. Mehta
Professor
Department of Physics
Indian Institute of Technology Kanpur

September 1977.

ACKNOWLEDGEMENTS

To me this thesis is the embodiment of about half a decade of endeavour marked by the cooperation, enthusiasm and affection of a large number of people who have contributed in various ways to varying extents in this 'struggle of scientific experiment'. It is therefore difficult to do full justice to the job of acknowledging all these people in these few paragraphs; however, I wish to mention some of those who have been directly associated with me in the laboratory during these past few years.

Dr. G.K. Mehta introduced me to the field of fission physics and improved my understanding in many areas of nuclear physics through lectures, discussions and through the innumerable tasks that we undertook in the laboratory. I would like to record my deep gratitude to him for his constant help and guidance during these years.

I thank Sri R.K. Choudhury, Dr. D.M. Nadkarni and Dr. S.S. Kapoor of BARC, Bombay for their extensive collaboration in the ^{235}U measurements. Their hospitality during my brief visit to BARC is also acknowledged. Ashok Gadgil helped me considerably during the initial stages of the trajectory calculations and I thank him for patiently helping me during those days.

The Central Nuclear laboratory has (and has had) a host of wonderful people whose constant cooperation was only superceeded by their merry disposition. Drs. S. Sen, S.N. Chaturvedi, H.R. Prabhakara and Raghuvir Singh gave me invaluable assistance during the experimental work. I am also grateful to them, and to the others, for those many scintillating hours we spent discussing everything from politics to poetry.

I acknowledge with deep gratitude the tremendous amount of help and affection I have received from Sarvashri A.K. Khanna, A.R. Korde, B.K. Jain, K.M.L. Jha, K. Masood, M.M. Gupta, Ram Nath, Shiv Prakash and V.K. Sharma during my stay in this laboratory. Without their assistance and efficiency in fabrication and manitenance work it would have been impossible to carry out the experiments.

Many others, both past and present, have made my stay in the laboratory and in the Institute a memorable experience and to all of them I express my sincere thanks.

The assistance of the Central workshop, the Physics workshop and the Computer Centre is gratefully acknowledged. Financial assistance from NCERT, New Delhi and the Dept. of Physics, I.I.T., Kanpur is acknowledged.

I thank Shri B.K. Jain for the excellent drawings, Sri L.S. Bajpai for efficient typing and Sri Lalloo Singh Rathaur for neat cyclostyling.

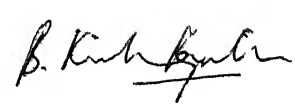

CONTENTS

LIST OF TABLES

LIST OF FIGURES

SYNOPSIS

The fission process continues to be a fascinating and challenging area of study even though almost four decades have elapsed since its discovery. During this period a large number of investigations on both the theoretical and experimental aspects of this process have been carried out. However, a clear picture, coherently linking all aspects of this complex process, is yet to emerge.

The charged liquid drop model corrected for shell effects has been quite successfully used in describing the main features of the fissioning nucleus, eg. the fission barrier with respect to deformation, fission isomers, intermediate structure in subthreshold fission cross sections etc. One of the crucial questions in the passage of the nucleus from saddle point to scission is the extent to which there is coupling between the collective and particle degrees of freedom. In other words, if the process is adiabatic with respect to the particle degrees of freedom, then the decrease in potential energy from saddle to scission remains associated with the collective degrees of freedom and appears primarily as kinetic energy of the nascent fragments. On the other

hand, if the motion is non-adiabatic then there will be transfer of collective energy into nucleonic excitation energy. A reasonable explanation based on this kind of motion is provided by the statistical theory of fission. Present experimental evidence does not allow an unequivocal decision in favour of either the adiabatic or non-adiabatic model. More information on the properties of the nucleus at the saddle point and scission point is necessary in order to shed more light on this question.

Experimental investigations on light-charged-particle-accompained (LCP) fission, also referred to as ternary fission, have indicated that, because of the time and place of LCP emission; a study of this mode of fission would contribute significantly to the understanding of the scission stage of fission.

The present thesis consists of two parts. The first describes some experimental work examining the effect of the saddle point configuration on ternary alpha (LRA) yield and average energy. The second part describes computational work aimed at studying the scission configuration of the fissioning nucleus.

The introductory chapter describes the salient features of the fission process. The characteristics of binary and ternary fission are compared in order to show the essential similarity of these two modes of fission. The emphasis on study of ternary fission is, however, motivated

by the fact that the LCP serves as a powerful probe of the scission process.

Chapter II summarizes the channel theory of fission, developed by A. Bohr, and its application to the explanation of some important characteristics of low energy neutron induced fission. The high light of this model is its emphasis on the role played by the saddle states (or channels) in determining the post-scission characteristics of fission. The question of validity of the adiabatic model is intimately linked to the success of this theory in the explanation of such fission characteristics.

The details of the experimental setup used in the LCP yield and energy measurements in low energy (thermal to 1 MeV) neutron induced fission of ^{235}U and ^{239}Pu are described in Chapter III. Details of data analysis, specifically the corrections for chance coincidences and energy loss effects, are also given.

The results of these measurements and their possible interpretation on the basis of the channel theory are presented in Chapter IV. The results on LRA yield and average energies and widths as a function of neutron energy indicate definite structure outside the limits of error. The structure in yield in ^{235}U is, however, more pronounced than in ^{239}Pu. The yield of the low energy component, attributed to tritons, also shows significant structure in the neutron energy region investigated. The results on LRA yield are

discussed in terms of the spins, parities and fission cross sections of the low lying saddle point states of these nuclei. However, no definite conclusions regarding the 'triton' yield could be drawn because of large errors due to poor statistics.

The method of trajectory calculations has been used to study the scission configuration. The post-scission motion of the fragments and alpha particle were simulated on a computer and by an interpolation method the scission configuration was obtained, Chapter V describes the method used and the calculations carried out for spontaneous ternary fission of ^{252}Cf. This nucleus was chosen because of the vast amount of experimental results available. The method used in this work differs from almost all previous methods in that no apriori restrictions were imposed on the initial parameters used as the starting point of the simulation i.e. in the approximate description of the scission configuration. The results indicate that such a method is valid and it has been possible to obtain hitherto unobtained distributions of initial parameters describing the scission configuration and some correlations between them.

Chapter VI contains a brief summary of the results of the experimental work and their interpretation and the results on the scission configuration obtained from trajectory calculations.

CHAPTER I

INTRODUCTION

1.1 The fission process

The fission process, that is, the breaking-up of a nucleus into two or more heavy parts, was discovered about 40 years ago by Hahn and Strassman (1938). It has since been extensively investigated both theoretically and experimentally. The first explanation for this process was given by Meitner and Frisch (1939) followed by a more quantitative description by Bohr and Wheeler (1939). In general nuclear reactions the question of whether the process is through a direct interaction or via compound nucleus formation is an important issue in itself. In contrast to this, fission is a clear case of a process via compound nucleus formation. This is because in fission we deal with collective nuclear motion and the characteristic time for such motion (vibration), $\sim 5 \times 10^{-21}$ sec., is long compared to the time for a nucleon to cross the nucleus $\sim 0.3 \times 10^{-21}$ sec. The compound nucleus in question may be formed by absorption of a particle or electromagnetic radiation - as in induced fission; or it may even fission from its ground state (spontaneous fission, Fig. 1.1). The compound nucleus

formed by absorption of a particle would be in an excited state and the excitation energy is distributed among a large number of degrees of freedom. The complex state of motion initiated thereby may be described in terms of collective nuclear rotations, vibrations and single particle excitations. In the compound system there is competition between the various modes of dissipation of the available energy: neutron emission, radiation or division. For fission to take place, it is necessary that a sufficient amount of energy becomes concentrated in the potential energy of deformation to enable the nucleus to pass through the saddle point shape - a shape corresponding to maximum potential energy of deformation. At the saddle point the repulsive Coulomb forces balance the attractive surface tension force (arising out of the nuclear interaction). Beyond the saddle point and till the scission point the repulsive forces increasingly dominate the attractive ones. The scission point is the point at which the nucleus divides into two or more smaller nuclei such that their nuclear forces cease to play a part as far as their mutual motions are concerned.

Thus the fission process may be described as the succession of three different phases. The compound nucleus undergoes a long series of oscillations until one of them leads to the passing of the saddle point, followed soon afterward ($\sim 10^{-21}$ sec.) by the splitting-up of the nucleus.

In most cases this division is mass asymmetric leading to light and heavy fragments. These primary deformed fragments move in opposite directions under the influence of their mutual Coulomb repulsion which results in their kinetic energy. They de-excite by emitting 'prompt' neutrons and gamma rays in time intervals of 10^{-15} and 10^{-11} sec., after scission, respectively. [An analysis of the angular distribution of neutrons emitted in fission (Milton and Fraser, 1965) indicated that a small fraction of neutrons (which are isotropic in the laboratory system) are probably emitted at scission]. These fission fragments are neutron rich and far from the stability curve and decay by delayed neutron and gamma emission and by beta emission to stable end products. Most physical measurements are carried out on the fission fragments whereas radiochemical measurements are performed on the fission products.

The total energy released in fission, comprising the kinetic energy of the fragments, the energy associated with neutron and gamma emission etc., is about 200 MeV and is equal to the difference in masses of the original compound nucleus and the two fragments. The explanation of this energy release was first provided by Meitner and Frisch (1939) and confirmed experimentally by Frisch (1939).

The most frequently occuring mode of fission is binary fission; in which the nucleus breaks up into two fragments. About 0.2% of such events result in three

fragments - this division is called ternary fission. Fission into four or more fragments is extremely rare.

A number of experiments have been done to study the characteristics of the fission process. However, no theory, which comprehensively explains all aspects of this process, has emerged. Bohr and Wheeler (1939) developed a theory of fission based on the conception of the nucleus as a liquid drop, Frenkel (1939) independently proposed a similar theory. Their application of this theory accounted for a number of features of the process, however, it did not explain the most striking feature of fission, namely, the asymmetric nature of the mass division. The liquid drop model has since been developed (Swiatecki and others) and is still used today as the starting point of calculations of binding energies and potential energy barriers (with respect to deformation) for heavy nuclei. There are, however, marked deviations from the predictions of the liquid drop model on binding energies etc., in the vicinity of the well-known neutron and proton shells. The first successful method for quantitatively introducing shell corrections to the liquid drop potential was introduced by Strutinsky (1967, 1968). This procedure is now widely used in calculating fission barriers etc. For actinides, calculations of this type give fission barriers with two humps separated by a second minimum (Fig. 1.1) which provides the possibility for very deformed

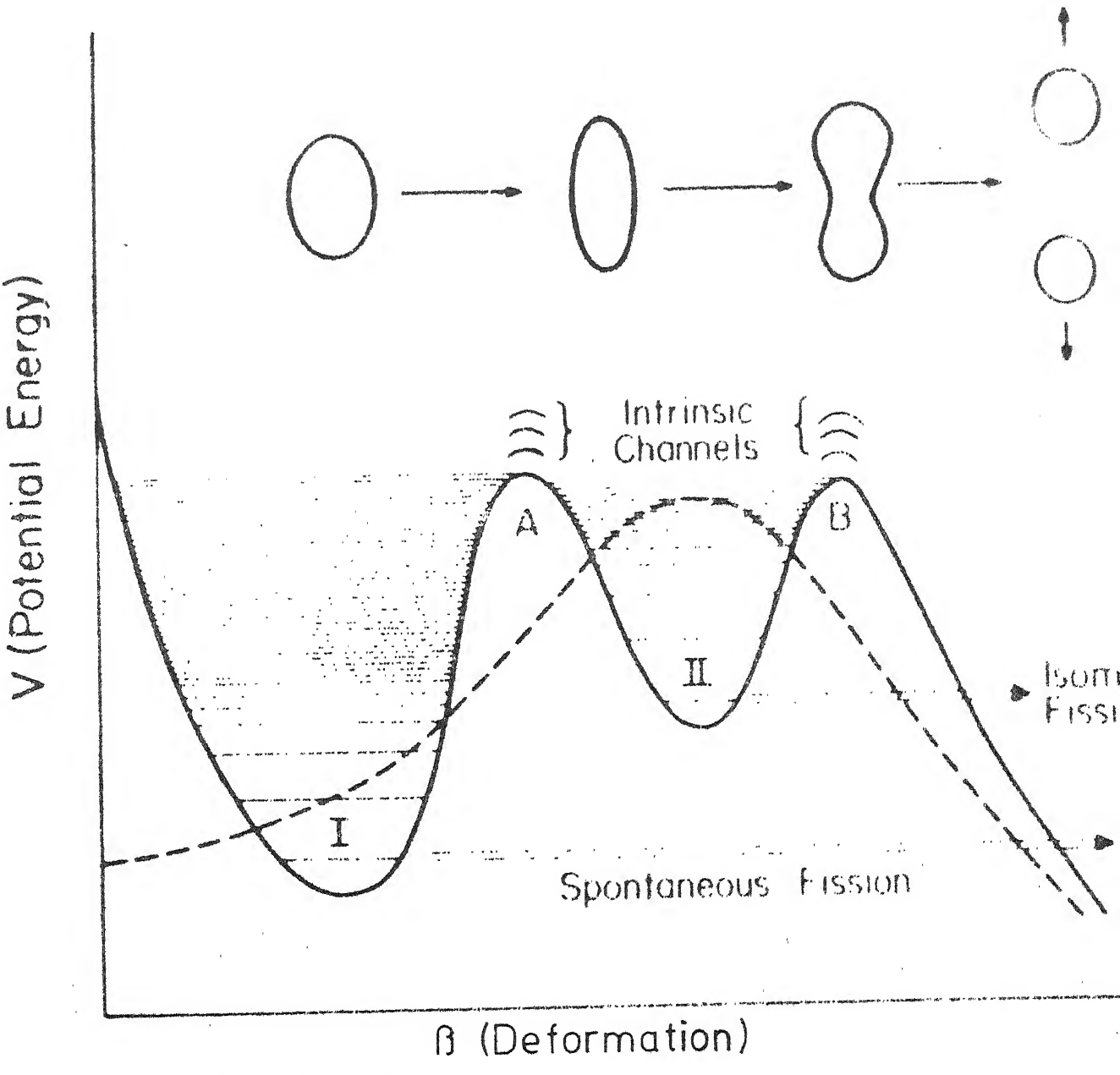

Fig. 1.1. Schematic illustrations of single-humped (---) and double-humped (——) fission barriers. Intrinsi excitations in the first and second wells are designated class I and class II states, respecti Intrinsic channels at the two barriers are also illustrated. The transition in the shape of the nucleus as a function of deformation is schematical represented in the u per part of the figure. [After Vandenbosch and Huizenga, 1973].

states (called class II states) to exist in the second well. The existence of such states can explain very well some important experimental results such as fission isomerism and structure in subthreshold fission cross-sections.

1.2 Binary fission

As mentioned earlier, the most commonly occuring division in fission is into two fragments of unequal mass. This asymmetric mass division is one of the most important characteristics of the process and is exhibited by all heavy nuclei with $A \geq 229$. The mass distribution is consequently double humped. Some nuclei, however, exhibit an anamalous mass distribution; Bismuth (in fact nuclei with $Z \leq 83$) exhibit predominantly symmetric mass distributions while Radium has a mass distribution which is triple humped indicating the presence of both symmetric and asymmetric divisions. A number of theoretical models have been suggested to explain these data, yet no one theory can explain all these observations. Other features of the mass distribution are that the mass distribution for a particular nucleus becomes more symmetric with increase in excitation energy and that the mass distribution depends on the mass number of the nucleus undergoing fission. The former observation has been explained in terms of the 'washing out' of shell effects at high excitation energies implying that the fissioning nucleus

'sees' only a liquid drop type of barrier (the liquid drop model predicts symmetric fission as the most probable mode).

Another important characteristic is the division of charge between the two fragments. Nuclear chemists have made many measurements to establish the character of this division of charge by measuring the yields of stable nuclei resulting from beta decay of the fission fragments. However, the quantity of most interest is the charge-to-mass ratio of the fragments just produced at scission prior to the emission of prompt neutrons i.e., of the primary fission fragments. The most probable charge (Z_p) of the fragments have been determined by measuring the characteristic K-x-rays in coincidence with the fragments (Reisdorf et al., 1971). The K-x-rays arise from internal conversion associated with the deexcitation of the primary fission fragments(10^{-10} sec., after scission). It has been observed that the charge division is such that the lighter fragment receives a larger fraction of the available charge than would be expected if the charge-to-mass ratio of the fissioning nucleus were preserved in the fragments. Various postulates have been used to explain these observations eg. the equal charge displacement postulate (Glendenin et al., 1951) which can be expressed as $(Z_p-Z_A)_{light} = (Z_p-Z_A)_{heavy}$ where Z_A represents the charge of the most stable isobar of that mass chain. This implies that there would be fewer

beta decays to stability in the case of the light fragment (relatively proton rich) than in the heavy fragment. Another postulate is that the charge division is such that the potential energy at scission is a minimum and another which requires a maximum of the total fragment excitation energy at scission (Wahl et al., 1962). One additional point to note is that the ratio of most probable charges of the fragments is very close to the mass ratio, eg., for ^{252}Cf the most probable mass and charge ratios are $\sim$1.31.

The largest fraction of the energy released goes into the kinetic energy of the fragments, resulting from Coulomb repulsion. The fragment energy distributions are related approximately to their mass distribution through the relation $M_L/M_H = E_H/E_L$. It is also noticed that the total fragment energy is a slowly increasing function of mass number or more precisely of the parameter, Z^2/A. One of the characteristics of the kinetic energy distribution (in low energy fission) is the decrease for symmetric fission and a prominent peak for asymmetric fission leading to heavy fragments with $A \approx 132$. This kinetic energy decrease has been qualitatively understood in terms of the relative increase in the number of prompt neutrons emitted in symmetric fission (this will be discussed later). The effect of increasing the compound nucleus excitation energy is to decrease the structure in this variation of kinetic energy

release. For nuclei lighter than Radium, which exhibit symmetric mass yield curves, the maximum kinetic energy release occurs for symmetric mass divisions and falls off with increasing mass asymmetry at a rate dependent on the compound nucleus excitation energy (Unik et al., 1969). However, in heavier nuclei, which exhibit asymmetric mass division, the total kinetic energy for the symmetric mode is lower than for the asymmetric mode. The dependence of total kinetic energy on compound nucleus excitation energy has been studied in detail and such studies indicate that the kinetic energy release in spontaneous fission is lower than that in thermal fission (Okolovich and Smirenkin, 1963) and for still higher excitations the variation in kinetic energy release is very small. This fact suggests that a large fraction of the compound nucleus excitation energy goes into fragment excitation and not into kinetic energy implying that the extent of stretching of the neck (the Coulomb potential energy at scission) remains more or less the same as the compound nucleus excitation energy increases. For symmetric mass division the drop in kinetic energy could, therefore, be related to the increase in fragment excitation leading to increased neutron emission.

Most of the energy release not appearing as kinetic energy of the fragments is dissipated by prompt neutron emission. The number of neutrons emitted is a direct consequence of the amount of energy stored in the fragments

either as internal (excitation) energy or as deformation energy converted to excitation energy as the fragments collapse to their equilibrium shapes. The neutron yield increases with increase in compound nucleus excitation energy which can be understood in terms of the weak dependence of kinetic energy on this excitation energy. As mentioned earlier the total number of neutrons increases for symmetric fission (Milton and Fraser, 1961; Apalin et al., 1964) with a corresponding decrease in kinetic energy. One of the most interesting aspects of neutronemission is the striking ('saw tooth') variation in neutron yield as a function of fragment mass. (Fraser and Milton,(1954) Apalin et al., 1965; Terrell, 1965). This behaviour led Terrell (1962, 1965) to the conclusion that the neutron yields are closely related to the deformabilities of the nascent fragments. Closed shell and near-closed-shell nuclei prefer spherical shapes and are resistant to deformation resulting in lower neutron yields. The 'saw-toothed' variation in neutron yield is fairly rapidly washed out with increasing excitation energy (Bishop et al., 1970).

The angular distribution of fission fragments has been studied in the excitation energy region up to several tens of MeV for many targets, for a variety of projectiles. (Gordon et al., 1960; Vandenbosch et al., 1961; Bate et al., 1963; Simmons and Henkel, 1960). The most striking

features of the experimental observations are (a) the fission fragments have largest differential cross sections in the directions forward and backward along the beam (b) the anisotropies are largest for the heaviest projectiles and smallest for neutron and proton bombardment (c) the anisotropies are approximately the same for odd A targets as for even-even targets and decrease with increasing Z^2/A. The angular distribution of the fragments depends on the angular momentum brought in by the projectile and the fraction of this converted into orbital angular momentum between the fragments (characterized by K in Fig. 2.3). The anisotropy has been successfully explained using the channel theory (discussed latter) using the assumptions that the fragments separate along the symmetry axis and that K is a good quantum number beyond the saddle point. Such anisotropies have also been observed in photofission (Baerg et al., 1959) however, the differential cross sections are largest in the directions perpendicular to the incident photon beam (electric dipole absorption).

Prompt γ rays emitted from the fission fragments provide useful information about properties of the fragments at scission. There are typically about 8 photons per fission (in spontaneous fission it is about 10) with an average of 1 MeV per photon. Both the average number (the multiplicity) and average energy per photon are functions of fragment mass. These γ rays differ from γ rays associated with neutron

capture because of the large amounts of angular momentum they carry away from the fragments ($\sim$10-12 $\hbar$). Extensive investigations of the characteristics of these fission γ-rays have been carried out (see for example the review in Vandenbosch and Huizenga, 1973) and have provided useful information about the de-excitation mechanism of the fragments.

1.3 Ternary fission

The term 'ternary fission' will be used with regard to that division resulting in two heavy fragments and a light charged particle (LCP) first observed by Alvarez (Farwell et al., 1947). Such a division normally occurs once in about every 500 fissions. Another possible mode of division is that resulting in three fragments of almost equal mass, however, such a division is very rare (Muga and Rice, 1969). A very large percentage ($\sim$90%) of these LCPs are long range alpha particles (LRA) having a mean energy of about 15 MeV (Cosper et al., 1967; Nadkarni and Kapoor, 1970), the remainder are mostly tritons, with an average energy of $\sim$8 MeV, and other particles such as protons, deutrons etc. The present study concentrates on certain aspects of LRA fission.

One of the most striking features about LCP emission is the angular distribution with respect to the

fragments. The fact that it is peaked in a direction perpendicular to the direction of the fragments (Titterton, 1951) has led to the belief that the LCP is emitted very close to the moment of scission from the 'neck' connecting the two fragments. Once these LCPs are emitted their motion would be influenced by the Coulomb field of the fragments and their final energies and angular distribution would be sensitive to the separation and speed of the fragments at the instant of their emission. Therefore, a study of LCP emission is expected to provide useful information about the scission-stage of fission.

The excitation energy dependence of LCP yield is fairly weak, decreasing by about 25 % for thermal neutron fission ($E^{*} \sim 7$ MeV) compared to spontaneous fission ($E^{*}=0$) e.g., for ^{240}Pu (Nobles, 1962). At excitation energies over 15 MeV there is some evidence of an increase in yield, (Thomas and Whetstone, 1966). It has also been noticed that the yield increases with increase in fissility parameter, Z^2/A (Nobles, 1962). This is consistent with the idea that the yield is dependent on the amount of deformation at scission i.e., a 'neck' should exist; which, as indicated by the liquid drop model, increases with increasing Z^2/A.

The kinetic energies of the various LCP vary quite significantly (Table 1.1). In $^{235}U+n_{th}$ fission the most probable LRA energy is 15 MeV (Nadkarni and Kapoor, 1970)

Table 1.1

LCP yield and energy characteristics in thermal neutron fission

LCP	Energy range of undistorted spectrum (MeV) ^{235}U	^{239}Pu	Relative intensity (extrapolated) ^{235}U	^{239}Pu	E(peak) (MeV) ^{235}U	^{239}Pu	FWHM (MeV) ^{235}U	^{239}Pu
p	4.5-17	4.0-18	1.15±0.15	1.9±0.1	8.6±0.3	8.4±0.15	6.9±0.5	7.2±0.3
d	5.5-17	4.5-19	0.5 ±0.1	0.5±0.1	7.9±0.3	8.2±0.3	7.0±1.0	7.2±0.5
	[4.8-15]*		[0.44±0.04]		[8.5±0.3]		[6.8±0.4]	
t	6.0-17	5.5-20	6.2 ±0.5	6.8±0.3	8.6±0.3	8.2±0.15	6.7±0.6	7.6±0.4
	[4.2-11.6]*		[6.3 ±0.2]		[8.1±0.2]		[6.2±0.2]	
α	12 -32	10 -29	100	100	15.7±0.3	16.0±0.1	9.8±0.4	10.6±0.2
	[10.6-34.2]*		[100]		[15.8±0.2] 15.0±0.1 a		[9.6±0.3]	
^4He	12.8-30	11 -28	1.1 ±0.2	1.9±0.2	12.9±0.5	11.8±0.4	8.7±0.7	10.6±0.6
	[9.0-20.1]*		[1.4 ±0.1]		[11.8±0.3]		[9.0±0.4]	

* measurable energy interval.

Ref: ^{235}U (Dakowski et al., 1967; Vorobiev et al., 1967 [...]) a : Nadkarni and Kapoor 1970.

^{239}Pu (Krogulski et al., 1969).

while the average triton energy is about 8 MeV. It has been observed that the average kinetic energy of the alpha particle increases as the angle of emission changes from the most probable angle (see Fig. 5.5).

Another striking feature of LRA fission is the observed anticorrelation between the average total fragment kinetic energy and the alpha energy. The value of this anticorrelation, averaged over all mass ratios, has been measured and found to be -0.44 i.e. $\partial \bar{E}_F / \partial E_\alpha = -0.44$ (Fraenkel, 1967; Gazit et al., 1970; Mehta et al., 1973). This anticorrelation decrease with mass ratio; in ^{252}Cf spontaneous fission it is about -0.2 in the far asymmetric region and increases to about -0.8 in the symmetric region (Mehta et al., 1973). This experimental fact will be used later in connection with trajectory calculations used to study the scission configuration.

1.4 Comparison of Binary and Ternary fission

A comparison of the mass-distribution in these two modes of fission e.g., in thermal neutron fission of ^{235}U (Schmitt et al., 1962) shows that the low mass sides of both fragment peaks are identical within the error of measurement whereas the high mass sides of the peaks are displaced towards the low mass side in ternary fission. The net shift in the peaks amounts to about 4 mass units corresponding

to the mass of the alpha particle.

The average total kinetic energy of the fragments in binary fission is almost equal to the sum of the average kinetic energies of the fragments and alpha particle. The average number of neutrons emitted in LRA fission of ^{252}Cf is 0.65 neutron less than in binary fission (Nardi et al, 1970; Piekartz et al., 1970). Using this figure it has been estimated that the excitation energy of the fragments is 5.7 MeV less in LRA fission than in binary fission. A remarkable similarity in these two modes is the 'saw tooth' variation of average neutron yield as a function of fragment mass. The total γ-ray energy in binary and ternary fission appears to be the same to within less than 1 MeV (Adamov et al., 1967; Ajitanand, 1969). These facts go to show the essential similarity of these two modes of fission.

1.5 The LRA as a probe of the fission process

There have been various conjectures about the extent to which the properties of the nucleus at the saddle point influence the various fission characteristics. For eg. the occurrence of negative parity states at the saddle point, for symmetric deformations, has been related to asymmetric fission. Another theory - the statistical theory, concentrates on the nucleus just at the moment of

scission where the characteristics of the process are believed to be decided. There does not exist adequate experimental evidence to decide to what extent the saddle states or statistical factors (at scission) influence the fission characteristics.

The present thesis reports experimental results on the yield and average energy of LRA in low energy neutron induced fission of ^{235}U and ^{239}Pu. The variation of LRA yield is sought to be linked up with some properties of the nucleus at the saddle point, thereby providing some more information which could help in moving toward a decision on the above questions. By using the method of trajectory calculations, the scission configuration in ternary fission of ^{252}Cf has been investigated. The results on the parameters describing the scission configuration, such as energies of the fragments and alpha particle, interfragment separation etc., could also throw some light on such questions.

CHAPTER II

CHANNEL EFFECTS IN FISSION

2.1. Introduction

A complete treatment of the fission process requires a dynamical study of the penetration of a multidimensional fission barrier. However, theoretical calculations mostly concentrate on the penetration of the potential energy barrier with respect to a deformation parameter. The potential energy surface (or fission barrier) with respect to the deformation parameter cannot be obtained, at present, using microscopic calculations which take into account the detailed structure of the nucleus. This is because of a lack of precise knowledge of the effective nucleon-nucleon interaction in the nucleus and also because of computational difficulties both in complexity and length. In addition, one would be faced with the problem of defining the deformation coordinates. Nevertheless, calculations of the fission barrier using Hartree-Fock methods have been carried out (Brack and Quentin, 1973; Flocard et al., 1973); but despite their considerable interest and the rapid improvements in accuracy such methods cannot as yet provide realistic barrier shapes.

Certain macroscopic methods based on classical concepts have been used with remarkable success. The first such calculation was made by Bohr and Wheeler (1939) employing the liquid-drop-model (LDM) to study the energy systematics of the fission process. In this model the nucleus is represented by a charged incompressible liquid drop and its potential energy is calculated in terms of the energies associated with the volume, surface area, Coulomb repulsion etc. The latter terms are shape dependent. These terms are summarized in the Weizacker (1935) semi-empirical formula for the nuclear ground state energy :

$$E = -U_v A + U_c \frac{Z(Z-1)}{A^{1/3}} + U_s A^{2/3} + U_T \frac{(A-2Z)^2}{4A} + \delta(Z,A)$$

where the first term is the volume energy term, the second the Coulomb repulsion energy term, the third the surface energy term, the fourth a term depending on the neutron-proton symmetry factor and an empirically observed term depending on the odd or even character of the nucleon numbers. From this formula it is possible to show that the energy of a heavy nucleus is considerably greater ($\sim$200 MeV) than the sum of the energies of two medium-weight nuclei of the same total mass, explaining the energy release in fission. It is also possible to obtain the ratio of the strengths of the repulsive coulomb forces to the strength of the restoring surface-tension forces for which the drop is in

unstable equilibrium - any small deformation will cause it to undergo fission. This ratio, denoted by the fissility parameter Z^2/A, has a critical value of about 50.

Much effort has been expended in studying the potential energy surface of the deformed liquid drop. Most studies (Bohr and Wheeler, 1939; Frankel and Metropolis, 1947; Cohen and Swiatecki, 1962) have employed the coefficients of a spherical harmonic expansion of the radius of the drop as a set of parameters describing deformation. If the potential energy surface is plotted as a function of one such deformation parameter (β_2) the curve shows a maximum (Fig. 1.1) and if it is plotted as contours on a surface using as coordinates the two principal parameters of symmetric deformation, β_2 and β_4; a saddle point would result for some (β_2,β_4) (Lynn, 1968). A similar saddle point would be apparent in a contour plot on a many dimensional surface defined by coordinates which included also the higher order coefficients of the expansion. It is the principal object of liquid-drop calculations to find the energy at the saddle point with respect to the energy of the undeformed drop, for this is the threshold of the fission reaction.

Despite the qualitative success of the liquid-drop model in explaining the fission phenomena it could not account for may observed characteristics such as mass asymmetry, isomer fission etc. The correction of the liquid-drop model for shell effects provided a great impetus

to the study of fission. Such corrections were first successfully incorporated by Strutinsky (1967, 1968) by an ingenious combination of the macroscopic and microscopic properties of the fissioning nucleus for all deformations along the fission path. The double-humped barrier (Fig. 1.1) which resulted from such calculations has been successful in explaining some of the above mentioned characteristics of fission.

2.2 The Unified Model of Fission

Before going into the formal discussion of this model it is necessary to understand the important feature of 'fission channels', especially for low excitation energies of the compound nucleus. In the formal theory of nuclear reactions, a channel is defined according to the quantum numbers of the asymptotic wave function of the system. Thus an entrance (exit) channel is specified by the state of the projectiles (products) before (after) any interactions occur. Bohr and Wheeler (1939) first introduced the concept of fission exit channels in terms of saddle-point configurations which are energetically available. By fission exit channels one means a well-defined type of fragmentation of the nucleus into two definite nuclear species in given excited states. The number of such channels would be extremely large (Wilets, 1964). Therefore

the variation in fission width should be practically constant from reasonance to resonance as are the radiative capture widths.(Michaudon, 1973). However, experiments indicate large fluctuations in fission widths.

The channel theory of A.Bohr (1956), also called the Unified model, gives a straight forward explanation for the large fluctuations in fission widths. Before discussing this theory it would be instructive to discuss the concept of 'open' fission exit channels as first introduced by Bohr and Wheeler (1939). The number, N, of such 'open' channel is given by

$$N = 2\pi \frac{\langle \Gamma_f \rangle}{\langle D \rangle}$$

where $\langle \Gamma_f \rangle$ and $\langle D \rangle$ are the average fission width and spacing of the reasonances, respectively. An effective number N_{eff}, of exit channels is defined for each spin and parity J^π as

$$(N_{eff})_{J^\pi} = 2\pi \frac{\langle \Gamma_f \rangle_{J^\pi}}{\langle D \rangle_{J^\pi}} = \sum_{i \varepsilon J^\pi} P_i$$

where $\sum P_i$ is the sum of penetrabilities P_i for all the ν channels i having the same spin and parity J^π, and

$$P_i = [1+\exp(-2\pi \frac{E^* - E_f^i}{\hbar w})]^{-1}$$

E_f^i is the height of the fission barrier associated with the transition state i.

$\langle \Gamma_f \rangle_{J\pi}$ has been calculated for low energy neutron induced fission of ^{235}U and ^{239}Pu using experimental data on integral fission widths. (Blons et al., 1970, 1971). The values of (N_{eff}) obtained for each of these resonances is usually less than or equal to one. This indicates that the effective number of fission exit channels in the case of low energy fission is very small. For example in the case of ^{239}Pu ($1/2^+$) resonances induced by s-wave neutrons have spin and parity 0^+ and 1^+. The value of N_{eff} for each of these two families of resonances is close to unity (Michaudon, 1973) indicating that in s-wave fission of ^{239}Pu there are two 'open' channels corresponding to the two resonances 0^+ and 1^+. This is the basic idea behind Bohr's channel thoory. Bohr had, however, proposed his theory, outlined below, before these calculations were made.

For excitation energies of the compound nucleus not too far above the fission threshold, the nucleus, in passing over the saddle point, is " cold'' since a major part of its energy is bound in the potential energy of deformation. The quantum states available to the nucleus at the saddle point (the fission channels) are then widely separated and represent relatively simple types of collective motion of the nucleus. These states are expected to resemble the ground state excitations of the deformed nucleus, that is, the channels at the saddle point form a spectrum similar to the low lying states of the stable deformed nucleus in its ground state.

Fig. 2.1 shows the spectrum of nuclear levels for an even-even nucleus as a function of a symmetric deformation parameter (for the sake of simplicity an LDM type of barrier has been chosen). It is assumed that the nuclear shape remains axially symmetric during the passing of the saddle point. The channels can then be characterized by the quantum number K, representing the component of the nuclear angular momentum J, along the symmetry axis. For even-even nuclei the lowest state of the nucleonic structure has K=0, corresponding to a paired nucleon configuration. With this intrinsic state is associated a rotational band with energies

$$E_{J,K} = E_K + \frac{\hbar^2}{2I} J(J+1)$$

where J is the total angular momentum (spin) and I is the effective moment of inertia. This latter quantity depends on deformation. For the ground states of the very heavy elements the value of $\hbar^2/2I$ is about 7 keV and at the saddle point the value would be smaller because of larger deformation.

For nuclei whose shapes possess reflection symmetry the spectrum, for K=0, contains only rotational levels with even J values: 0, 2, 4 ..... all of which have positive parity. The separation of these transition states comprising the the lowest rotational band would be smaller than observed in the heavy nuclei (ground state) spectra - the factor $\hbar^2/2I$ being smaller. The 2^+ state is about 11 keV and the 4^+ state

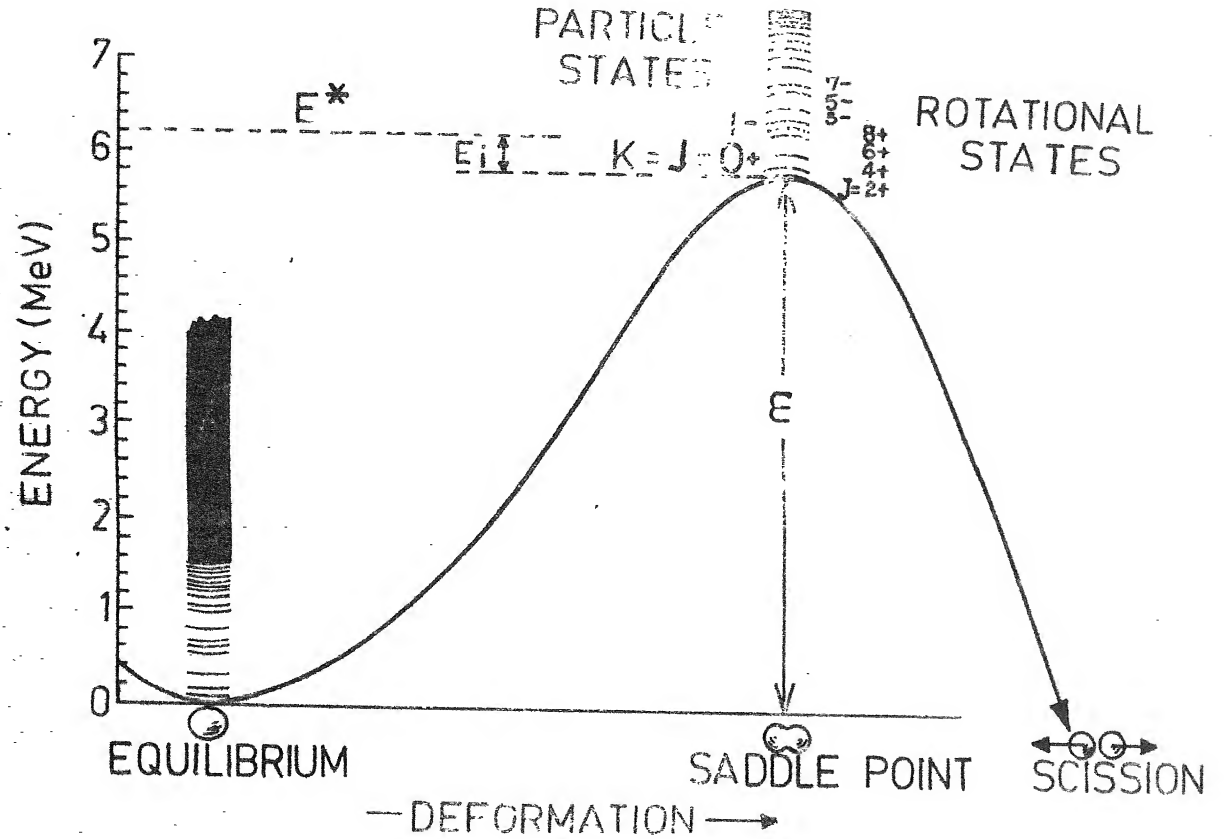

Fig. 2.1. Schematic representation of the fission process, as proposed by A. Bohr (1956). The level scheme at the saddle-point deformation is for an even-even nucleus.

about 37 keV above the 0^+ threshold (Lynn, 1968). The rotational band also contains odd J values having negative parity. These states correspond to excitations of the vibrational states of the deformed nucleus which do not possess reflection symmetry [the 'sloshing' mode of vibration, Wheeler (1956)]. These states are antisymmetric with respect to rotations about 180 deg and hence give rise to negative parity states such as 1^-, 3^-..... . They are displaced with respect to the positive parity states by an amount $\hbar w$, where w is the frequency of 'tunnelling' motion between the mirror shapes of the preferred asymmetry. The higher the degree of asymmetry the smaller the w. These low lying (1^-) excitations of the nuclear ground state have been observed to occur in the even isotopes of Ra and Th with energies in the region of 200 to 300 keV (Stephens et al., 1954). The energies increase as one goes to heavier elements.

At the saddle-point shape one expects even-even nuclei to have a lowest state of $J^\pi = 0^+$ and close lying collective excitations of 2^+, 4^+... type as well as states like 1^-, 3^-.... at somewhat higher energies.

Apart from these collective rotational excitations, the nucleus possesses states corresponding to the excitation of the nucleonic configuration i.e. single particle excitations. Since these require the breaking of a nucleon pair there will be a significant energy gap ($\sim$1 MeV) between the

lowest configuration (K=0) and the first excited configuration. After this gap the spacing between intrinsic excitations is only of the order of a 100 keV, corresponding to the average spacing of individual particle orbits. With each such intrinsic excitation, characterized by a definite K, there is associated a rotational band with J=K, K+1, K+2... and both parities.

In odd-A nuclei the lowest K value is given by the component of angular momentum of the last odd nucleon in its lowest binding state. At saddle point this lowest K value differs in general from the nuclear ground state. The spacing between the states of the last odd particle is of the order of a few hundred keV, and the intrinsic excitations in odd-A nuclei involve no energy gap similar to that characterizing the paired configuration in even-even nuclei. With each particle configuration is associated a rotational band with J = K, K+1.... and both parities. Similarly in odd-odd nuclei the intrinsic excitations would be closely spaced.

It must be mentioned that whether the single-humped or double-humped barrier is considered for the purpose of the Unified model the conclusions are not altered. As shown in Fig. 1.1 both saddle points (A and B) have intrinsic channels associated with them and hence the channel which would be relevant to the fission process would be the one corresponding

to the higher hump. For light actinides the inner barrier A is lower than the outer a barrier B whereas the opposite situation prevails for heavy actinides.

2.3 Low-energy fission and the characteristics of transition states

Slow neutron capture by an even-odd nucleus of spin J_o leads to a compound nucleus of even-even type with $J = J_o \pm 1/2$ and with the same parity (if $l = 0$) as the target nucleus. As explained in the last section the spectrum of states at the saddle point (the transition states) will contain only one of these spin parity combinations in the rotational band associated with the lowest nucleonic configuration $K = 0$. Therefore, the fission threshold is expected to differ appreciably ($\sim$1 MeV) for the two types of compound nucleus levels formed. Hence, in slow neutron fission, the transition state is essentially well defined and is expected to influence some of the characteristics of the process such as (i) angular distribution of the fission fragments (ii) fission widths of the resonances (iii) mass distribution of the fission fragments (iv) kinetic energy of the fragments (v) average number $\bar{\nu}$ of prompt neutrons emitted and (vi) emission probability and energy spectrum of light charged particles (LCP) emitted in fission. These characteristics are discussed in section. 2.5.

In the discussion so far only neutrons with l = 0 (s-wave) neutrons have been considered. However, the fission cross-sections for different partial waves differ significantly depending upon the energy of the incident neutrons. Rae et al (1958) have calculated the neutron capture and elastic scattering cross-sections of ^{235}U upto 1.1 MeV on the basis of the statistical theory of nuclear reactions. In the course of these calculations, the partial wave fission cross-sections, upto l=3, were computed and these are shown in Fig. 2.2. The curves are dashed above 500 keV because above that energy they depend on the assumptions used concerning the low-lying level structure of ^{235}U. It is seen that the p-wave (l=1) cross-section rises rapidly with energy and becomes equal to the s-wave (l=0) cross section for a neutron energy of 100 keV. From there on to 500 keV, the p-wave component represents at least 50% of the total fission cross-section; the d-wave having risen to equal the s-wave component by 500 keV.

It follows, therefore, that depending upon the incident neutron energy different channels would influence the fission process to differing extents. For example, in s-wave fission of $^{235}U(7/2^-)$ the states accessible to the nucleus would be 3^- and 4^- and when the energy is increased so that p-wave interactions become probable, the levels of character 2^+, 3^+, 4^+ and 5^+ would also be accessible. The relative

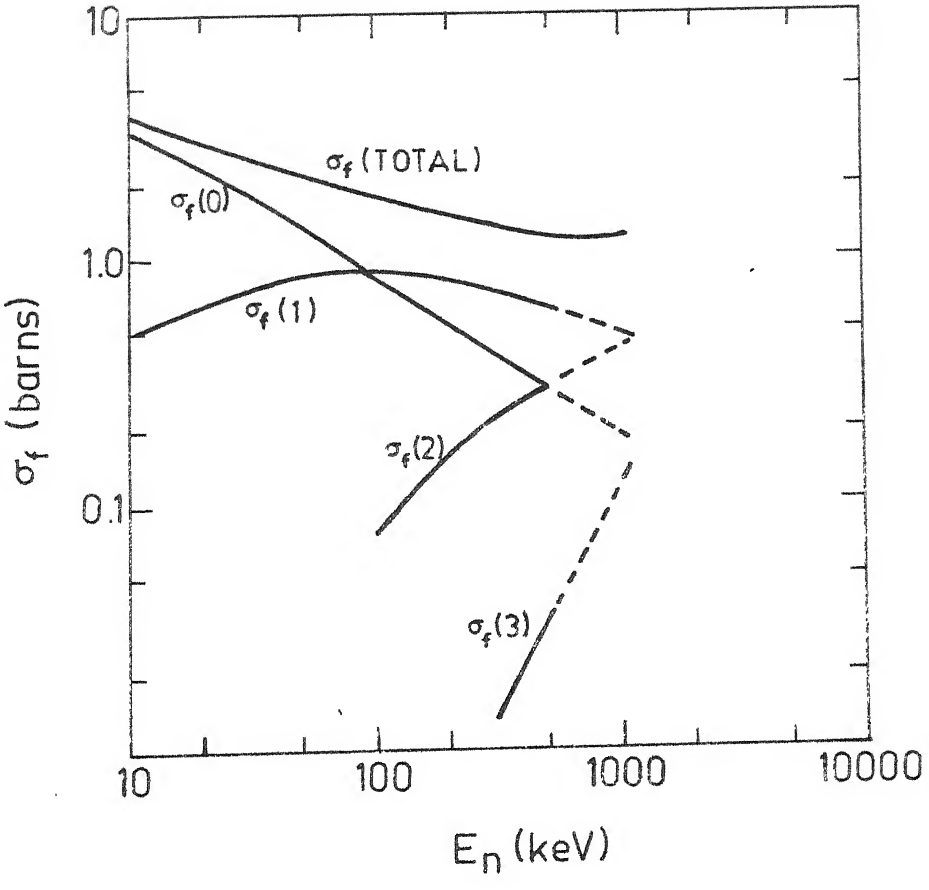

Fig. 2.2. Calculated partial wave fission cross sections for neutron induced fission of ^{235}U. [After Cuninghame et al., 1961].

predominance of either of these states i.e. odd or even parity states, would depend on the relative predominance of the partial fission cross-sections in the neutron energy region under study. Hence, if the neutron energy spread is not too large it should be possible, in principle, to selectively excite one or a few of these states and study the characteristics of fission resulting thereby. As the neutron energy increases the channel density also increases (since the level spacing decreases) and thus many channels would participate, and the channel effects are expected to average out.

It should be noted that the assumption that the fission characteristics are influenced by the properties of the transition states depends on the fact that the scissioning nucleus retains some information (over and above the rigidly conserved quantum numbers) as to which channel it passed through. In order to further understand this it is necessary to consider the descent of the nucleus from saddle to scission.

2.4 Motion from saddle to scission: Adiabatic and Statistical Models

The excitation energy of the compound nucleus may be represented as

$$E^{*} = E_i + \varepsilon$$

where E_i is the excitation energy of the i channel above the ground state and ε is the fraction of E^{*} stored as the potential energy of deformation (Fig. 2.1). As has been mentioned, ε would constitute a major fraction of E^{*}, in slow neutron fission, such that the nucleus is 'cold' at the saddle point and E_i would be of the order of a few tens of keV.

Most models of fission can be divided into two groups depending on whether or not the motion from saddle to scission is assumed to be adiabatic with respect to the particle degrees of freedom (Vandenbosch and Huizenga, 1973). If the change in deformation during descent is sufficiently slow or the coupling to internal degrees of freedom (residual interaction) sufficiently weak so that the single particle degrees of freedom can easily readjust to each new deformation (i.e. no nucleonic excitation) as the distortion proceeds, an adiabatic approximation may be valid. In this situation the decrease in potential energy from saddle to scission remains in the collective degrees of freedom at scission and appears primarily as kinetic energy associated with the relative motion of the nascent fission fragments. Hence the motion will become faster as fission proceeds. If, on the other hand, the change in deformation is somewhat faster or the coupling somewhat stronger there will be transfer of collective

energy into nucleonic excitation in a manner analogous to viscous heating. If there is sufficient non-adiabatic mixing of the energy among the single particle degrees of freedom by the time scission is reached, then a statistical model may be a reasonable approximation. The transfer of collective energy to the internal degrees of freedom can be thought of as arising due a nuclear viscosity. In this case less energy will be available for kinetic energy of motion of the fragments hence the descent would become slower. There is thus a feedback mechanism tending to prevent either approximation from becoming increasingly valid as the motion from saddle to scission proceeds.

At the other end of the time scale is the 'sudden' (impulse) approximation. Here it is assumed that the descent is so rapid that the nucleonic motion cannot readjust at all to the change in potential. A condition for this approximation to be valid is that the descent time is short compared to nucleon times. ($\sim 3\times10^{-22}$ sec.). An estimated descent time of $\sim 3\times10^{-21}$ sec has been derived from LDM calculations (Hill, 1958). (Blyumkina et al.,(1964) had obtained $\frac{t_{desc}}{t_n} \approx 10$). Thus the descent is slow enough for the impulse approximation to be invalid. However, the actual tearing of the neck and the collapse of the nascent fragments may be sufficiently rapid for this approximation to be valid at scission.

It is difficult to make theoretical estimates which are sufficiently reliable to decisively indicate whether an adiabatic approximation is valid. Wilets (1964) has examined this question from the point of a level crossing model (Hill and Wheeler, 1953) and concluded that although the process is unlikely to be adiabatic, it is also unclear whether the non-adiabatic mixing is sufficiently strong to assume the validity of the statistical model. Wilets has emphasized that the large energy gap associated with pairing may cause fission of even-even nuclei at low excitation energy to be mostly adiabatic. In reality the descent from saddle scission is undoubtedly very complicated, with near adiabaticity occuring for some degrees of freedom and sufficient non-adiabatic mixing for others. Experiments on low energy neutron induced fission might, however, indicate the extent to which channel effects show up after scission. Such information could help decide which of the descent models is most applicable.

2.5 Channel Effects in low-energy neutron induced fission

2.5.1 Angular distribution of fission fragments

Perhaps the most striking phenomenon explained by the channel theory of Bohr (1956) was the angular distribution of fission fragments, using the simple symmetric top model and the quantum numbers characterising the fission

channels. The angular momentum of the compound nucleus J, and its projection on the symmetry axis K are schematically shown in Fig. 2.3. The direction of motion of the fission fragments is along the symmetry axis. For relatively small neutron energies the angular momentum vector remains predominantly perpendicular to the symmetry axis, (as also to the incident direction) hence only smaller K values play a role and the distribution of fission fragments is peaked in the forward direction. This explanation, of course, implies that during descent, the value of K does not change. For larger incident energies, a larger number of channels may enter the picture, nevertheless, a systematic tendency for anisotropy in fragment emission results from the fact that the values of M (the projection of J on the incident neutron direction) and K are not distributed from - J to +J but are concentrated towards numerically small values. Such anisotropies have been experimentally observed (eg. Nesterov et al., 1967; Bekhami et al., 1968; Nadkarni, 1969) confirming the results of the channel theory. Anisotropies in photo-fission (Baerg et al., 1959) and in fast neutron-induced fission (Brolley et al., 1954) and other particle induced fission, such as (d,pf) and (t,pf),reactions have been explained similarly (Bohr, 1956; Wilets and Chase, 1956; Griffin, 1960).

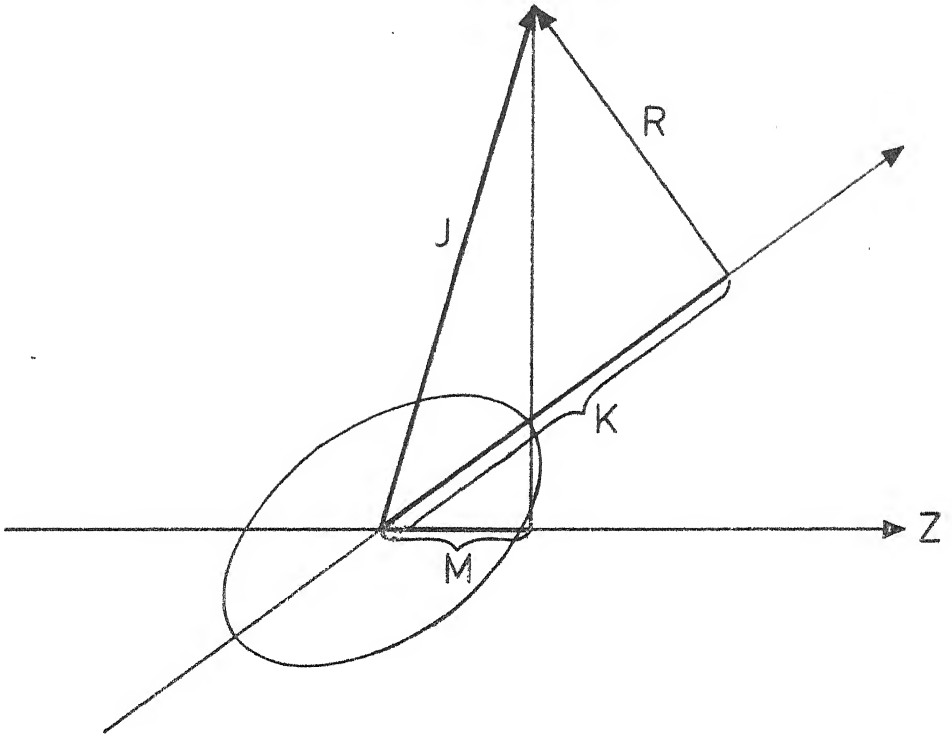

Fig. 2.3. Angular momentum coupling scheme for a deformed nucleus. The vector J defines the total angular momentum. The quantity M is the component of J on the space-fixed Z axis (the beam direction). The quantity K is the component of J along the nuclear symmetry axis. The collective rotational angular momentum R is perpendicular to the nuclear symmetry axis [After Vandenbosch and Huizenga, 1973].

2.5.2 Fission Widths

Since slow neutrons absorbed by odd mass nuclei form states with either of two spins and a parity well defined by the parity of the target, one expects a division of observed resonance fission widths into two groups with different average values of Γ_f, depending on the spin of the resonance state. As an illustration we can examine the well studied ^{239}Pu fission resonances. Resonances induced by s-wave neutrons in ^{239}Pu have $J^\pi = 0^+$ or 1^+. The low spin value of these resonances leads to relatively large spacings and neutron widths. For the $J^\pi = 0^+$ fission resonances, there is at least one fully open 0^+ fission exit channel, that of the ground state, since it lies about 1 MeV below the neutron separation energy, S_n. (The $K^\pi = 0^+$ channel is the main fission mode). In contrast, no simple 1^+ collective excitation seems to exist below S_n+1 MeV where two-particle states start to be excited.

The large energy difference between the lowest 0^+ and 1^+ transition states is actually reflected in the fission width distribution obtained experimentally (Blons et al., 1970). Two families of resonances are clearly visible and these two groups of narrow and wide fission resonances have been shown to have $J^\pi = 1^+$ and $J^\pi = 0^+$ respectively. This is in excellent agreement with the predictions of the channel theory.

2.5.3 Mass distribution of fission fragments

A suggestion stemming from the nature of the saddle states is that for resonance fission the mass asymmetry of the fragments may also depend upon the spin and parity of the resonance state. A tentative mechanism for such a dependence was suggested by Bohr (1956), Wheeler (1956) and discussed by Wilets and Chase (1956). One assumes that the mass asymmetry may be influenced by the state of asymmetric vibration at the barrier through which the nucleus passes en route to scission. In particular, fission via the first excited state of the asymmetric vibration could show a decreased probability for symmetric mass division relative to fission via the ground state of this vibrational mode. Hence one would expect that fission proceeding via the even parity band e.g. states based on 0^+, would show a more symmetric mass distribution (higher valley in the mass yield curve) than that proceeding via the odd parity band e.g. states based on 1^-. Odd-spin even-parity (1^+, 3^+....) or even-spin odd-parity (2^-, 4^-....) levels, which belong to neither band, would contain wave functions of both the symmetric and antisymmetric type (in the vibration parameter) so that their mass distributions might be intermediate in character between the other two groups. A very large number of radiochemical ond other measurements of the peak-to-valley ratio have been carried out for a

large number of resonances in low energy (upto 600 eV) fission of ^{239}Pu (e.g. Cowan et al., 1966; Burgus, 1962; Melkonian and Mehta, 1965; Ryabov et al., 1972) and of ^{235}U (Regier et al., 1960; Cowan et al., 1961; 1963, 1970; Simpson et al., 1971; Ryabov et al., 1971; Melkonian and Mehta, 1965). The results indicate that this ratio, R, does change from resonance to resonance and that they appear to fall into two symmetry classes characterized by different average values of R. In the case of ^{239}Pu, the average values of R for these two groups were in the ratio 3:5 corresponding to the two spin states 0^+ and 1^+. As expected from theory, low-R and high-R groups belong to the 0^+ and 1^+ spin states, respectively. There was also a correlation between the R values and Γ_f. The widths were larger, on the average for the low-R group of resonances. In the case of ^{235}U, the distribution in R values was narrower but they also appeared to be composed of two groups of resonances though the separation was not as clear as for ^{239}Pu (Michaudon, 1976). No correlation was observed between R and Γ_f.

In s-wave (l=0) fission the levels accessible in the case of $^{235}U(7/2^-)$ are 3^- and 4^- and for $^{239}Pu(1/2^+)$ are 0^+ and 1^+. In p-wave (l=1) fission the levels are 2^+, 3^+, 4^+ and 5^+ for ^{235}U and 1^- and 2^- for ^{239}Pu. Using the considerations developed in the channel theory one would

expect more symmetric fission (smaller R) for the even parity states, in particular the even spin states i.e. 2^+, 4^+ for ^{235}U and 0^+ for ^{239}Pu, than for the odd parity states. Such effects have been observed (Cuninghame et al., 1961, 1964; Mehta et al., 1967). Cuninghame et al., (1961, 1964) measured these ratios for fission by neutrons in the energy range between 65 keV and 1 MeV with emphasis on the region around 125 keV.

The results on ^{235}U fission indicated a large increase in R below 200 keV incident neutron energy. The measured value of R at 125 keV was approximately 45% above the thermal neutron value. The increased ratio in the energy region of 60 to 125 keV especially at 125 keV is quite contrary to what one would expect from channel theory considerations. The explanation of these anomalous results was not conclusive and some of the suggestions to account for these were (i) in thermal fission the mass distribution is only averaged over a mixture of a few levels of opposite J and statistically this type of fission may not be truly representative of s-wave fission; as the energy was increased the relative number of fissions via even parity levels increased hence the proportion of symmetric fission increased, however, the large increase in the 125 keV region remained unexplained (ii) the abiabatic model does not hold good so that between saddle and scission there is a mixing of

expect more symmetric fission (smaller R) for the even parity states, in particular the even spin states i.e. 2^+, 4^+ for ^{235}U and 0^+ for ^{239}Pu, than for the odd parity states. Such effects have been observed (Cuninghame et al., 1961, 1964; Mehta et al., 1967). Cuninghame et al., (1961, 1964) measured these ratios for fission by neutrons in the energy range between 65 keV and 1 MeV with emphasis on the region around 125 keV.

The results on ^{235}U fission indicated a large increase in R below 200 keV incident neutron energy. The measured value of R at 125 keV was approximately 45% above the thermal neutron value. The increased ratio in the energy region of 60 to 125 keV especially at 125 keV is quite contrary to what one would expect from channel theory considerations. The explanation of these anomalous results was not conclusive and some of the suggestions to account for these were (i) in thermal fission the mass distribution is only averaged over a mixture of a few levels of opposite J and statistically this type of fission may not be truly representative of s-wave fission; as the energy was increased the relative number of fissions via even parity levels increased hence the proportion of symmetric fission increased, however, the large increase in the 125 keV region remained unexplained (ii) the abiabatic model does not hold good so that between saddle and scission there is a mixing of

adiabatic model states; however, in order to provide lower symmetry for p-wave fission, one would have to assume mixing between levels of different K. In other words, it would be necessary to violate K-conservation which appeared so necessary to explain angular distribution data.

The ^{239}Pu results indicate an increase in ratio in the region 30 keV to 200 keV above the thermal value, the increase being very significant around 30 keV. Beyond this region the ratio is more or less the same as the thermal value. The region (30 keV to 200 keV) of increase is the region where p-wave fission competes with s-wave fission and the increasing asymmetry (large R) would be due to the relative predominance of negative parity levels populated due to the p-wave interaction. These results are quite consistent with the predictions of the channel theory unlike the ^{235}U results.

2.5.4 Kinetic energy of fission fragments

The kinetic energy of the fragments arises out of the Coulomb repulsion at scission with the possible addition of prescission kinetic energy which depends on viscosity effects. Measurements of kinetic energy distribution in resonance neutron induced fission of ^{235}U (Melkonian and Mehta, 1965; Moore and Miller, 1965) and ^{239}Pu (Melkonian and Mehta, 1965) showed that it was possible to separate the variations in the kinetic energy distribution into two

groups corresponding to the two different J values in s-wave fission. Similar measurements on the average total fragment kinetic energy in ^{235}U fission in the incident neutron energy region upto 2 MeV (Bolshov et al., 1968; Blyumkina et al., 1964) have indicated that the average total fragment kinetic energy shows definite structure around 200 keV - it drops by about 0.6 MeV in this region. This drop in kinetic energy has been explained as resulting due to the predominance of the p-wave interaction leading to increased excitation of the fragments. (The number of prompt neutrons emitted (ν) is a measure of this excitation). The positive parity states populated by the p-wave interaction lie about 0.6 MeV below the negative parity states populated by the s-wave interaction. Measurements on ^{233}U (Okolovich and Smirenkin, 1963; Boldeman et al., 1976) which has a ground state parity opposite to that of ^{235}U; showed an opposite effect in average total fragment energy around 200 keV. These results go to show that channel effects persist even in gross quantities such as average total fragment kinetic energy.

2.5.5 Prompt neutron emission

A major portion of the energy not appearing as kinetic energy is dissipated by emission of prompt neutrons. Thus the average number of prompt neutrons emitted ($\bar{\nu}$) would be a direct measure of a fairly large amount of energy stored in the nascent fragments at scission. This

energy may either be in the form of internal (excitation) energy, or be stored in the form of deformation energy and converted into excitation energy as the fragments collapse to their equilibrium shapes. The linear dependence of $\overline{\nu}$ on incident neutron energy was postulated by Fowler [Fowler's hypothesis, Leachman (1956)]. According to this hypothesis $\overline{\nu}$ increases linearly with neutron energy as a result of increasing excitation energy - the average total kinetic energy being independent of neutron energy. Andreev (1961) had predicted that in the energy region $E_n \lesssim 1$ MeV the fission channels would effect the distribution of energy between kinetic energy and excitation energy of the fragments leading to deviations from Fowler's hypothesis. This prediction is based on the fact that because discrete channels are available, the average kinetic energy must increase linearly with incident neutron energy and $\overline{\nu}$ remain constant for fission through a particular channel. When a new channel opens, the kinetic energy decreases in a step and $\overline{\nu}$ increases proportionately. Andreev (1961) had assumed that the energy that goes into deformation of the fragments, as the energy is increased from one channel to the next (higher barrier), is converted into kinetic energy of the nascent fragments, whereas Fowler's hypothesis requires this deformation energy to go into nucleonic excitation. The validity of these two lines of thought are, we see once again, connected with the

nature of the descent from saddle to scission.

The variation of $\bar{\nu}$ from resonance to resonance has been studied for the fission of ^{239}Pu (Shapiro, 1968; Weinstein et al., 1974) and ^{235}U (Ryabov et al., 1972; Trochon et al., 1973). These studies showed definite variations in $\bar{\nu}$ which could be correlated, though not quite consistently, with the different values of J^{π} (Michaudon, 1976). However, with the establishment of the existence of the (n, γf) reaction from results obtained on measurements on $\bar{\nu}$ and $\bar{E}_{\gamma}$ (the mean fission γ-ray energy) (Frehaut and Shackleton, 1974); the variation in $\bar{\nu}$ could be explained without invoking the influence of the transition states. The conclusion is that there is a weak spin effect on $\bar{\nu}$ but most of the variation in $\bar{\nu}$ is due to the effect of the (n, γf) reaction and not to the fission channels.

Measurements on $\bar{\nu}$ for higher incident neutron energies (upto 1 MeV) in the fission of ^{235}U (Blyumkina et al., 1964; Meadows and Wahlen, 1967) and ^{233}U (Blyumkina et al., 1964; Boldeman et al., 1976) have indicated the presence of structure around 200-300 keV neutron energy. The increase around 200 keV relative to thermal energies was correlated with the decrease in average total kinetic energy of the fragments ($\sim$0.6 MeV) in this region. The interpretation of the energy division was that the energy associated with collective motion (eg., rotation) was weakly coupled to the nucleon degrees of freedom and hence this energy went mostly

into kinetic energy of the fragments. Thus, whenever a new channel opens, there would be change in kinetic energy and 'between' channels $\bar{\nu}$ would increase. In the case of ^{235}U, since the even parity states (populated by the p-wave interaction) lie ~0.6 MeV lower than the odd parity states, the kinetic energy would also register a drop in the region where p-wave fission becomes important (~200-300 keV) and the 'extra' energy made available would go into fragment excitation and subsequently result in an increase in $\bar{\nu}$. Beyond 600 keV channel mixing effects would probably result in the averaging out of $\bar{\nu}$ and $\bar{E}_k$ as observed.

2.5.6 Light charged particle (LCP) emission

For the scissioning nucleus to be able to emit a light charged particle (LCP) it is necessary that a certain amount of energy be concentrated on a degree of freedom which facilitates LCP emission, for example Halpern (1963) has calculated that for alpha particles (LRA) this energy is about 29 MeV. Since the distribution of energy between the various degrees of freedom eg., kinetic energy, fragment excitation etc., at the saddle point, is influenced by the properties of the saddle states it would be reasonable to expect that the emission probability (yield) and average energy of LCP may also be affected by these states.

Measurements on LRA emission probability (P_{LRA}) have been carried out for fission induced by neutrons in the resonance energy region (Deruytter and Neve de Mevergnies, 1965; Melkonian and Mehta, 1965; Schröder et al., 1965; Wagemans and Deruytter, 1972). The results indicate that the variation in P_{LRA} (as indicated by the LRA yield) and average energy of LRA is in correspondence with the J value of the compound nucleus resonance i.e., fission channel. Measurements with fast neutrons (Drapchinski et al., 1964) and with fast charged particles (Thomas and Whetstone, 1966; Loveland et al., 1967) have also been made. At high incident energies the probability for second and third chance fission increases, hence the observed P_{LRA} would be an average over several nuclear species fissioning at different excitation energies leading to uncertainties in P_{LRA}. Hence, it would be necessary to measure P_{LRA} at those energies where only first chance fission occurs. In the case of ^{235}U and ^{239}Pu this (incident neutron) energy range lies below 5 MeV.

Investigations on P_{LRA} in neutron induced fission of ^{235}U upto 4 MeV, in intervals of 1 MeV (Nadkarni and Kapoor, 1970) showed that P_{LRA} was equal to the thermal neutron value within the statistical error of 10%. Subsequent measurements with neutrons in the range 0.75 to 1.75 MeV also gave the same result (Nadkarni et al., 1975) however, the low-energy component of the spectra showed variation with neutron energy. In the energy range above 500 keV channel mixing

effects could result in an average value of P_{LRA} close to the thermal value. Hence, in order to determine the presence of structure in yield or average energy one would have to concentrate on the region from thermal to 1 MeV.

The present measurements on P_{LRA} were for neutron induced fission of ^{235}U $(7/2^-)$ and ^{239}Pu $(1/2^+)$ in the energy range from thermal to 1 MeV, with a view to determine whether or not channel effects show up in the yield and average energy of the LRA.

CHAPTER III

EXPERIMENT

3.1 Experimental setup

The present work was done with the 2 MV Van de Graaff accelerator at the Indian Institute of Technology, Kanpur. It is a standard H.V.E.C. machine capable of providing positive ion beams upto a total current of about 100 μA with an energy resolution better than ± 5 keV (without the stabilization system). A schematic diagram of the beam transport system is shown in Fig. 3.1.

The quadrupole lens (Q_1Q_2) used to focus the beam, was fabricated locally. The pole gap of this doublet is large enough to allow a $1\frac{1}{2}$'' diameter beam pipe to pass through. The stand on which the lens is mounted has facilities for easy up-and-down movement of the lens. With this lens it was possible to focus the beam to a spot less than 5 mm in diameter at the target located about 6 meters away from the lens.

The neutron counter used to monitor the neutron flux was a standard long counter.(Hanson and Mckibben, 1947). It consists essentially of a BF_3 counter axially embedded in a paraffin cylinder. The exact geometry and other

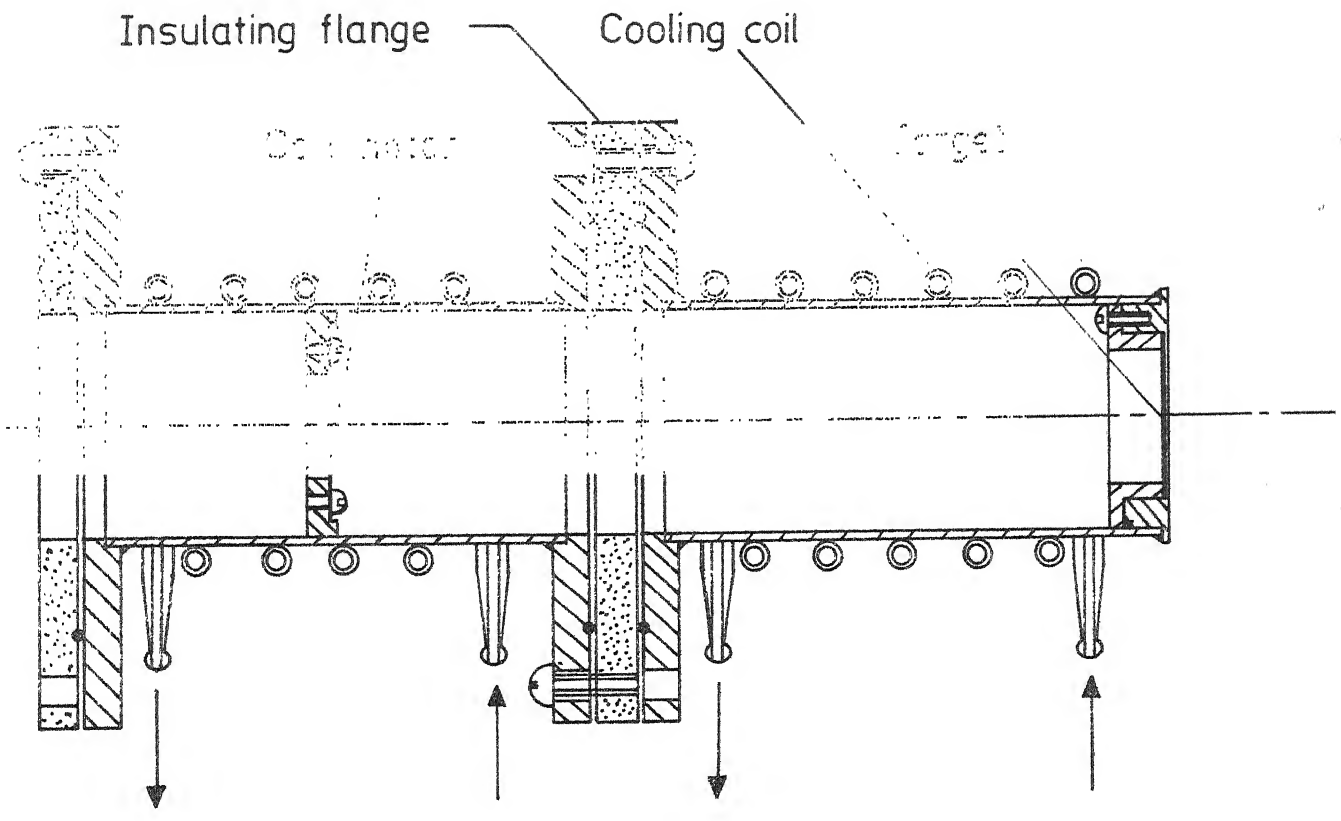

Fig. 3.2. The target holder and collimator.

details are described in the reference quoted above. This type of counter has a flat response to neutrons above 1 MeV The response to thermal neutrons is about 70% of the response to 1 MeV neutrons (Allen, 1960). The counter was placed at a distance of about 3 meters away from the neutron target. It served essentially as a monitor of neutron target deterioration.

The neutron target holder assembly, shown in Fig. 3.2, consisted of a water cooled collimator and a target holder made of copper. With this assembly it was possible to use proton currents upto 50 μA on the target without significant target deterioration for periods over 24 hours. Neutrons were produced by the $^{7}Li(p,n)^{7}Be$ and $T(p,n)^{3}He$ reactions. The lithium targets, of about 20 keV thickness to 2 MeV protons, were prepared by vacuum evaporation of lithium metal on to copper backings. The tritium targets were obtained from the Isotope Division, BARC, Bombay. The tritium targets of activities upto 12 Ci consisted of titanium deposited on a copper disc in which tritium was adsorbed such that the ratio of number of atoms of tritium to titanium was 1:1. In order to calculate the thickness of these targets in keV the following procedure was adopted

Consider a 1 Ci target:

$$\frac{dN}{dt} = -\lambda N = 3.7\times10^{10} \text{ sec}^{-1}$$

$$\therefore N = 3.7\times10^{10}\times12.33\times3.15\times10^{7} \text{ atoms}$$

$$= 1.44\times10^{19} \text{ atoms.}$$

Hence the number of Ti atoms $= 1.44\times10^{19}$

If this titanium is deposited over an area of 1 cm^2 then the thickness of the titanium layer would be

$$\frac{1.44\times10^{19}\times48}{6\times10^{23}} = 1.14 \text{ mg/cm}^2$$

The protons lose most of their energy in titanium hence using the energy loss of protons in titanium in units of MeV/mg/cm^2, obtained from tables, the nett loss for any target of specified activity may be calculated. For example the energy loss of 2 MeV protons in titanium is 94 keV/mg/cm^2; hence in a 4 Ci target the protons would lose about 130 keV i.e. the target thickness of a 4 Ci target to 2 MeV protons is ~130 keV.

The fissile targets consisted of deposits of ^{235}U and ^{239}Pu on nickel discs. The ^{235}U target of 93.9% enrichment, obtained from the Isotope Division, BARC, had a thickness of ~5 mg/cm^2 and an active area of ~4 cm^2. The ^{239}Pu targets of 96.97% enrichment, obtained from the Oak Ridge National Lab., USA, had a thickness of ~880 μg/cm^2 with an active area of ~3 cm^2.

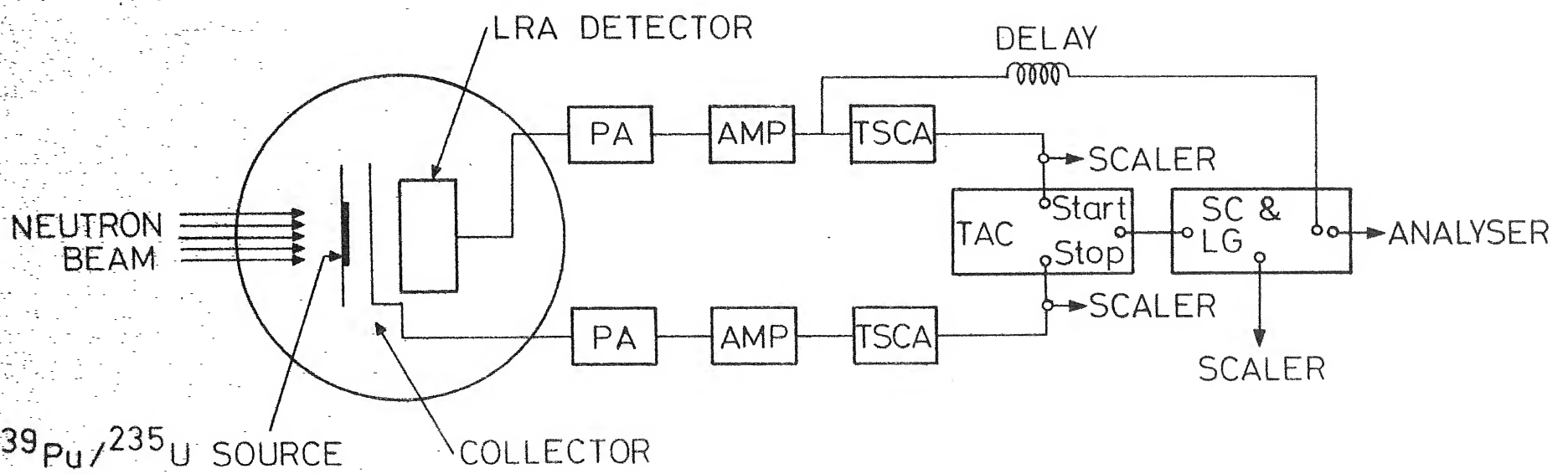

Fig. 3.3. Schematic diagram of the ionization chamber and electronics used.

and 410 amplifiers and fed to timing single channel analysers (Ortec 420) to get the timing signals. The discriminator on the fission side was set to cut off natural alphas (~6 MeV) and on the LCP side the cut off was ~6 MeV in the ^{235}U runs and ~8 MeV in the ^{239}Pu runs i.e. the cut off was just above the highest alpha energy of the calibration source. The timing signals were fed to a time-to-pulse-height converter (Ortec 437, 2τ = 0.5 μsec.) in the ^{235}U runs and to a slow coincidence unit (Ortec 409, 2τ = 1 μsec.) in the ^{239}Pu runs. The LCP detector pulses after suitable delay (Ortec 427) were gated with these outputs and recorded on a Packard 400 channel analyser. The fission and alpha count rates were simultaneously monitored.

3.2 Procedure

Neutrons of five different energies in the range 100 to 1100 keV were produced. The Li(p,n) reaction was used to produce neutrons upto 300 keV (Gibbons and Newson, 1960) and the T(p,n) reaction for neutrons between 500 and 1100 keV (Coppola and Knitter, 1967). The neutron energy spread was calculated using energy loss and angular spread considerations (the fissile target intercepted the neutron 'beam' in a 30° cone). Thermal neutrons were produced by interposing a 5 cm thick paraffin block between the neutron target and the fission chamber.

The average proton current used was 30μA. The fission rate in the ^{235}U runs was $\sim 2.5 \times 10^{3}$ per sec and in the ^{239}Pu runs it was $\sim 2.6 \times 10^{2}$ per sec. The neutron flux at the fissile target estimated from these rates was $\sim 10^{7}$ n/cm^{2}/sec. The average LCP count rate was 1-2 per min. and each spectrum was collected for about 20 hours.

After each coincidence run an ungated (singles) spectrum of the LCP was recorded for a fixed time. This was used in the correction of the coincidence spectra for chance coincidences. Each 'fast' run was preceeded and followed by a thermal run. These thermal runs served as a monitor for possible drifts and also provided a normalization for the 'fast' runs. The stability of the system was monitored frequently using an on-line precision pulser. The bias on the detector changes with increase in leakage current because of the increase in voltage drop across the series resistance in the preamplifier. When the bias drops so low that the depletion depth is not sufficient to stop the high energy LCPs, the spectrum gets distorted. Hence the leakage current in the detector was continuously monitored and the bias was adjusted when this current increased(due to neutron damage) so that the high energy tail of the LCP spectrum was not lost. Detector deterioration due to radiation damage was quite severe and during the course of the experiment several detectors were used. Several coincidence runs (with similar calibrations) were added to give the final coincidence spectra.

3.3 Data Analysis

The LCP spectra were first corrected for chance coincidences using the singles LCP spectra. The chance coincidence rate is given by

$$N_{ch} = 2\tau \frac{N_1 N_2}{T_1 T_2} \text{ sec}^{-1}$$

$$= 2\tau \frac{N_\alpha^s N_f^s}{T^s T^c} \text{ sec}^{-1}$$

where N^s is the number of events in the singles run.

T^c is the time period of the coincidence run during which the fission rate was monitored.

T^s is the time period of the singles run.

The number of chance coincidences in time T^c is therefore

$$N_{ch} = 2\tau \frac{N_\alpha^s N_f^s}{T^s}$$

The number of chance coincidences per fission event is

$$N_{ch} = 2\tau \frac{N_\alpha^s}{T^s} .$$

hence the number of chance coincidences during the coincidence run is

$$N_{ch} = 2\tau \frac{N_\alpha^s N_f^c}{T^s}$$

or

$$\sum_{i=1}^{n} N_{ch,i} = \frac{2\tau N_f^c}{T^s} \sum_{i=1}^{n} N_{\alpha,i}^s$$

Therefore, if $N^{s}_{\alpha,i}$ is the number of counts in a particular channel i then $N_{ch,i}$ gives the chance coincidence correction for that channel. In this manner a channel by channel correction was made. The maximum correction (~5%) was in the low energy region.

These spectra were then corrected for energy loss in the source, gas and aluminium foil. This was done by estimating the average thickness of source, gas and aluminium foil encountered by the particles by comparing the observed LCP peak energy in the thermal runs with the known value of LRA energy in thermal fission of ^{235}U (Nadkarni and Kapoor, 1970) and in ^{239}Pu (Krogulski et al., 1969). The shift in peak energy represents the average energy loss (ΔE) of the LRA, with initial energy (E_o) corresponding to the known peak value, in the source, gas and foil. The average thickness of argon corresponding to this energy loss was obtained from tables (Northcliffe and Schilling, 1970). Using this value a plot of initial energy (E_o) versus residual energy ($E_o - \Delta E$) was made using energy loss tables. It was thus possible to determine the energy loss for any initial LRA energy. The energy loss values obtained this way were also cross-checked by calculating the energy loss in the source, gas and foil step by step and the results indicated that the method adopted above was very satisfactory.

The experimentally measured energies, which are the residual energies, were thus converted into initial energies. The final spectra were obtained by adding the counts in channels falling within equal initial energy intervals of 0.5 MeV each.

CHAPTER IV

RESULTS AND DISCUSSION

4.1 ^{235}U fission

The LCP energy spectra in thermal and fast neutron runs are shown in Fig. 4.1 (Krishnarajulu et al., 1977). The least squares Gaussian fits to the spectra are shown as continuous curves. The lower limit of the Gaussian fitting function was fixed at 12 MeV since the yield in the region beyond 12 MeV is predominantly due to alpha particles (see Table 1.1). The spectra show more low-energy particles than that given by the Gaussian.

From these fits, the most probable value ($\bar{E}_\alpha$) and standard deviation (σ_{E_α}) were obtained as a function of neutron energy and these values, tabulated in Table 4.1, are shown in Fig. 4.2. It can be seen that there is some structure ($\sim$0.6 MeV) in the neutron energy range of 200 to 700 keV. There is no indication of a systematic trend with neutron energy. The width, σ_{E_α}, seems to be insensitive to variation in incident neutron energy.

The results on LCP yield above 6.5 MeV (Table 4.1) are shown in Fig. 4.3(a). There is a marked increase of about 20% in the range 200 to 500 keV as compared to the thermal neutron yield. At higher neutron energies the yield tends towards the thermal value. This yield has

Table 4.1

Average LRA energies, widths and Normalized Yields (^{235}U fission)

Neutron Energy (keV)	$\bar{E}_\alpha$ (MeV)	σ_{E_α} (MeV)	LCP Yield >6.5 MeV	LRA Yield >12 MeV	'Triton' Yield 6.5 to 12 MeV
THERMAL	15.0 ±.1	4.87±.16	1.0 ±.01	1.0 ±.01	1.0 ±.1
120±40	15.1 ±.09	5.09±.16	1.09±.03	1.07±.03	0.92±.19
180±40	14.3 ±.06	4.56±.16	1.22±.03	1.21±.03	0.63±.16
500±180	15.66±.1	4.72±.16	1.21±.03	1.11±.03	2.66±.38
800±180	15.06±.1	4.38±.16	1.01±.03	0.97±.02	1.79±.27
1020±180	15.16±.08	5.41±.16	1.04±.03	1.00±.03	1.33±.19

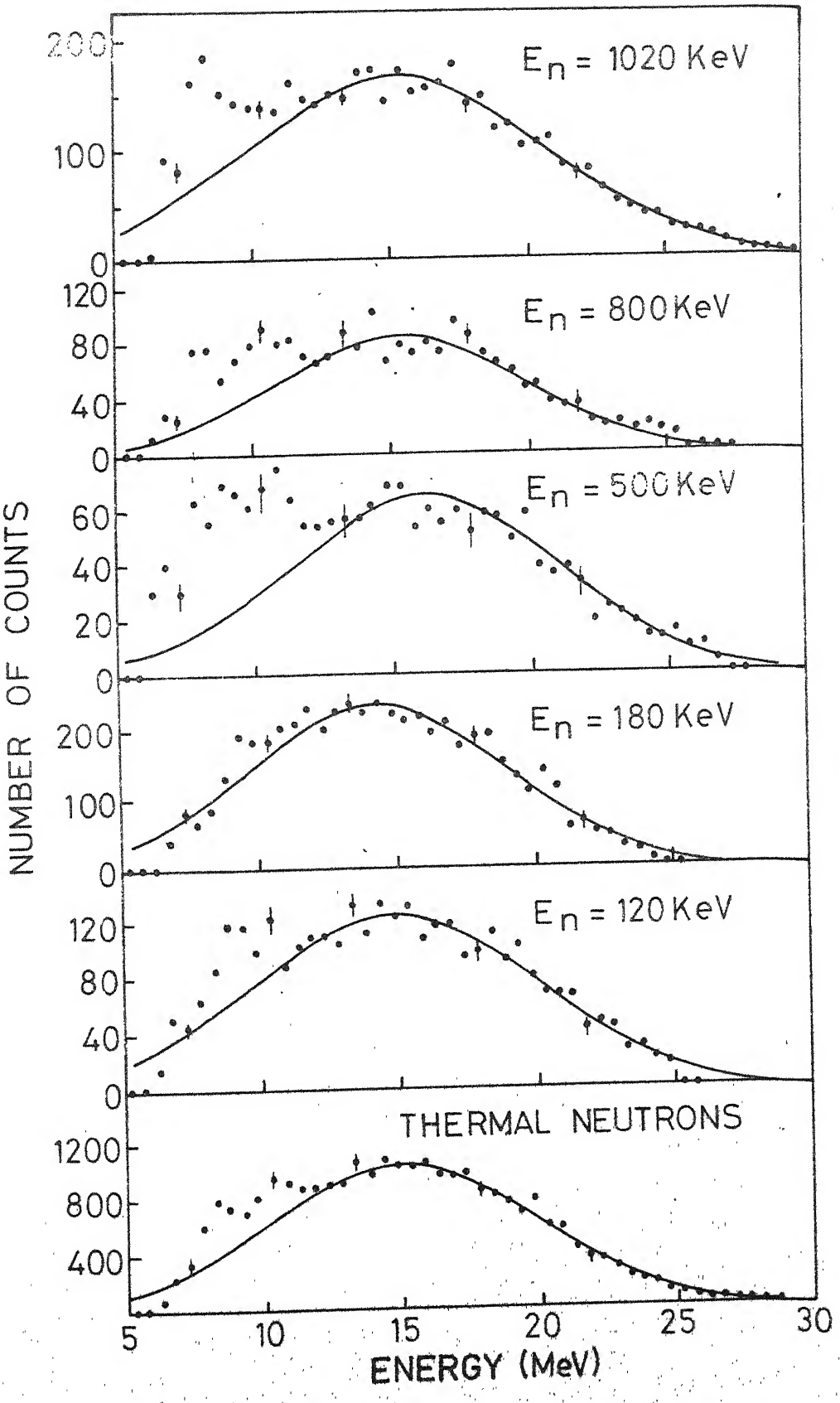

Fig. 4.1. The LCP energy spectra for various neutron energies. (^{235}U fission)

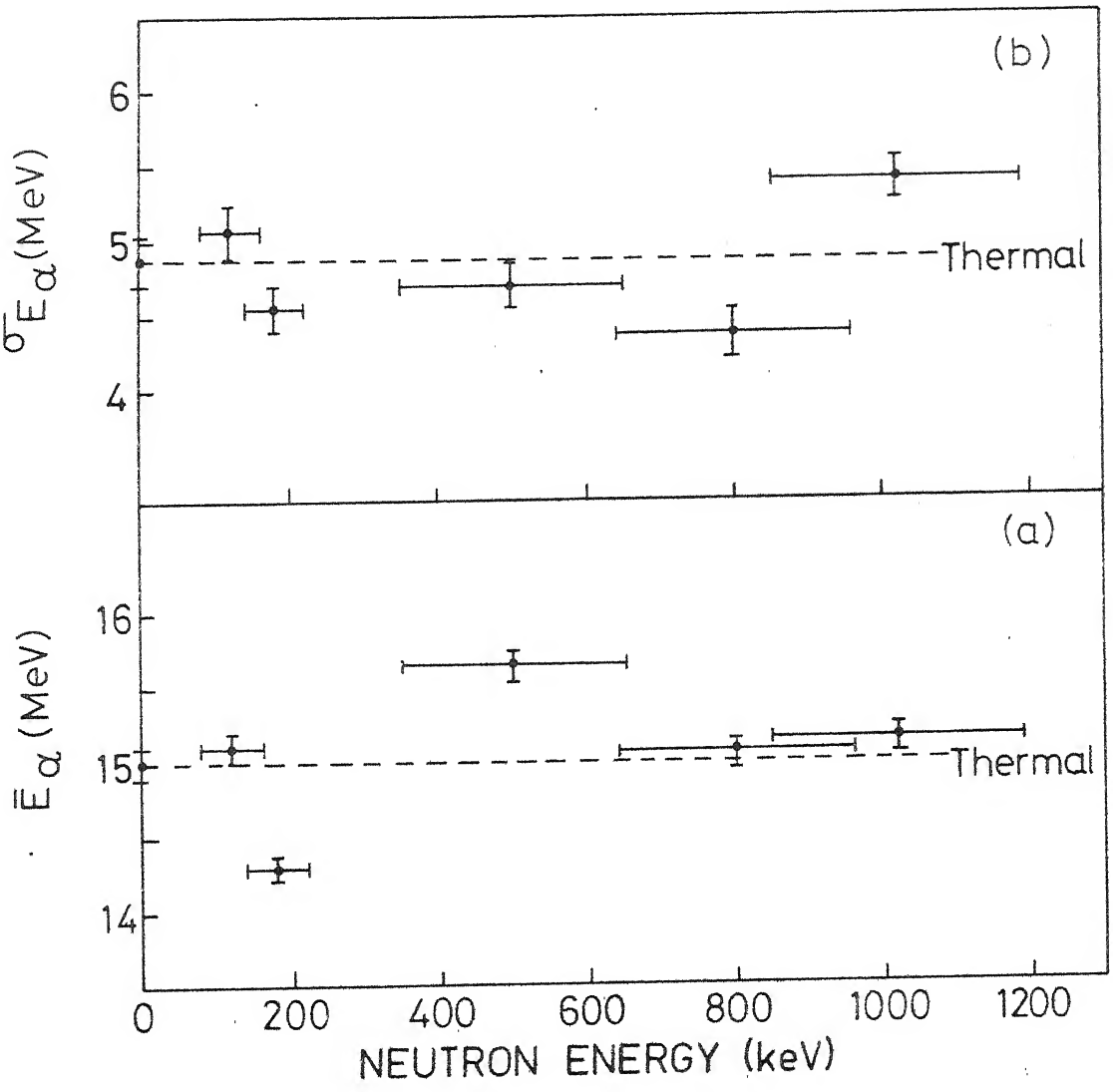

Fig. 4.2. Variation of (a) the average alpha energy ($\bar{E}_\alpha$) and (b) standard deviation (σ_{E_α}), with neutron energy.
(^{235}U fission)

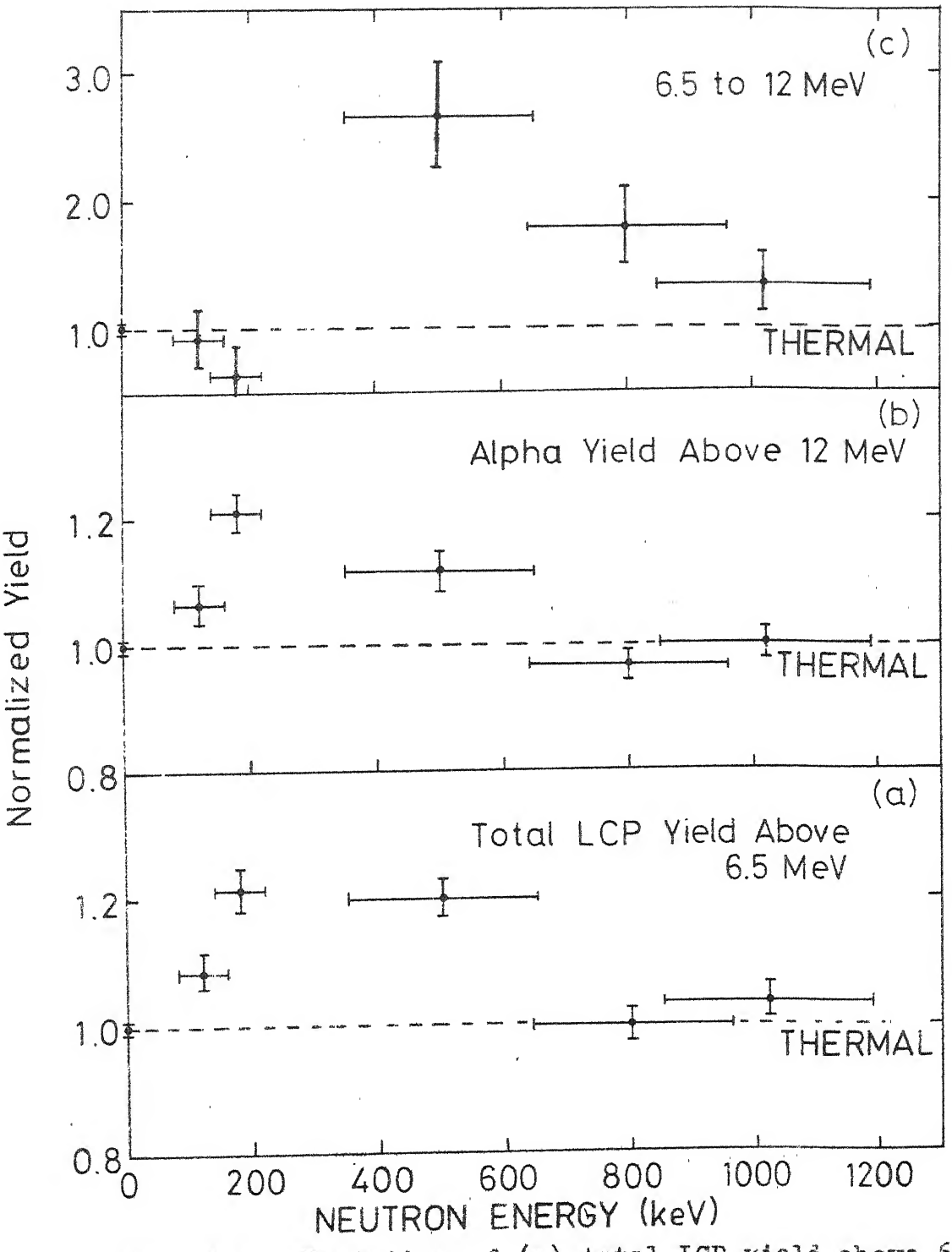

Fig. 4.3. Variation of (a) total LCP yield above 6.5 Me
(b) alpha yield above 12 MeV and (c) LCP yiel
between 6.5 and 12 MeV, with neutron energy.

(^{235}U fission)

contributions from both LRA and other light particles, the majority of which would be tritons (Table 1.1). Assuming that above 12 MeV the contribution to LCP yield is only due to LRA, an attempt has been made to estimate the yields of LRA and 'tritons' separately.

The observed LRA yield for $E_{LCP} > 12$ MeV as a function of neutron energy is shown in Fig. 4.3 (b). There is an increase of about 20% in the energy region 200 to 500 keV similar to the LCP yield results. At higher neutron energies the yield is the same as that for thermal energies. Beyond 1 MeV this yield has been measured (Nadkarni and Kapoor, 1970) and found to be equal to the thermal value within the limits of error.

The yield in the energy region $6.5 < E_{LCP} < 12$ MeV has contributions from both LRA and 'tritons'. To estimate the yield of 'tritons' alone, the low-energy tails of the Gaussian fits to the spectra have been subtracted from the observed yields to give the 'triton' yield. The extracted 'triton' yield for different neutron energies is shown in Fig 4.3(c). For neutron energies around 200 keV this yield is equal to the thermal value but it shows a significant increas (2 - 2.5 times) over the thermal value, around 500 keV. Beyond 500 keV the yield decreases but is always higher than the thermal value.

4.2 ^{239}Pu fission

The LCP energy spectra in thermal and fast fission are shown in Fig. 4.4. The continuous curves represent the Gaussian fits. Since the out-off in this case was larger than in the ^{235}U runs (see section 3.2) the lower limit of the spectra are shifted towards the high energy side. The fits were obtained in the same manner as before, setting the lower limit of the fitting function at 12 MeV.

The most probable energy ($\bar{E}_\alpha$) and the standard deviation (σ_{E_α}) as a function of neutron energy (Table 4.2) are shown in Fig. 4.5. As in ^{235}U fission, the average energy and width do not vary significantly with neutron energy and the values are very close to the thermal value. There is, however, an indication of a drop in $\bar{E}_\alpha$ ($\sim$0.7 MeV) in the region 250 to 300 keV.

The results on LCP and alpha yield (Table 4.2) shown in Fig. 4.6(a), indicate that the variation of yield in this case is not similar to or as pronounced as in the case of ^{235}U fission. The alpha yield increases slightly ($\sim$7%) around 250 keV, 600 keV and 1 MeV. One point to note is that the alpha yield shows a drop ($\sim$14%) in the range 250 to 300 keV. In the other regions of neutron energy the yield is equal to the thermal yield.

Since the low-energy cut-off was large ($\sim$8 MeV), the low-energy yield data could not be obtained and a part

Table 4.2

Average LRA energies, widths and Normalized Yields (^{239}Pu fission)

Neutron Energy (keV)	$\bar{E}_\alpha$ (MeV)	σ_{E_α} (MeV)	LCP Yield >9 MeV	LRA Yield >12 MeV	'Triton' Yield 9 to 12 MeV
THERMAL	16.0 ±.1	4.61±.1	1.0 ±.03	1.0 ±.03	1.0 ±.1
140±30	15.6 ±.09	4.59±.1	0.98±.03	0.99±.03	0.24±.05
175±30	16.03±.1	4.25±.1	1.02±.03	1.0 ±.03	2.5 ±.49
200±30	15.79±.18	5.04±.1	1.06±.04	1.04±.04	1.19±.24
265±30	16.44±.1	4.41±.1	1.08±.03	1.07±.04	3.5 ±.86
300±30	15.63±.1	4.76±.1	0.97±.03	0.93±.03	2.0 ±.43
575±100	15.87±.12	5.31±.1	1.04±.03	1.08±.03	0.29±.05
790±115	15.48±.11	4.93±.1	0.97±.03	1.01±.03	0.07±.02
990±130	15.82±.14	4.73±.1	1.02±.04	1.07±.04	0.31±.08

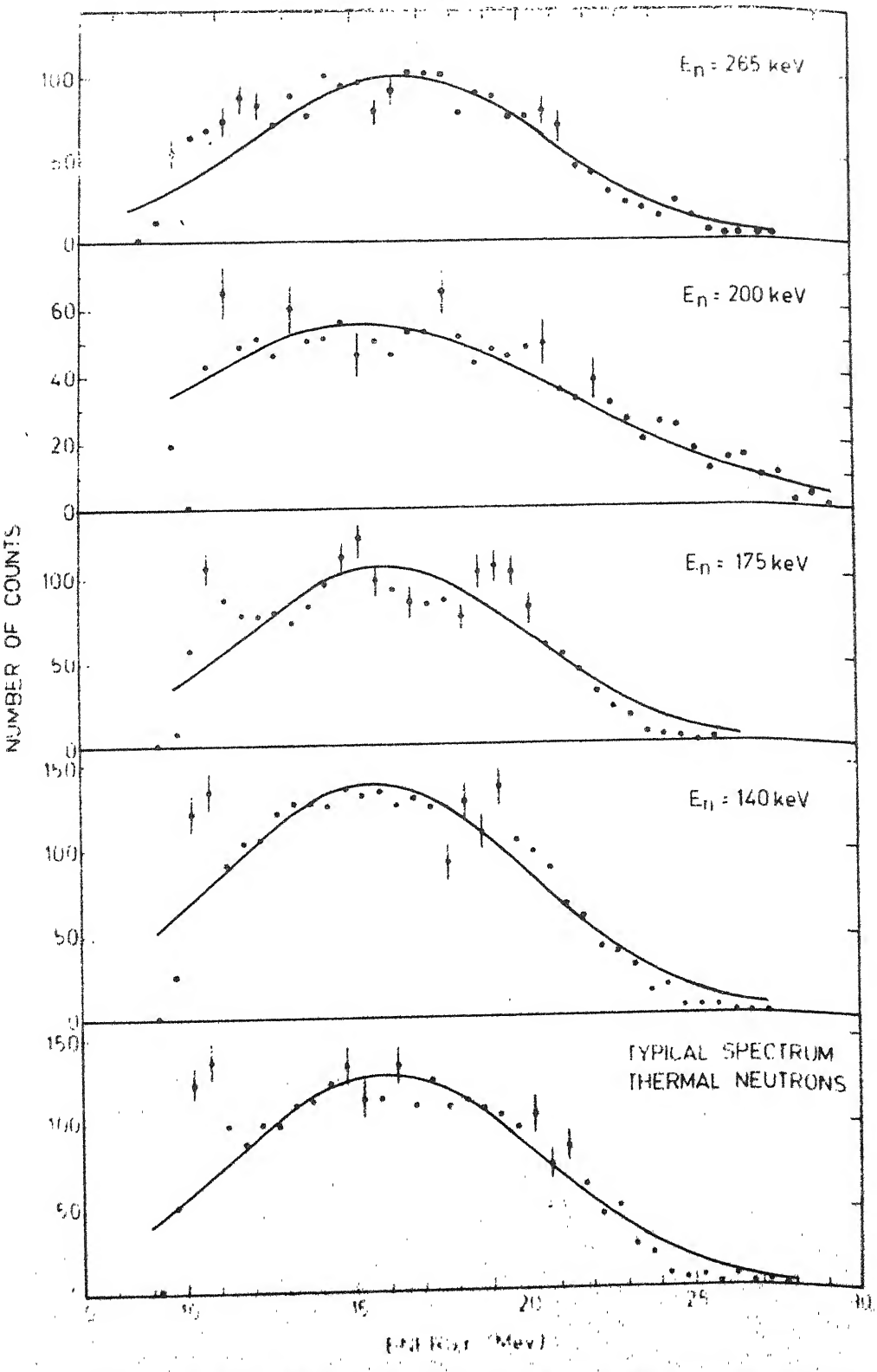

Fig. 4.4. The LCP energy spectra for various neutron energies.
(^{239}Pu fission)

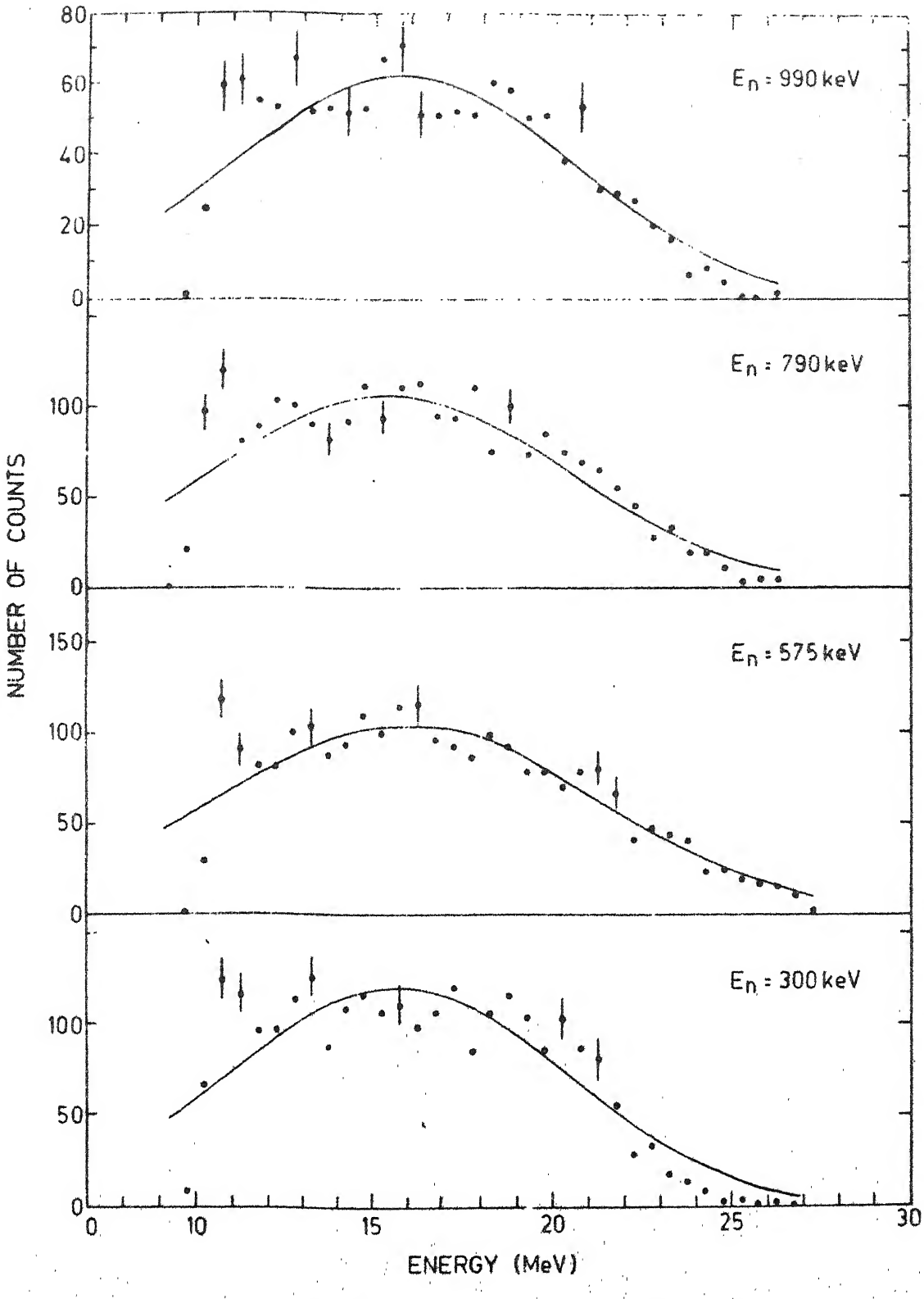

Fig. 4.4. (Contd.) The LCP energy spectra for various neutron energies.

(^{239}Pu fission)

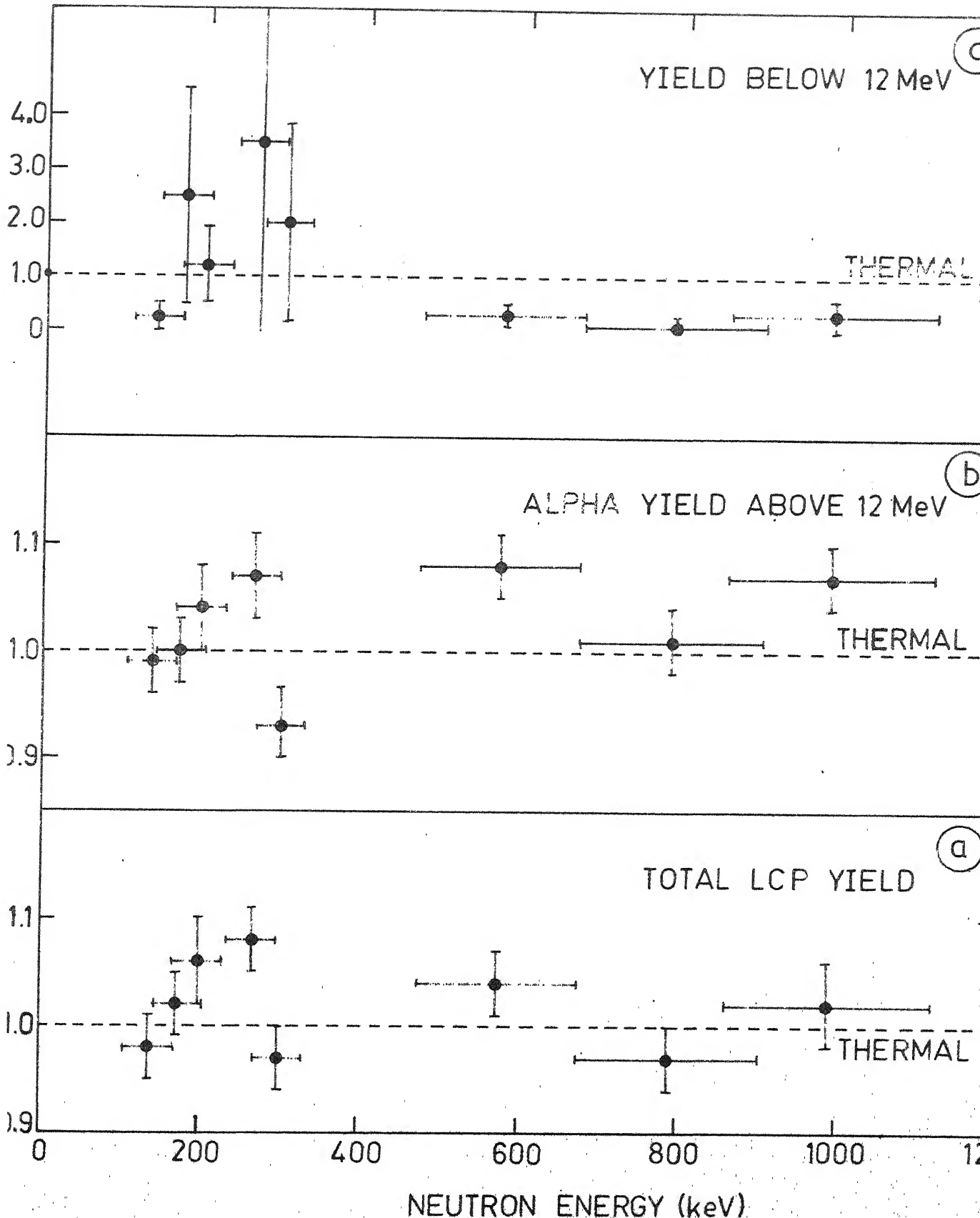

Fig. 4.6. Variation of (a) total LCP yield above 9 MeV (b) alpha yield above 12 MeV and (c) LCP yield between 9 and 12 MeV, with neutron energy.

(^{239}Pu: fission)

of the 'triton' spectrum was lost. Hence the results on 'triton' yield have a large statistical error as indicated. [Fig. 4.6 (c)]. The results indicate that, within the limits of error, the yield upto 500 keV is almost equal to the thermal value. However, one observes that there is an indication that the average yield in the region 200 to 350 keV is larger than the thermal value. Beyond 500 keV the yield drops below the thermal value unlike the ^{235}U results where the 'triton' yield was above the thermal value in the entire region beyond 200 keV. This decrease in 'triton' yield is not apparent in the total LCP yield because the 'triton' emission probability is an order of magnitude lower than that of LRA.

4.3 Discussion

4.3.1 LRA yield

The increase in LRA yield for ^{235}U fission in the neutron energy region 200 to 500 keV cannot be attributed to any excitation energy dependence of LRA yield since the change in compound nucleus excitation energy is very small and the observed yield does not vary monotonically with neutron energy, moreover, beyond 1 MeV previous measurements (Nadkarni and Kapoor, 1970) have shown that the yield levels off to the thermal value. Thus the increase in LRA yield around

200 keV may be associated with the increase in relative number of fissions proceeding via the even parity states populated by the p-wave interaction at these energies. Since the positive parity states lie lower ($\sim$0.6 MeV) than the negative parity states, the extra energy available at the saddle point in p-wave fission can go into the degrees of freedom such as deformation, kinetic energy of relative motion of the fragments, fragment excitation or into LCP emission. In binary fission Blyumkina et al. (1964) and others have observed a drop in average kinetic energy of the fragments and an increase in the number of prompt neutrons at these neutron energies as compared to thermal energies. The higher LRA yield observed in this energy region indicates that the extra energy may also be available for LRA emission. At higher energies higher l-waves contribute to the fission cross-section and this may result in the averaging out of channel effects resulting in an LRA yield equal to the thermal value.

Fluss et al. (1972) had measured the triton and LRA yields in neutron induced fission of ^{235}U in the range thermal to 700 keV. They used both radiochemical and particle identifier methods. Their results indicate a trend of decreasing LRA yield with increasing neutron energy, however, the yield in the entire region was close to the thermal value of 2×10^{-3} per fission. No structure was observed in this region. They had remarked that the reproducibility of their results was poorer than the counting uncertainty ($\sim$5%).

They had also claimed that their data on σ_{E_α} indicated a broadening of the spectra at 380 keV, however, an examination of their spectra does not indicate this.

It is not possible to explain the structure in the ^{239}Pu LRA yield in as clear terms especially the small increases in the 200 keV, 800 keV and 1 MeV regions. However, the drop in yield between 250 and 300 keV may be explained in terms of the domination of the p-wave interaction in this region. Fission induced by p-wave neutrons would take place via negative parity states eg. 1^- state, which lies higher (Lynn, 1968) than the 0^+ ground state. This means that the energy which was available for LCP emission is 'reduced' and this is reflected in the drop in yield as also in the drop in average alpha energy in this energy region. In the region beyond 350 keV various partial waves would contribute to the fission cross section and the variation in yield possibly reflects the result of the admixture of states through which fission takes place.

It is therefore clear that since there is no monotonic increase in yield with neutron energy, the structure in yield cannot be due to a dependence on compound nucleus excitation energy. The observed structure in $\bar{\nu}$ and $\bar{E}_F$ in this region for ^{235}U (eg. Blyumkina et al., 1964) has been explained in terms of channel effects and there is indication that the LRA yield also reflects these channel

effects. More accurate measurements with better neutron energy resolution would have to be carried out in order to establish this result more firmly. However, decreasing the thickness of the neutron target or reducing the solid angle; in order to improve neutron energy resolution, would reduce the count rates considerably and each spectrum which was collected over a few days would perhaps take weeks.

4.3.2 'Triton'yield

The method used to extract 'triton' yields is far from satisfactory and since the low-energytails of the spectra could not be obtained, especially in the case of ^{239}Pu, there are large errors in the estimates of this yield. However, some points are worth noting. The first is that the variation in 'triton' yield is quite different from that of LRA yield indicating that the emission mechanism may be different in the two cases. The second point is that this yield shows a distinct increase, outside the limits of the estimated errors, around 500 keV in the case of ^{235}U. Whether an increase exists for ^{239}Pu around 300 keV or not would have to be established by further measurements (in which the out-off is lower). In the 500 keV region both p and d-waves contribute to significant extents hence no clear picture based on channel effects is possible.

The results of Fluss et al. (1972) on triton yield indicate that the yield for the entire region from 170 to 700 keV is about 2 to 2.5 times the thermal value. However, their data indicate some structure at 350 keV (particle identifier method shows a decrease of ~20%) and at 700 keV (radiochemical method shows an increase of ~50%) about the straight line which can be drawn through their data points. The two methods they used, radiochemical and particle identifier, do not complement each other in the entire neutron energy range and where they do overlap the results (specifically the decrease at 350 keV) are not consistent. They had remarked that their data were not sufficiently precise to establish the energy dependence of the yields they observed.

In order to establish the structure in 'triton' yield more accurate measurements using ΔE-$\bar{E}$ systems for particle identification are being carried out.

4.3.3 Comparison of ^{235}U and ^{239}Pu results

The results on the variation of average energies and widths indicate that there is no significant difference between the two cases. The average energies are equal to the thermal values within error except in the region around 200 to 300 keV where there is indication of some structure.

The total LCP yields indicate some difference especially in the region 200 to 500 keV but since the 'triton'

yields in ^{239}Pu have large errors, any comparison of the total LCP yield or 'triton' yield may not be justified. However, the LRA yields in the two cases show clear differences. The LRA yield beyond 500 keV in ^{235}U levels off to the-thermal value , whereas in ^{239}Pu it is on the average more than the thermal value. The ^{235}U LRA yield indicates a fairly smooth variation from 200 to 600 keV whereas in ^{239}Pu the yield shows structure (~7%) in this region. In the region below 200 keV the yield variations are identical. Cuninghame et al. (1961, 1964) had expected the mass asymmetry in binary fission to show opposite behaviour in these two cases (below 200 keV) but their experiments indicated an essential similarity in the two cases.

The difference in structure in the entire region beyond 200 keV cannot be correlated with the parities of these nuclei, that is, since their parities are different one would expect opposite effects in LRA yield. It is observed, however, that in the region 200 to 350 keV the ^{239}Pu LRA yield indicates a drop to below thermal values which is opposite to that observed in ^{235}U. In this region therefore, the opposite parities of these two nuclei seem to manifest themselves. In the region beyond 350 keV the specific level schemes of these two nuclei and the effect of higher l-waves contributing to the fission cross-section could possibly account for the difference in variation of LRA yield.

CHAPTER V

TRAJECTORY CALCULATIONS

5.1 Introduction

The method of trajectory calculations has been extensively used to study of the scission configuration. This method consists of following the motion of the fragments (the trajectories) after scission. During this period the fragments accelerate under the influence of their mutual Coulomb fields and the initial conditions of their motion would be given by the state of the nucleus at scission eg. the extent of stretching (hence the initial separation), initial kinetic energy etc. The final conditions of this motion would correspond to experimentally measurable quantities such as kinetic energies, angular distributions etc. Therefore, if the connection between the initial conditions and the final quantities was established, it would be possible to obtain quantitative information on the state of the fissioning system at scission.

The calculation of these trajectories has been carried out classically using a limited but representative choice of initial conditions, and the main features of the final conditions of motion, such as average energies and

angles have been reproduced. The method used in such calculations is as follows: a set of conditions are chosen to describe the scission configuration and using these as the initial conditions of motion the trajectories are calculated. The 'final' configuration is the one obtained after the lapse of a sufficient period of time at the end of which the fragments are well separated and the Coulomb interaction is consequently very small ($\sim$1% of the original value). These 'final' conditions are compared with experimental results and the intial conditions are modified until a set of initial conditions are obtained which produce 'final' conditions which are in good agreement with experimental results. This procedure has a limitation - the derivation of such a set of initial conditions only indicates that at a given moment the kinematical variables of the system coincide with these initial conditions; however, they may not coincide with the values of the kinematical variables at the moment of scission. In order to obtain information on the moment of scission, the 'earliest' set of initial conditions which produce satisfactory final conditions should be obtained. It is apriori not obvious that an 'earliest' set of initial conditions can be found (except for the trivial one corresponding to zero kinetic energy) from an examination of the experimental distributions. This ambiguity in localizing the 'moment of scission' in time is an inherent feature in such calculations. It is therefore not

surprising that such calculations when carried out for binary fission produced a large number of sets of initial conditions, all of which could produce satisfactory final conditions. However, in the case of ternary fission (eg. LRA fission) this ambiguity can be reduced because of the nature of ternary alpha emission. The angular distribution of the alpha particles is very sharply peaked perpendicular to the fission fragment direction (Titterton, 1951) indicating that the alpha particle is emitted from the region between the fragments when they are still close together, at the moment of scission (Tsien, 1948). [A very small fraction of alpha particles are emitted from the fragments diametrically opposite to those emitted from the neck (Piasecki et al., 1970). It has however, not been established that these 'polar' alphas are emitted at the instant of scission.] . This rather accurate localization of the moment and point of emission of the alpha particle would help fix the moment of scission with less ambiguity. It is for this reason that the alpha particle represents a powerful tool for the study of the scission configuration.

A large number of experiments have been carried out in which certain features observed in normal binary fission have been compared with the same features in LRA fission. The main conclusion reached from such comparisons (eg. Fraenkel, 1967) is that, LRA fission has all the essential

characteristics of binary fission except for alpha particle emission. It is therefore believed that the scission configuration as obtained from a study of LRA fission would represent the general characteristics of the scission configuration for normal binary fission too.

The assumptions made in such calculations are that

(i) the scission configuration defines the initial conditions of the three-body motion, that is, a fissioning nucleus is practically simultaneously separated into three bodies and the state of motion of the whole system, induced by the preceeding nuclear interactions, develops under the influence of the Coulomb force only.

(ii) non-relativistic classical mechanics and electrostatics provide the necessary theoretical basis for the calculations.

The motion of the three-particles cannot be calculated in closed form hence the trajectories are computed numerically.

5.2 Approximations

For such a three-body calculation there are 18 variables, for each of the three particles there are three spatial variables describing the position of each particle and three conjugate momenta. The condition of conservation of linear and angular momenta reduce the number of independent variables to 12. Since the fragments are confined

to the fission axis the number of independent variables reduces to 10.

In order to simplify the calculation, the number of dynamical variables used to describe the system must be small. The minimum number of variables (as described above) is obtained when no internal degrees of freedom are allowed. The three particles may be assumed to behave like point charges - the point-charge approximation. Strictly speaking, the particles should not be taken as points because they have nonspherical spatial extension over which their charge is distributed. The effect of the charge distribution ought not to be neglected especially at the beginning of motion when the fragments are highly deformed. These charge distributions change with time as the deformation changes. An attempt has been made to study the effects of deformation, this will be discussed later.

The point-charge approximation effectively anulls the effect of higher multipoles on the fragment fields; hence it would be necessary to estimate the error involved in using this approximation. For this purpose the fragments are taken to be prolate ellipsoids and a calculation of the effect of the dipole and quadrupole interactions in comparison with the monopole interaction is used to estimate the error involved. The potential due to a prolate ellipsoid of charge Ze at (r,θ) is given by

$$V(r,\theta) = 3Ze \sum_{n=0}^{\infty} \frac{(a^2-b^2)^n \, P_{2n}(\cos\theta)}{(2n+1)(2n+3)r^{2n+1}}$$

where only symmetric deformations are considered and 'a' and 'b' denote the major and minor axes of the ellipsoid. If R_o is the radius of an undeformed sphere of the same volume, then

$$\pi ab^2 = \pi R_o^3$$

and the eccentricity can be defined as

$$\varepsilon^2 = \frac{a^2-b^2}{R_o^2}$$

thus

$$V(r,\theta) = \frac{3Ze}{R_o} \sum_{n=0}^{\infty} \frac{\varepsilon^{2n} \, P_{2n}(\cos\theta)}{(2n+1)(2n+3)(r/R_o)^{2n+1}}$$

considering terms till n=1 i.e. only till the quadrupole term

$$V(r,\theta) = \frac{3Ze}{R_o} \left[\frac{1}{3(r/R_o)} + \frac{\varepsilon^2}{15} \frac{P_2(\cos\theta)}{(r/R_o)^3} \right]$$

The first term is the monopole term

$$V_{mono} = \frac{Ze}{r} \quad \text{and} \quad E(r) = \frac{Ze}{r^2}$$

This field induces a dipole moment in the other fragment, that is, it polarizes the other fragment. The force on

each charge is therefore

$$F = eE = \frac{Ze^2}{r^2}$$

Since each charge is bound under the action of this restoring force

$$F = \frac{Ze^2}{r^2} = -mw_o^2x$$

where m is the mass of the charge and w_o is the frequency of oscillation about equilibrium. Hence the induced dipole moment is

$$p = ex = \frac{Ze^3}{mw_o^2r^2}$$

$$\therefore \quad w_o = \sqrt{\frac{Ze^2}{mr^2x}} = \sqrt{\frac{k}{m}} \quad \text{where} \quad k = \frac{Ze^2}{r^2x}$$

For a fragment with Z charges

$$w_o = \sqrt{\frac{Z^2e^2}{r^2xM}}$$

where M is the reduced mass of the oscillating system and is equal to one fourth the fragment mass. From the location of giant dipole resonances in those nuclei which have such masses it is known that (Halpern, 1963)

$$\hbar w \approx 15 \text{ MeV} \quad \therefore \quad k = \frac{225}{\hbar^2/M} = \frac{Z^2e^2}{r^2x}$$

with $\frac{h^2}{M} \approx 4/3$ MeVf^2; $\frac{Z^2e^2}{r^2} \approx 160$ MeV, r $\approx$20 f

$$x = 1/20 \text{ f}$$

The energy stored in this polarization is $1/2kx^2$ which is about 0.2 MeV. Since the initial potential energies for r = 20 f are of the order of 100 MeV the contribution due to the induced dipole moment is less than 1% of the monopole potential and can hence be neglected.

The second term corresponds to the quadrupole moment of the fragment. Clearly, for undeformed spheres $\varepsilon=0$ and this term does not contribute. However for $\varepsilon\neq0$ we have

$$V_{quad} = \frac{Ze\ \varepsilon^2}{5\ R_o} \frac{P_2(\text{Cos } \theta)}{(r/R_o)^3} = \frac{Ze}{5} (a^2-b^2) \frac{P_2(\text{Cos } \theta)}{r^3}$$

The quadrupole moment is given by

$$Q = Ze/5\ (a^2-b^2)$$

At a distance 'r' from the centre of the ellipsoid along the axis, the ratio of the quadrupole to monopole potential is

$$\frac{V_{quad}}{V_{mono}} = 1/5 \frac{(a^2-b^2)}{r^2}$$

thus at the centre of the adjacent fragment, r=2a, and

$$\therefore \quad \frac{V_{quad}}{V_{mono}} = \frac{1}{4a^2} \quad \frac{a^2-b^2}{5} = \frac{1}{20}\left[1-(b^2/a^2)\right]$$

for $\varepsilon \approx 0.7$, $(b/a)^2 \simeq 0.6$ for a = 10f and $R \approx 8.5$ f

$$\therefore \quad \frac{V_{quad}}{V_{mono}} \approx 0.02$$

Thus the interaction energy between the fragments is $\sim 4\%$ greater than it would be if the quadrupole moments were ignored. The alpha particle is released midway between the fragments i.e. $r \approx a$, hence V_{quad}/V_{mono} is four times the value at the centre of the fragments. Hence the potential the alpha particle sees is about 1.1 times that seen without quadrupole effects. Since the alpha particle moves away quickly it would see an effective time average of the quadrupole moment close to the original value. In view of the smallness of the induced electric dipole and quadrupole moments the effect of higher multipoles can be neglected. These results are similar to those obtained by Halpern (1963). To keep the calculation of trajectories simple it is therefore justifiable to consider the fragments and alpha particle as point sources of their Coulomb fields. It must be pointed out that even in the point-charge approximation the fragments are considered to have a size, in the sense that if the alpha particle, in the course of its motion, happened to come within a distance of $\sim$8f from the fragment centre it was considered to be absorbed.

The second major approximation is that of restricting the motion of the three particles to a plane, that is, the calculation is two-dimensional. The justification for this assumption lies in the fact that most experimental measurements on alpha emission are made in a plane, that is, the fragment and alpha particle detectors are normally placed in a plane. Hence a comparison of experimental results with the results of trajectory calculations using the two-dimensional approximation would be meaningful. Halpern (1963) had carried out calculations of alpha particle trajectories in three dimensions and the results, for example, on energy and angular distribution of alpha particles, compare very well with a large number of subsequent calculations (eg. Boneh et al., 1967) using the two-dimensional approximation. Thus the restriction to two-dimensions would be a justifiable approximation. Using this approximation the number of independent variables necessary to describe the three-body motion reduces to seven.

5.3 The motion of the fragments and alpha particle

The motion of the three particles under the influence of their mutual Coulomb fields are calculated numerically. The equations of motion are (Boneh et al., 1967)

$$\frac{dX_{ij}}{dt} = U_{ij} \quad \text{and} \quad m_i \frac{dU_{ij}}{dt} = F_{ij}$$

where X_{ij} is the j th coordinate if the i th particle, U_{ij} is the j component of velocity U_i and F_{ij} is the j component of the force F_i acting on the i th particle of mass m_i. These equations are replaced by difference equations :

$$X_{ij}^{n+1} = X_{ij}^{n} + U_{ij}^{n} \Delta t$$

$$U_{ij}^{n+1} = U_{ij}^{n} + \frac{1}{m_i} F_{ij}^{n+1} \frac{\Delta t}{2}$$

where $$U_{ij}^{n} = U_{ij}^{n} + \frac{1}{m_i} F_{ij}^{n} \frac{\Delta t}{2}$$

is the average or intermediate velocity and is used to improve the accuracy of the calculation. F_{ij}^{n} is the j compoment of the force acting on the i th particle at position $\vec{X}_i^n$

$$\vec{F}_i^n = e^2 Z_i \sum_{k=1}^{2} Z_k \frac{\vec{X}_i^n - \vec{X}_k^n}{\left|\vec{X}_i^n - \vec{X}_k^n\right|^3}$$

The subscript k refers to the other two particles, and the superscript n refers to the value of the parameter after the n th time interval.

The time interval is chosen such that when the particles are close together, that is, just after scission and the forces are rapidly changing; it is small and when the particles are far apart their directions etc., are slowly changing; the intervals are relatively larger. Such a procedure ensures

that uniform accuracy is maintained at all stages of the dynamical process succeeding scission. The total time t_n after n intervals is given by

$$t_n = t_o e^{na}$$

hence the size of the n th interval is

$$t_n = t_n - t_{n-1} = t_o(e^{na} - e^{(n-1)a})$$

$$= t_{n-1}\,(e^a - 1)$$

Thus 't_o' determines the time scale and 'a' determines the rate of exponential growth. Roughly 't_o' determines the accuracy at the beginning of the trajectory (t=0) and 'a' determines the accuracy towards the end ($t=\infty$). The parameters 't_o' and 'a' are so chosen that the accuracy remains more or less constant during all intervals. For the present calculations the choice was

$$t_o = 10^{-22} \text{ sec} \quad \text{and} \quad a = 0.1$$

The calculation was terminated after 81 time intervals, that is, after 3.3×10^{-19} sec by which time the distance between the particles would be $\sim 10^2$ times their initial distance and hence the potential $\sim 10^{-2}$ times the initial value. The final energies are given by

$$E_i(t_n) = \sum_j 1/2\; m_i [v_{ij}(t_n)]^2$$

and the angle the alpha particle makes with the fission axis is

$$\theta_\alpha(t_n) = \tan^{-1} \frac{v_y^\alpha (t_n)}{v_x^\alpha (t_n)}$$

The calculation rigorously conserves linear and angular momentum of the system. The maximum percentage error in value of total energy after 81 time intervals was estimated to be $\sim .15\%$.

5.4 Choice of variables

The seven initial dynamical variables used to describe the scission configuration are shown schematically in Fig. 5.1. They are :

(i) The mass ratio $R = m_H/m_L$ which is approximately equal to the charge ratio. However, the charges were determined using the relations (Mukherji, 1969)

$$Z_H = M_H/2.587 \quad \text{and} \quad Z_L = Z_{tot} - Z_H$$

Z_{tot} is the charge of the nucleus minus the charge of the alpha particle. The present calculations are for the nucleus $^{252}_{98}Cf$ and thus $Z_{tot} = 96$.

(ii) The line joining the two fragments is defined as the fission axis (x-axis) and the origin is the zero field point. The x coordinates of the fragments are inversely proportional to their charges except for the correction

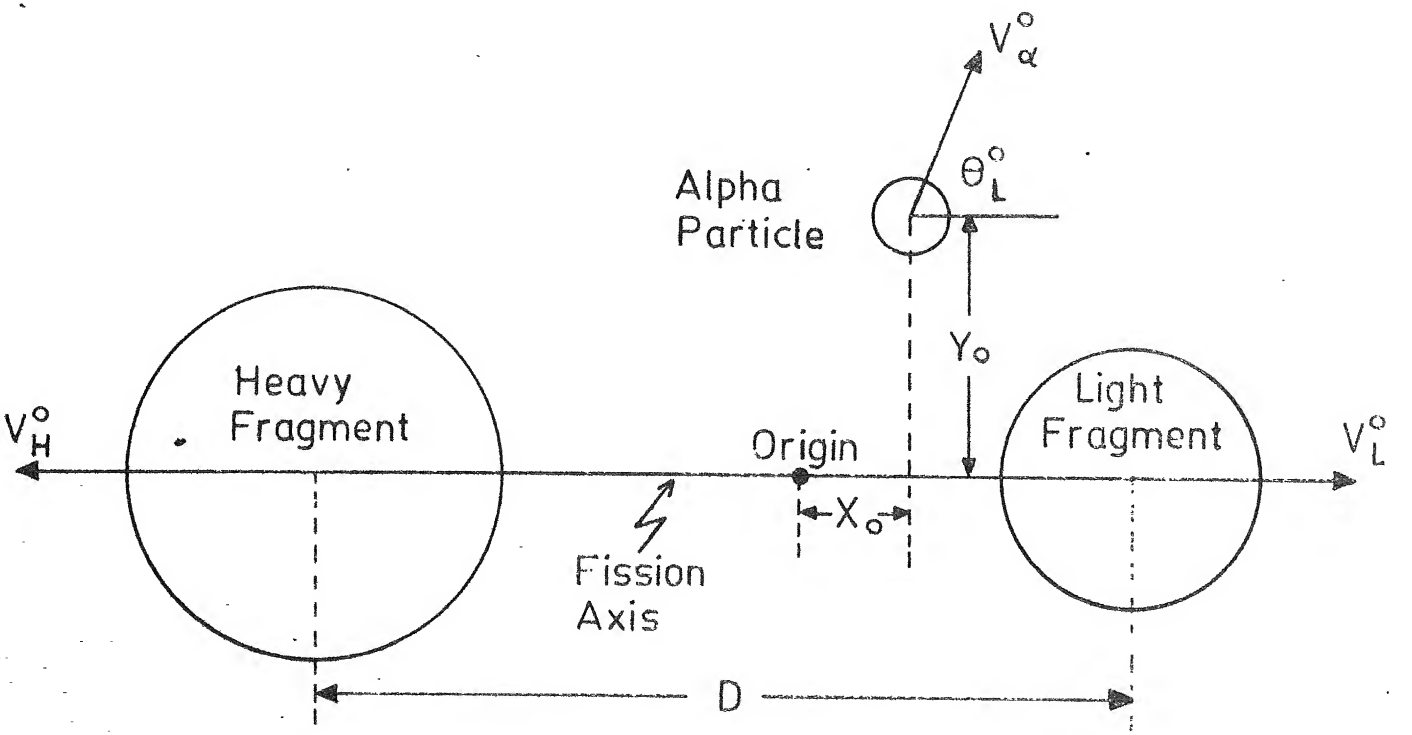

Fig. 5.1. Schematic diagram of the initial parameters of the calculation

introduced due to the alpha particle. The coordinates are denoted by D, the separation between the charge centres of the fragments.

(iii) The x coordinate of the alpha particle X_o

(iv) The y coordinate of the alpha particle Y_o, which indicates that the alpha particle is created off the fission axis at a distance Y_o.

(v) The initial velocities of the fragments in the y direction are zero since their motion is confined to the fission axis and the velocities along the x axis, v_L^o and v_H^o are combined to give the intial total fragment kinetic energy, E_F^o.

$$E_F^o = 1/2(m_H v_H^{o\,2} + m_L v_L^{o\,2})$$

(vi) The initial energy of the alpha particle, E_α^o.

$$E_\alpha^o = 1/2\, m_\alpha\, v_\alpha^{o\,2}$$

(vii) The initial angle between the direction of motion of the alpha particle and the direction of motion of the light fragment, θ_L^o.

In most calculations the choice of dynamical variables is the same as the one used here. However, some calculations have used t, the time of emission of the alpha particle, as a variable. This is equivalent to a different choice of initial

velocities for the fragments or alternatively a different separation between them.

5.5 Review of previous calculations

The calculations that have been made so far can be divided into two categories: the ones whose initial conditions lend support to the predictions of the statistical theory of fission (Fong, 1969) and those whose intial conditions support the predictions of dynamical theories such as the adiabatic model or sudden snap model (Halpern, 1963, 1965, 1971). Broadly speaking the statistical model demands that the initial energies be low ($\sim$1 MeV) for the fragments and $\sim$0.5 MeV for the alpha particle) whereas the adiabatic model predicts large values for the initial energies ($\sim$30 to 40 MeV for the fragments and $\sim$3 MeV for the alpha particle). The former condition implies that at scission the particles are almost at rest whereas the latter implies that at scission the particles are already moving with a considerable fraction ($\sim$20%) of the final velocities. One general similarity in a large majority of these calculations is that most of the initial variables had fixed starting values and the final values (distributions) were generated by varying one or two of these variables. These calculations are briefly reviewed below (see also Feather, 1969; Asghar et al., 1971; Vandenbosch and Huizenga, 1973).

5.5.1 Calculations supporting the Statistical model

According to the statistical theory, the fission fragments have about 0.5 MeV initial kinetic energy at the moment of scission associated with their three degrees of freedom. Hence for the alpha particle a value of 0.5 MeV is chosen as its initial kinetic energy (Ertel, 1968). An extreme case of this model would be one where the initial kinetic energies are zero.

Tsien (1948) assumed the initial kinetic energies of the fragments and alpha particle to be zero and discussed their initial coordinates in terms of two parameters; the distance of the alpha particle from the fission axis and parameters defining the change of radii of the fragments as functions of excitation energy. The velocity distribution calculated for the alpha particles emitted in ternary fission of ^{236}U was in agreement with experiment in the high energy region.

Geilikman and Khlebnikov (1965) had performed these calculations using the droplet model. Nuclear deformations upto the α_3 term were considered. The initial alpha energy lay in the range 0 to 2 MeV. The best agreement between the calculated and experimental results, on energy and angular distribution, was observed at an energy E_α^o=1.0 MeV. The significant point about the method used was the

absence of the point-charge approximation. The deformation, however, was assumed to be independent of time, that is, the change in α_2 and α_3 during motion was neglected. The mean values of the final energy and angle agreed very well with experimental results, however, the calculated widths were smaller due to the rapid fall in the distribution at about 18 MeV.

Ertel (1968) carried out trajectory calculations using initial energy values of 1 MeV and 0.5 MeV for the fragments and alpha particle, respectively. He was able to successfully reproduce the experimental results (Fraenkel, 1967) on the angular correlation of the alpha particle, that is, the variation of θ_L with R.

Vitta (1970, 1971) used initial energies as predicted by by the statistical theory and was able to satisfactorily reproduce the final kinetic energy distribution. The final angular distribution could be reproduced if delayed emission was assumed. He also obtained the variation of the final alpha kinetic energy and angle with X_o as well as its (E_α) variation with initial kinetic energy.

Fong (1970) extended Ertel's calculations and showed that the angular correlation of the alpha particle obtained for E_α^o below 0.5 MeV was quite different from the experimental results. The also obtained the variation of the alpha energy distribution with R and compared them with

the results of Fraenkel (1967). The effect of assuming that the alpha particle is created off the fission axis ($\sim$3f), on these results was shown to be very small. It was also noticedthat the value of E_α^o was influenced by the choice of X_o, and based on prompt neutron data, the value of 0.5 MeV was found to be appropriate and the point of emission (for R = 1.4) was closer to the heavy fragment (X_o= 12f measured from the centre of the heavy fragment; the zero field point would be at about 15f).

Cavallari et al., (1971) used a range of values for the initial parameters, E_α^o, X_o, Y_o and θ_L^o. These ranges were divided into a number of intervals. The trajectories were computed for fixed R using different sets of initial values selected from these intervals and for 5 different values of E_F^o. Using experimental results (specifically $\bar{E}_\alpha$) they assigned a 'weight' to each trajectory and were thus able to obtain statistical distributions for the initial parameters. These distributions could be obtained only when E_F^o = 0 MeV. The E_α^o distribution showed a strong peak at 0.5 MeV and a weak one around 2 MeV. The X_o distribution indicated that the alpha particle was emitted at the zero field point. The θ_L^o distribution was double peaked. The most probable values obtained by them are given in Table 5.1.

More recently Choudhury (1976) has been able to reproduce the experimental distributions as well as some

Table 5.1

Initial values of calculations supporting the Statistical model

Author	Nucleus	R	E_α^o (MeV)	E_F^o (MeV)	D (f)	Y_o (f)	X_o (f)	σ_{X_o} (f)	θ_L^o	t_o (10^{-21} sec)
Tsien (1948)	^{236}U	1.44	0	0	18	6	a	-	$90^o \pm 20^o$	-
Geilikman, Khlebnikov (1965)	^{236}U, ^{242}Cm ^{252}Cf	1.44	1.0	-	20	0	a	-	-	-
Ertel (1969)	^{252}Cf	1.3, 1.4	0.5	1.0	20	0	a	-	-	-
Vitta (1970)	^{252}Cf	1.4	1.2	0	24.3	0	b	2.2	90^o	0.3
Fong (1970)	^{252}Cf	1-2	0.5	1.0	24	0	a	1.8	-	-
Cavallari et al.(1971)	^{252}Cf	1.33	0.25	0	19.8	0	c	1.5	115^o-165^o	-
Choudhury (1976)	^{252}Cf	1.41	0	0	20.5	1.0	8.5, 13.62	1.47, 2.31	d	-

a:- alpha particle in the region between the two touching fragments; b:- X_o not specified because of delayed emission; c:- zero field point; d:- isotropic.

observed correlations using zero initial kinetic energy for both the fragments and alpha particle. In particular, the observed anticorrelation between the average final fragment kinetic energy and the final alpha energy has also been reproduced.

The results of the calculations which lend support to the predictions of the statistical theory are summarized in Table 5.1.

5.5.2 Calculations supporting Adiabatic models

Halpern (1963) developed the three-point-charge model and computed the energy and angular distribution of the alpha particle in ternary fission of ^{236}U. He estimated the initial alpha energy to be 4.4 MeV from the volume of the neck at scission using the uncertainty principle. The initial angular distribution of the alpha particle was assumed to be isotropic and the final angular distribution was found to be insensitive to the location of the point of emission of the alpha particle and to its initial energy. The average final alpha energy showed appreciable variation with initial alpha and fragment energies. In order to reproduce the observed distribution in alpha energy he concluded that the initial fragment energy had to be about 15 to 20% of the final fragment energy if the initial alpha energy was 4.4 MeV.

Boneh et al., (1967) computed trajectories of the alpha particle in ternary fission of ^{252}Cf using the three-point-charge model in the two dimensional approximation. A 'standard' set of values were chosen for the seven initial parameters. This 'standard' set was obtained from some preliminary calculations. The value of R was chosen to be 1.4 since this is roughly the mean value observed experimentally. The preliminary calculations consisted of the determination of the effect of the variation of one initial parameter on the final values, the other initial values being fixed. Using this standard set they reproduced most of the experimental results of Fraenkel (1967). In order to reproduce the correct widths in angular distribution and the anti-correlation between the final fragment energy and the final alpha energy, they concluded that the initial energies had to be high, that is, $E_\alpha^o \approx 3$ MeV and $E_F^o \approx 35$ MeV. The emission angle of the alpha particle was found to depend principally on the emission point (on the fission axis) and the mass ratio. They had also attempted to calculate the initial distributions using empirical relations connecting various initial and final parameters. Using some of these distributions they could successfully reproduce the experimental angular and energy distributions of the alpha particle. The initial fragment energy distribution was found to be Gaussian with a mean of ~39 MeV and the initial alpha energy

distribution was a Maxwellian dependent on the point of emission of the alpha particle. No unique distribution for X_o could be obtained.

Katase (1968) carried out similar calculations for the fission of ^{236}U and ^{252}Cf. The results of the calculations for ^{236}U were compared with experimental results and the dependence of certain final parameters on initial ones were identified. On this basis empirical relationships between the final and initial angles and between the alpha energy and various initial parameters were obtained. The parameters of the latter expression (about 8 of them) were obtained by a least squares method, that is, the values of the coefficients that gave the best fit to the values of E_α obtained from trajectory calculations, were determined. Using these expressions the final distributions for ^{252}Cf were determined and compared with experiment. The agreement with experiment was good and he concluded that the fragments had about one third of their final energy at scission and the initial alpha energy was about 3 MeV.

Raisbeck and Thomas (1968) obtained a good fit to the experimental kinetic energy spectrum of the alpha particles from ^{252}Cf in terms of a model in which the alpha particle materialises at a point (the zero field point) on the fission axis, at a time 't' after binary fission has occured. At the instant of scission the fragments were

assumed to have zero velocity and the alpha energy was described by a Gaussian distribution. They obtained the best fit with $t = 0.4 \times 10^{-21}$ sec and $E_\alpha^o \sim 2$ MeV. At the instant of emission of the alpha particle the fragments had a mean kinetic energy of ~8 MeV. They had also carried out similar calculations for other light particles such as protons, tritons and ^{6}He in an attempt to determine whether a single set of parameters could account for the energy spectra of these particles. They concluded that the emission mechanism of all light particles was essentially identical.

Blocki and Krogulski (1968), carried out computations for alpha emission in the fission of ^{236}U. Using the sudden approximation i.e. abrupt scission they assumed the fission fragments to be at rest at scission. The initial alpha energy was described by a Maxwellian distribution of the type $E_o^{\frac{1}{2}} \exp(-E_o/T)$ with T = 0.35 MeV. They could reproduce the experimental distributions quite well. The calculations were also used to study the emission of other light particles such as ^{1}H, ^{2}H, ^{3}H, ^{6}He and other heavier particles upto ^{16}O. They concluded that the emission conditions of these nuclei were very similar to those of the alpha particle. In a subsequent calculation (Krogulski and Blocki, 1970) for ^{252}Cf, the effects of the various initial conditions on the final energy and angle were examined. The results led them to conclude that the initial

conditions for the emission of alpha particle, tritons and ^{6}He were quite similar. However, an extremely elongated configuration was needed for the emission of protons and deutrons; which led them to conclude that the emission mechanism for these particle was different from that of alphas for eg. emission from the surface of the fragments instead of from the neck.

Gazit et al., (1971) used trajectory calculations to complement their measurements on ^{236}U fission. Their calculations included corrections for alpha recoil effects. They obtained good agreement with their experimental results.

Musgrove (1971) obtained a set of initial values quite close to those of Boneh et al., The angular distributions he obtained were however, narrower.

Rajagopalan and Thomas (1972) using initial conditions similar to those used by Raisbeck and Thomas (1968) obtained angular distributions which agreed very well with their measurements on angular distribution.

The results of the calculations which lend support to the dynamical theories are given in Table 5.2.

Table 5.2

Initial values of calculations supporting Adiabatic models.

Author	Nucleus	R	E_α^o (MeV)	E_F^o (MeV)	D (f)	Y_o (f)	X_o (f)	σ_{X_o} (f)	θ_L^o	t_o (10^{-21} sec)
Halpern 1963	^{236}U	1.44	4.4	40	27	0.5	b	-	d	1.1
Boneh et al.1967	^{252}Cf	1.4	3	35	26	0	c	-	90°	-
Katase 1968	^{252}Cf	1.3	4.35	63	26.75	0	c	-	90°	-
Raisbeck and Thomas 1968	^{252}Cf	1.33	2	7.5	21.5	0	b	1.5	90°	0.4
Nardi et al.1969	^{252}Cf	1.4	3	28	24	0	c	4	d	-
Krogulski and Blocki 1970	^{252}Cf	1.4	2	40	26	0	c	-	90°	-
Musgrove 1971	^{252}Cf	1.2-1.6	2.75	25	23.7	0	c	2.3	a	-
Gazit et al.1971	^{236}U	1.44	3.4	31	24	2	12	2.6	d	-
Rajagopalan and Thomas 1972 Rajagopalan 1972	^{252}Cf	1.33	2	7.5	21.5	0	b	2.5	90°	0.4

a:- initial angular distribution given by $\cos\theta = P_x/\sqrt{P_x^2+P_y^2}$; b:- X_o not specified because of delayed emission; c:- zero field point; d:- isotropic.

5.6 Present calculations

5.6.1 Motivation

The common feature of most of the calculations that were reviewed in the previous section, is that of assigning a set of fixed values to the initial parameters. Using this fixed set, certain final distributions and correlations have been obtained. In some of these calculations eg. Halpern (1963) and Vitta (1970) the initial set was chosen based on the assumptions or predictions of some model of fission.

The initial set of values used in the calculations supporting the predictions of either the statistical or adiabatic models are quite different, yet they both reproduce final distributions and some correlations quite satisfactorily. The inability to resolve the apparent ambiguity in the initial values could be due to the imposed limitation of choosing essentially fixed values for the parameters, whereas in reality each parameter would have a distribution, however small. This argument is also supported by the fact that in many calculations it was found necessary to assume some small widths for certain initial parameters in order to obtain the correct widths for the final distributions eg. Vitta (1970) had to assume a spread in X_o of about 2f to account for the observed spread in θ_L, similarly Boneh et al., (1967) had to assume certain widths for E_α^o to account for the width in θ_L. The mean values of these

distributions - usually Maxwellian or Gaussian - represent the fixed values. While reproducing the experimentally observed anticorrelation between $\bar{E}_F$ and E_α, Boneh et al., and others used fixed values for the parameters; however, they had remarked that distributions in initial parameters would effect their results. Thus such methods of obtaining final correlations are open to question.

It would therefore appear realistic to begin with a distribution of values for the initial parameters and then attempt to reproduce the final distributions and correlations. The nature of initial distributions obtained this way can then possibly indicate the validity of one of the two models discussed above.

So the method of attack should be to remove all artificial restrictions on the values of the initial parameters and make a model independent calculation. Such a procedure had been adopted by Cavallari et al., (1971). The philosophy of the present calculations is similar. The initial parameters are allowed a range of values covering all regions studied so far. Each value in the range initially has an equal probability of occurance. Furthermore the parameters are initially uncorrelated. These assumptions, in fact represent one extreme choice of initial values, however, they impose no restrictions on the behaviour of the calculated final values.

5.6.2 Choice of values

The range of values for each of the seven parameters, were essentially decided by performing some preliminary calculations (Gadgil, 1973) similar to those done by Boneh et al., (1967). In these calculations all initial parameters were held fixed except one and the sensitivity of the asymptotic values of E_α, E_F, and θ_L etc. to this parameter were checked. A representative set of results of these calculations is shown in Figs. 5.2 (a) to (f). The (fixed) values of all parameters except the one being varied are also indicated. It was seen [Figs. 5.2 (e) and (f)] that for variations in θ_L^o between 40^o and 140^o and Y_o between 0 and 2.5 f; the final values in E_α, E_F and θ_L did not change as significantly as for the variations in other initial parameters. Hence in the subsequent calculations θ_L^o was allowed an isotropic variation between 45^o and 135^o and Y_o was fixed at 0 f i.e. the alpha particle was assumed to be emitted from the fission axis. The assumption on Y_o contradicts the philosophy of allowing all parameters free variation within a range of values, however, since the preliminary calculations and many previous calculations indicated that for Y_o = 0 to 5 f the results were not altered significantly and because of limitations imposed on computing time; such an assumption had to be accepted.

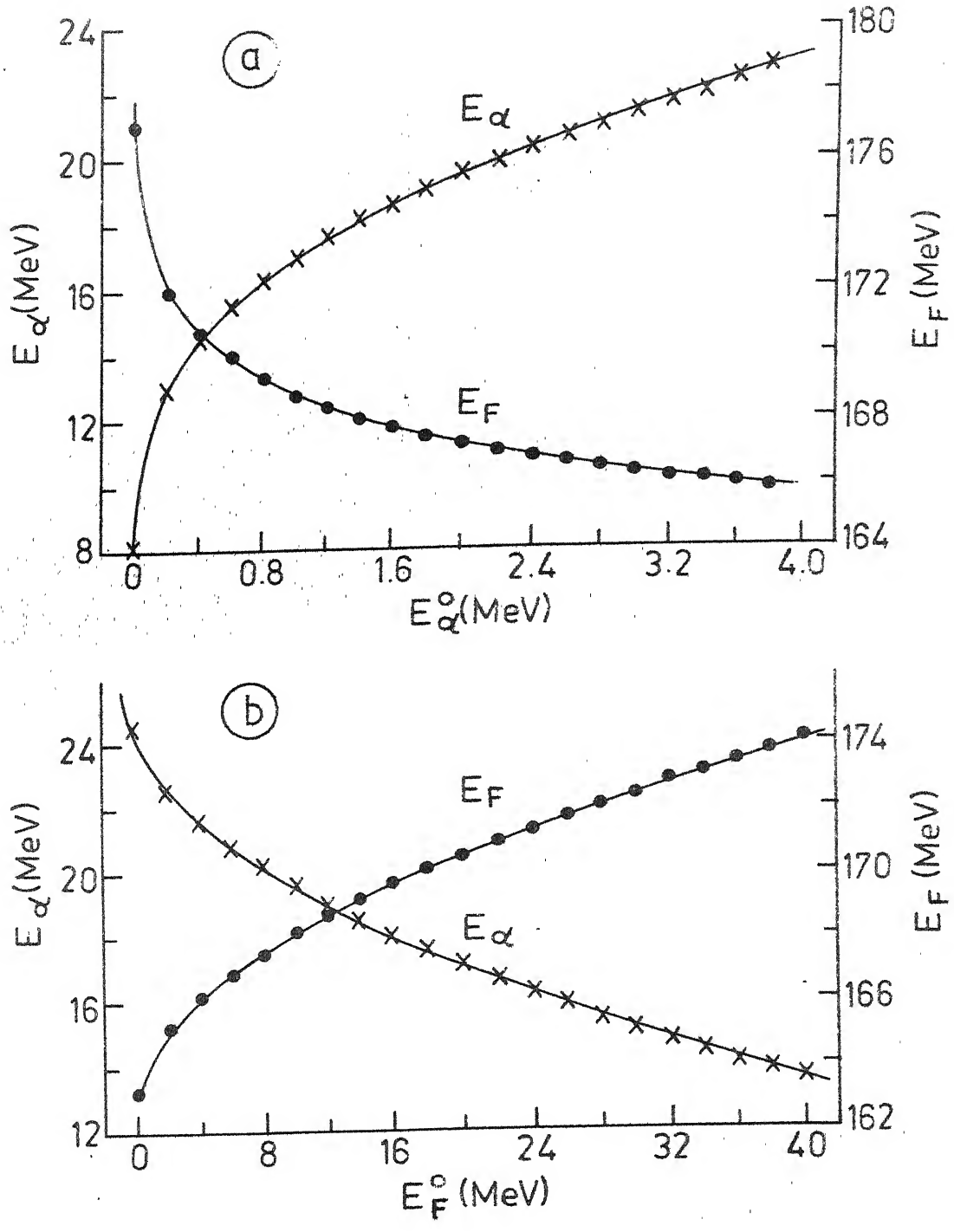

Fig. 5.2. Results of preliminary calculations. Variation of (a) E_α and E_F with E°_α and (b) E_α and E_F with E°_F [with R = 1.1, X_o = 0f, Y_o = 1.0f, Θ°_L = 60°, D = 21.8f and for (a) E°_F = 7 MeV (b) E°_α = 2 MeV.

The other parameters, namely D, E_α^o, E_F^o and X_o were allowed values in the ranges given in Table 5.3. Each range was divided into ten intervals thus allowing each parameter to take any of the ten values. The calculations were perfo-rmed for seven different values of mass ratio (Krishnarajulu and Mehta, 1975).

Table 5.3

The input parameters and their range of values

	Parameter	Symbol	Range of values
1.	Mass ratio	R	1.0 to 1.8
2.	Interfragment distance	D	17f to 28 f
3.	Initial distance of alpha particle from zero field point	X_o	-7.0f to 6.5 f
4.	Initial distance of alpha particle from fission axis	Y_o	0 f (fixed)
5.	Initial alpha energy	E_α^o	0.4 to 4.0 MeV
6.	Initial fragment energy	E_F^o	0.5 to 40 MeV
7.	Initial angle of emission of alpha particle	θ_L^o	35^o to 145^o

5.6.3 Details of calculations

Each trajectory was computed using a set of initial values for the parameters, characterized by a five digit

number - corresponding to the five varying initial parameters R, E_α^o, E_F^o, D and X_o (θ_L^o varied isotropically). It took 0.44 sec to calculate a trajectory on an IBM7044 computer and 70,000 such trajectories were calculated. The five digit number specifying the initial values of the trajectory and the final values of E_α, E_F and θ_L were written on magnetic tape and stored thus enabling subsequent analysis to be performed with relative ease and minimal computer time.

In order to pick out the physically significant trajectories, the final results of each trajectory were compared with experimental distributions and a relative 'weight' was assigned to the trajectory as follows. The experimental distributions in E_α and E_F for different values of mass ratio (Mehta et al., 1973) were used. These distributions were assumed to be Gaussian and were defined by specifying the mean value and the variance of the distributions for various mass ratios. The 'weight' was a product of terms of the type

$$P_x = \exp\left(-|x-\bar{x}|^2/2\sigma^2\right)$$

where $\bar{x}$ and σ^2 are the mean value and variance of the experimental distribution being compared with the calculated value x of the variable (E_α or E_F in the present case). All trajectories with $P \geqslant 0.1$ where $P = P_x P_y$, were used in subsequent analysis.

5.7 Results

5.7.1 E_α and E_F distributions

In order to check the calculations the mean values of the E_α and E_F distributions obtained from the calculations were compared with the experimental ones used in assigning weights. The comparison is shown in Table 5.4.

Table 5.4

Comparison of experimental and calculated values of $\bar{E}_\alpha$, $\bar{E}_F$

R	$\bar{E}_\alpha$		$\bar{E}_F$	
	Exp	Calc	Exp	Calc
1.0	17.5±0.5	17.54±1.03	173 ±1.0	172.85±1.32
1.2	16.0±0.1	16.2±0.98	173.5±0.5	173.29±1.26
1.3	15.95±0.1	16.12±0.98	170.5±0.5	170.39±1.24
1.4	15.95±0.15	16.16±0.98	166.75±0.5	166.87±1.18
1.5	16.0±0.2	16.43±0.98	162.75±0.5	163.99±1.08
1.6	16.05±0.25	16.98±0.88	158.75±1.0	161.70±0.94
1.8*	16.25±0.55	16.94±0.73	152.5±1.0	162.29±1.15

* Statistics were poor for this mass ratio.

As can be seen from the table the agreement is quite satisfactory.

5.7.2 Variation of $\bar{\theta}_L$ with R and the dependence of $\bar{E}_\alpha$ on θ_L

The angular distributions of alpha particles for different values of mass ratio were obtained and were compared with the experimental results of Fluss et al., (1973). These results, for a few values of R, are shown in Fig. 5.3. The agreement is satisfactory indicating the validity of the method used. The variation of the average angle of emission, $\bar{\theta}_L$, with mass ratio, R, is shown in Fig. 5.4. The results are compared with those of Fraenkel (1967) and Fluss et al., (1973). The average angle of emission decreases with increasing mass ratio. This trend of variation is in agreement with experimental results and for R = 1.3 amd 1.4 the actual values are very nearly equal to the observed ones. However, there is disagreement between the calculated and experimental results in the region $1.5 < R < 2$ and also for R = 1.0. This could be due to the inherent experimental inaccuracies in these regions of mass ratio. However, the value of $\bar{\theta}_L \approx 90^\circ$ obtained for R = 1 in the present calculations represents a physically meaningful result since both fragments exert an equal force on the alpha particle it should come out in a direction perperndicular to the fission axis. If one takes into account the recoil due to the emission of the alpha particle - the departure from colinearity is about 4.3° (Fluss et al., 1973) - then the value of θ_L for R = 1 could be about 92°. In the case of large values of

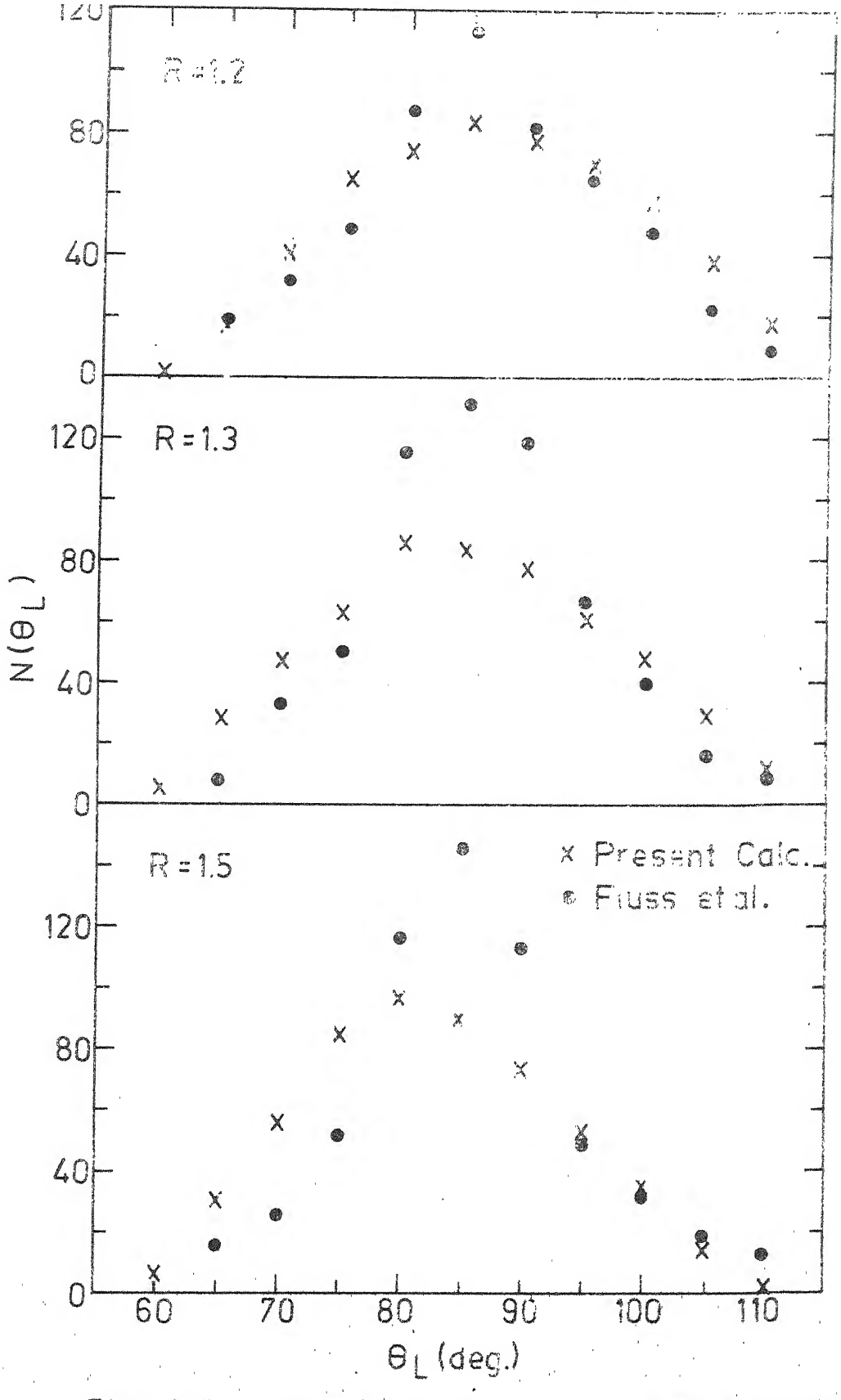

Fig. 5.3. The calculated final angular distribution for a few values of mass ratio, (R). Also shown are the experimental results of Fluss et al., (1973). The ordinate is in arbitrary units.

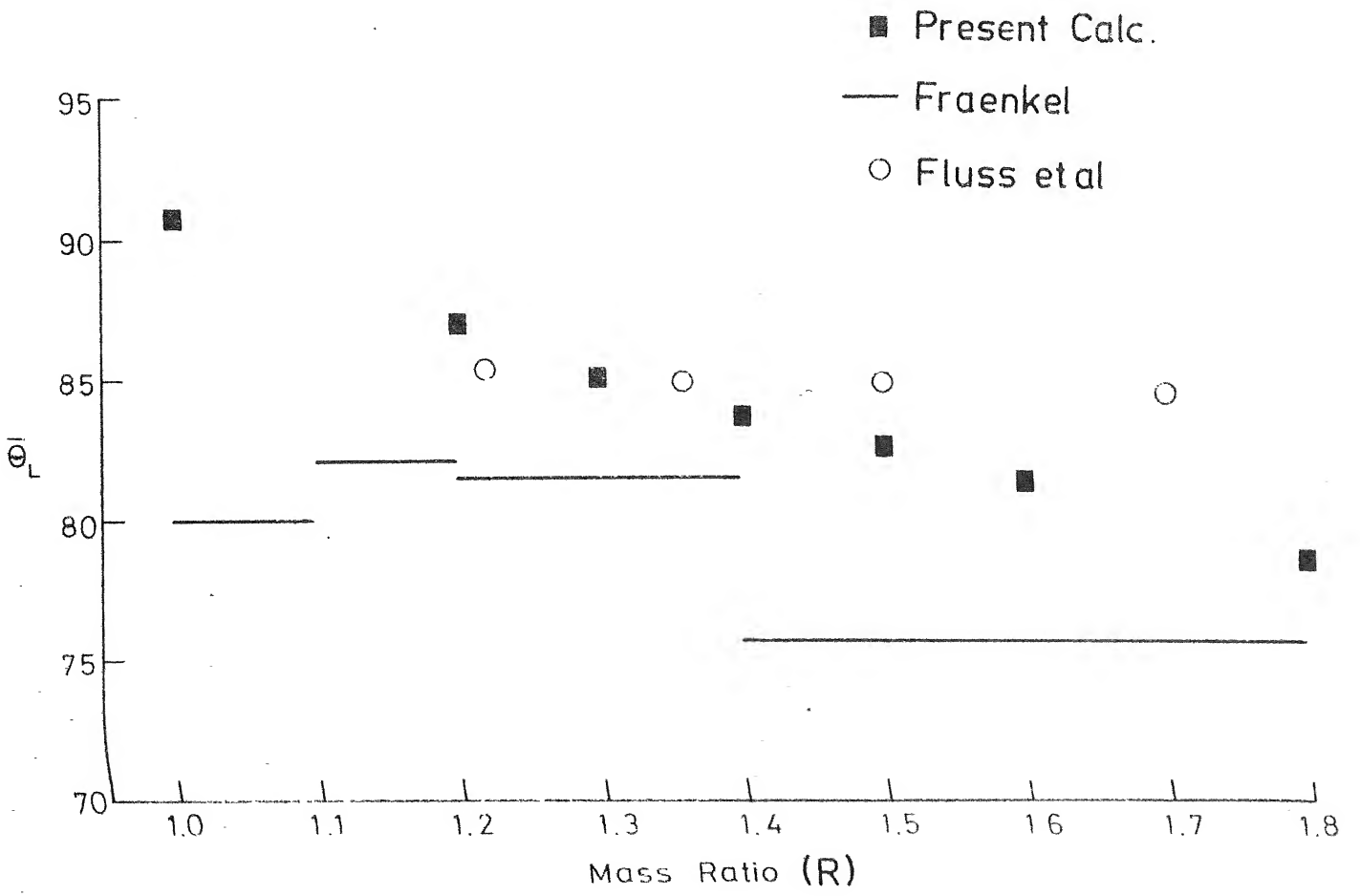

Fig. 5.4. The variation of the average angle of emission of the alpha particle ($\bar{\theta}_L$) with mass ratio (R). Also shown are the results of Fraenkel (1967) and Fluss et al., (1973).

R, Fraenkel's results (1967) show an appreciable decrease in $\bar{\theta}_L$ whereas those of Fluss et al., (1973) indicate a very small decrease. This is because of the stated poor mass resolution in the latter case. The present results lie between these two experimental results.

A second correlation which is significant is that between the angle of emission of the alpha particle and its energy. The variation of the average alpha energy, $\bar{E}_\alpha$, with the angle of emission θ_L is shown in Fig. 5.5. There is quantitative agreement between the present calculated results and the experimental ones. The results of the calculations of Boneh et al., (1967) are also shown for comparison. It is seen that the average value of the alpha energy is minimum at the most probable angle of emission ($\sim 84^\circ$) and increases as θ_L changes in either direction. The calculated values of $\bar{E}_\alpha$ are, in general, higher than the experimental ones, especially when compared with the results of Fluss et al., (1973). This could be because the alpha energy averaged over all angles obtained by Fluss et al., is about 1 MeV less than the accepted value of 16 MeV.

It has been thus demonstrated that all these experimental results can be reproduced with the initial parameters having distributions, using the method adopted here; that is, of assigning statistical 'weights' to the trajectories using a few experimental distributions namely

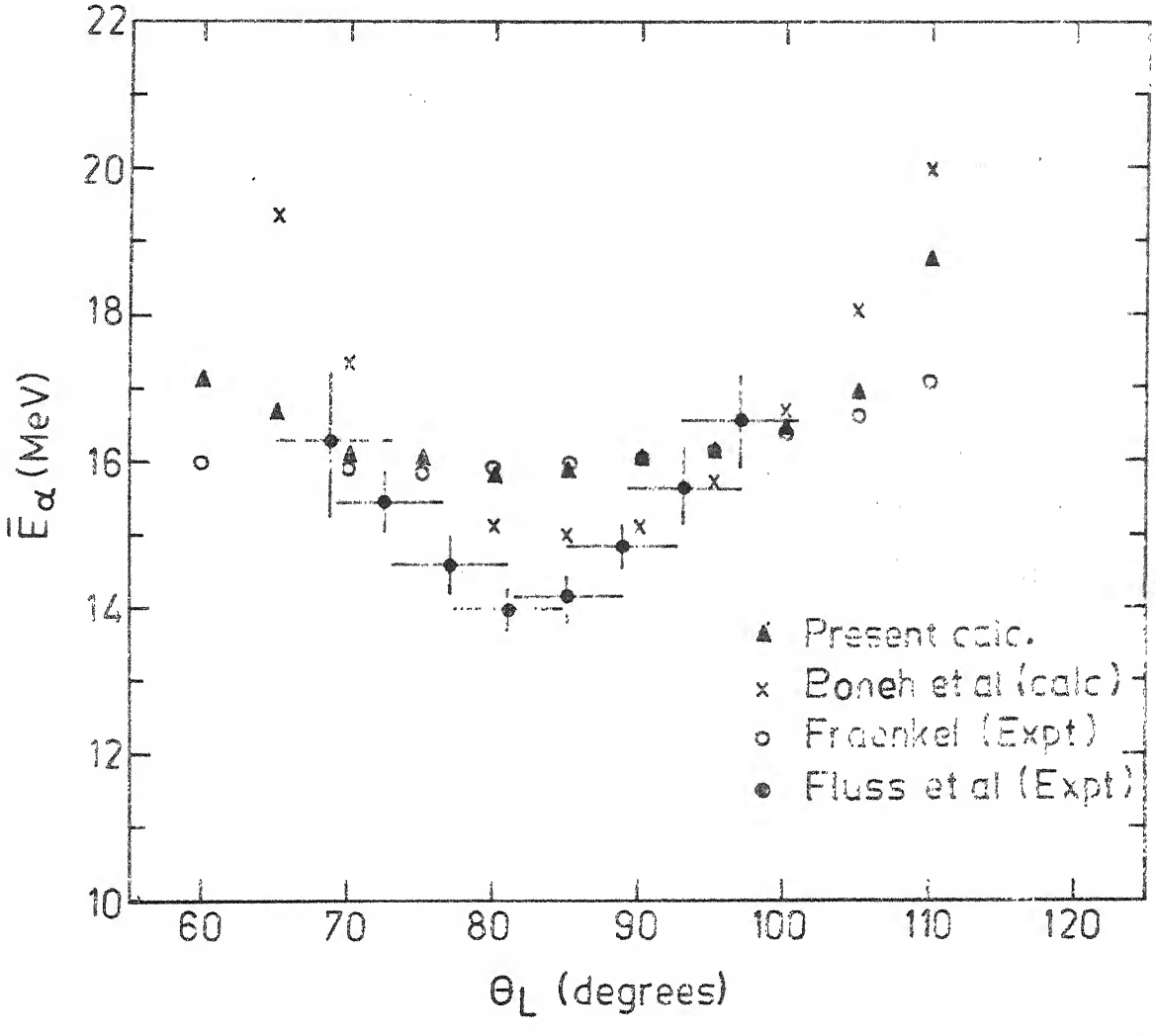

Fig. 5.5. The variation of the average alpha energy ($\bar{E}_\alpha$) with angle of emission (θ_L). Also shown are the results of Fraenkel (1967), Fluss et al., (1973) and Boneh et al., (1967).

the E_α and E_F distributions. When only the E_α and θ_L distributions were used it was seen that the average total fragment energy $\bar{E}_F$ was independent of mass ratio contrary to experimental results. This result was interpreted to mean that in order to account for the deformation energy of the fragments (which is inherently neglected due to the point charge approximation) it was necessary to include the E_F distributions while assigning weights.

5.7.3 The anticorrelation between $\bar{E}_F$ and E_α

The total kinetic energy of the three-particle system is a conserved quantity in the framework of such trajectory calculations. If the average initial energy of the fragments is uncorrelated with the initial kinetic energy of the alpha particle then an increase in one of these quantities during motion must be accompained by a decrease in the other quantity. If the initial energies are small and fixed (that is, the scission configuration were always the same) then an increase in alpha energy must be compensated by a decrease of equal size in fragment energy i.e. $\delta\bar{E}_F/\delta E_\alpha=-1$. However, if the initial energies were large or if they had a distribution of values (implying different scission configurations) then the degree of correlation would, in general, be smaller than unity.

Experimental measurements on this anticorrelation (Fraenkel, 1967; Mehta et al., 1973) have shown that its value averaged over all mass ratios for ^{252}Cf is -0.44. Boneh et al., (1967) had in their calculations, obtained the correct anticorrelation by keeping all initial variables fixed except E_α^o which was varied between 1 and 5 MeV. With lower values for the initial energies they obtained a stronger anti-correlation. This led them to conclude that at the moment of scission the three particles had already acquired about 20% of their final kinetic energy. Choudhury (1976) has obtained fair agreement with experimental results starting with zero kinetic energies and narrow distributions for D, X_o and Y_o. He attributed the stronger anticorrelation obtained by Boneh et al., (1967) to their fixing of D and Y_o. It must be emphasized that in the results quoted above the initial fragment and alpha energies were assumed to be uncorrelated. The presence of distributions in the initial parameters and/or correlations between them could alter the conclusions regarding the scission configuration. Therefore, in order to get a clearer picture of the scission configuration it would be necessary to examine the effect of distributions in the initial parameters and also, if possible, the correlations between them.

The method adopted in the present calculations has therefore been directed by such requirements. The initial

parameters have been allowed a distribution in values and the anticorrelation obtained is shown in curve A of Fig. 5.6. The degree of anticorrelation obtained is very small. However, the correct anticorrelation was obtained when the fragment separation D, was held fixed(curve B) while all the other parameters were allowed to have distributed values. In particular, no regard was given to the initial energies being high or low. This result indicates that when the interfragment distance D is held fixed a negative correlation between $\bar{E}_F$ and E_α is obtained with no restrictions on the E_α^o or E_F^o distributions. One, therefore, cannot conclude that at scission the particles have very small energies or that their energies are about 20% of their final values.

The result that the anticorrelation almost disappears when all the parameters, including D, are allowed to have distributed values; could be due to an initial positive correlation between E_α^o and E_F^o. Boneh et al., (1967) had pointed out that a distribution in the values of D could give rise to a positive correlation between E_α^o and E_F^o. They had, however, stated that this positive correlation would be partially compensated by the negative correlation due to the distribution in initial heavy fragment velocity (i.e. in effect a distribution in E_F^o). There exists no quantitative support for this conjecture. The present calculations

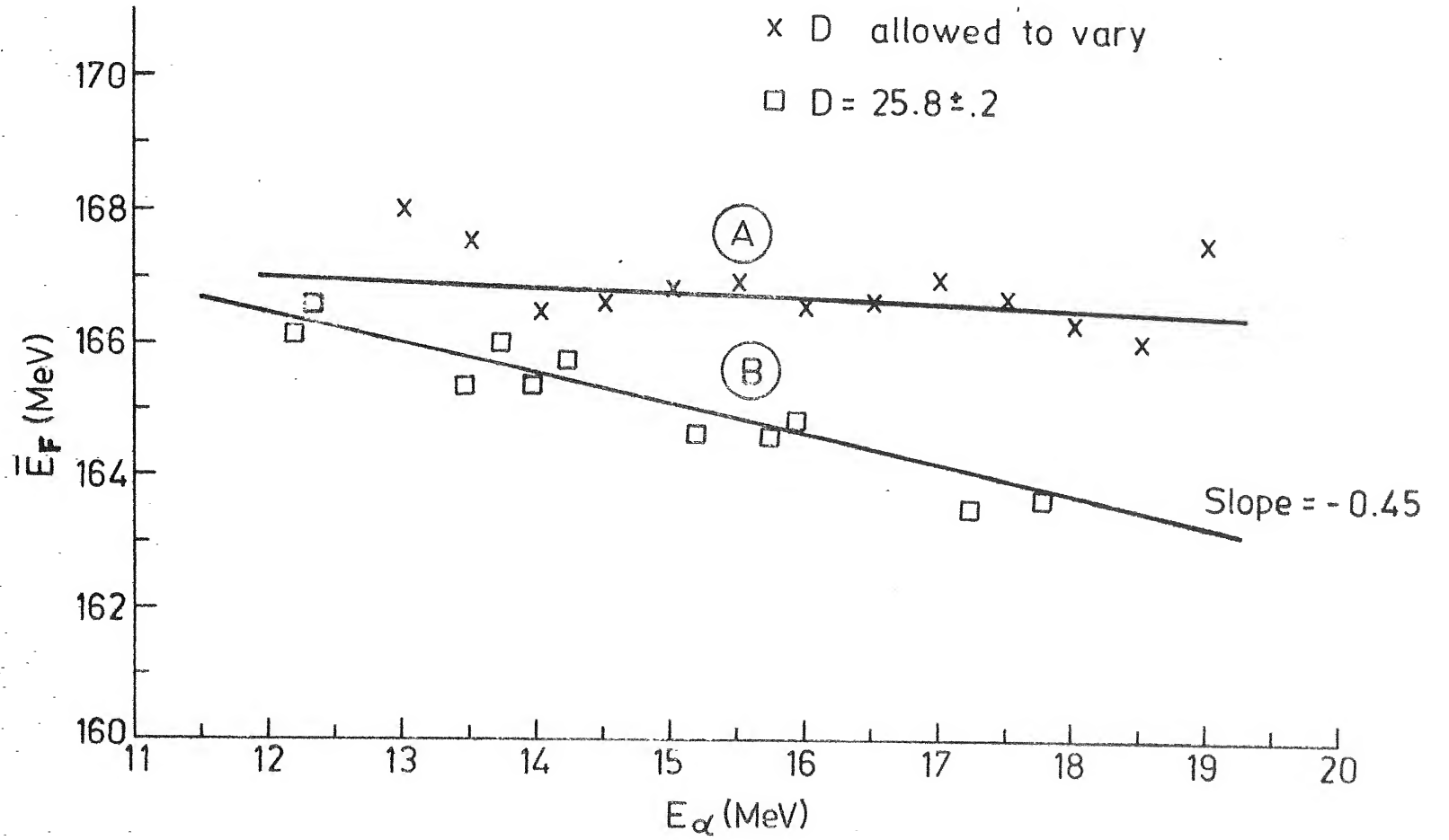

Fig. 5.6. The anticorrelation between the average total fragment energy ($\bar{E}_F$) and the alpha energy E_α; for a fixed value of D and for D having a distribution of values.

indicate that the distributions in the other parameters (apart from D) could account for this (possible) positive correlation.

In the results presented above only the effects of distributions have been considered however one cannot exclude the possibility of some initial correlations which could be responsible for the final anticorrelation. With fixed D it was possible to obtain the correct anticorrelation hence this could mean that fixing D gives rise to a negative correlation between E_α^o and E_F^o which more than compensates the positive correlation in these two quantities due to the distribution in all other parameters. In the foregoing conjecture it has been assumed that the initial correlation between E_α^o and E_F^o largely determines the sign of the final correlation between $\bar{E}_F$ and E_α.

As illustrated in Fig. 5.6 the correct anticorrelation was obtained with D = 25.8±0.2 f. When the variation was increased to 1.0 f the anticorrelation became very small indicating that the anticorrelation depends quite sensitively on the spread in value of D. In other words, the D distribution necessary to produce the correct anticorrelation is very narrow. This result indicates that the alpha particle is emitted when the fragments effectively maintain a constant separation. This could be pictured as follows : the motion of the fragments just after scission and the

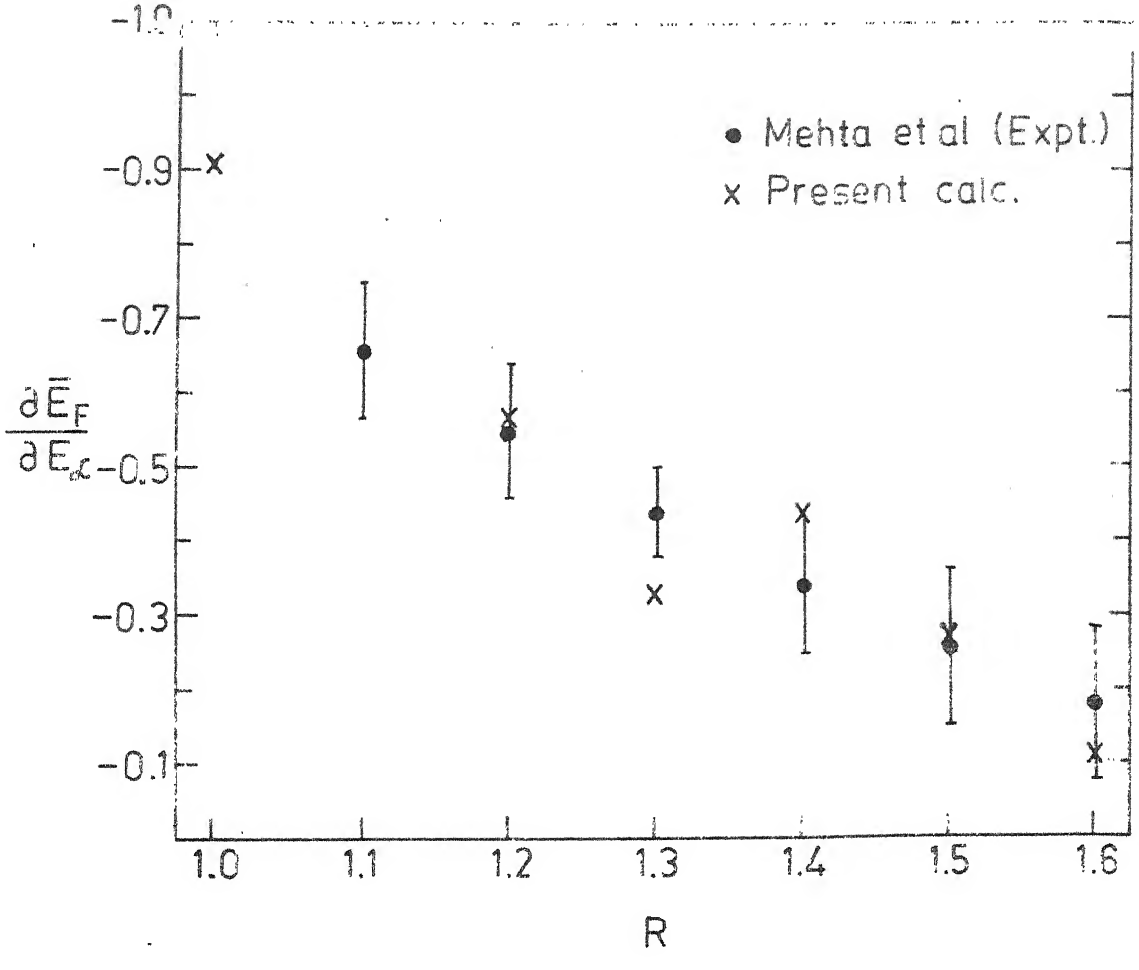

Fig. 5.7. The variation of the anticorrelation with mass ratio. The results of Mehta et al., (1973) are also shown.

change in their deformations in this period, could result in zero nett displacement of the charge centres of the fragments thereby resulting in a fixed D during this small time interval .

The variation of the value of the anticorrelation with mass ratio was studied. The value of D chosen for this purpose was 26.2±0.2 f. The results, shown in Fig. 5.7 are compared with the experimental results of Mehta et al., (1973). The calculated values agree quite well with that of experiment.

5.7.4 Initial distributions

Each trajectory was assigned a 'weight' by comparing the final E_α and E_F values with experimental distributions. This 'weight', denoted by P, with $P = P_x P_y$ as explained earlier, expressed the probability that the initial values characterizing the trajectory had of reproducing the mean values of the experimental distributions in E_α and E_F. In choosing the trajectories for analysis a lower limit on P was imposed; only those trajectories which had $P \geqslant 0.1$ were considered. This cut off though not physically significant as such, does however, imply that only those initial values having more than 30% chance of resulting in each of the mean experimental values of E_α and E_F were considered. This cut off was also chosen with a view to obtain good statistics. The mean values of E_α and E_F were not altered when $P \geqslant 0.01$ or $P \geqslant 0.001$.

These initial values were then plotted against their frequency of occurrence, that is N(x) vs x, to give the initial distributions. Thus, while counting the number of times a particular initial value occured, no regard was given to P. That is, once the trajectories had been selected they were treated on equal footing. In this manner the distributions in E_α^o, E_F^o, X_o and D were obtained.

The distribution in E_α^o is shown in curve A of Fig. 5.8 (a) (curve B will be discussed later). It is clear that this distribution does not give the much-sought-for information on whether the initial energy is low or is an appreciable fraction of the final value. The indication is that the distribution is broad with possible peaking in the 1 and 2 MeV regions. The E_F^o distribution, shown in curve A of Fig. 5.8 (b) is also quite broad and shows possible multiple peaking. In order to examine this possibility the variation in E_F^o was extended to 60 MeV and the result is shown by the dotted extension in the figure.

The distribution in the point of emission of the alpha particle along the fission axis is shown in Fig. 5.8(c). It is seen that the most probable initial starting position for the alpha particle is close to the zero-field point. Several previous trajectory calculations eg. Boneh et al., (1967), Raisbeck and Thomas (1968) also gave the same result. Fong (1970) remarked that the main difference, which accounts

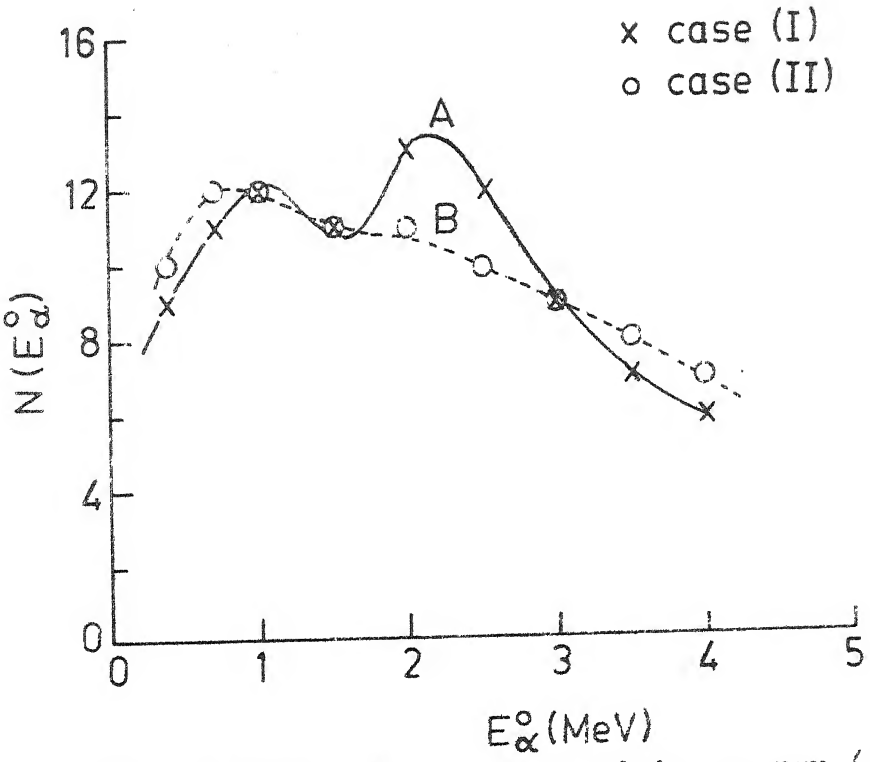

Fig. 5.8(a). The initial alpha energy (E°_{α}) distribution for R = 1.4.

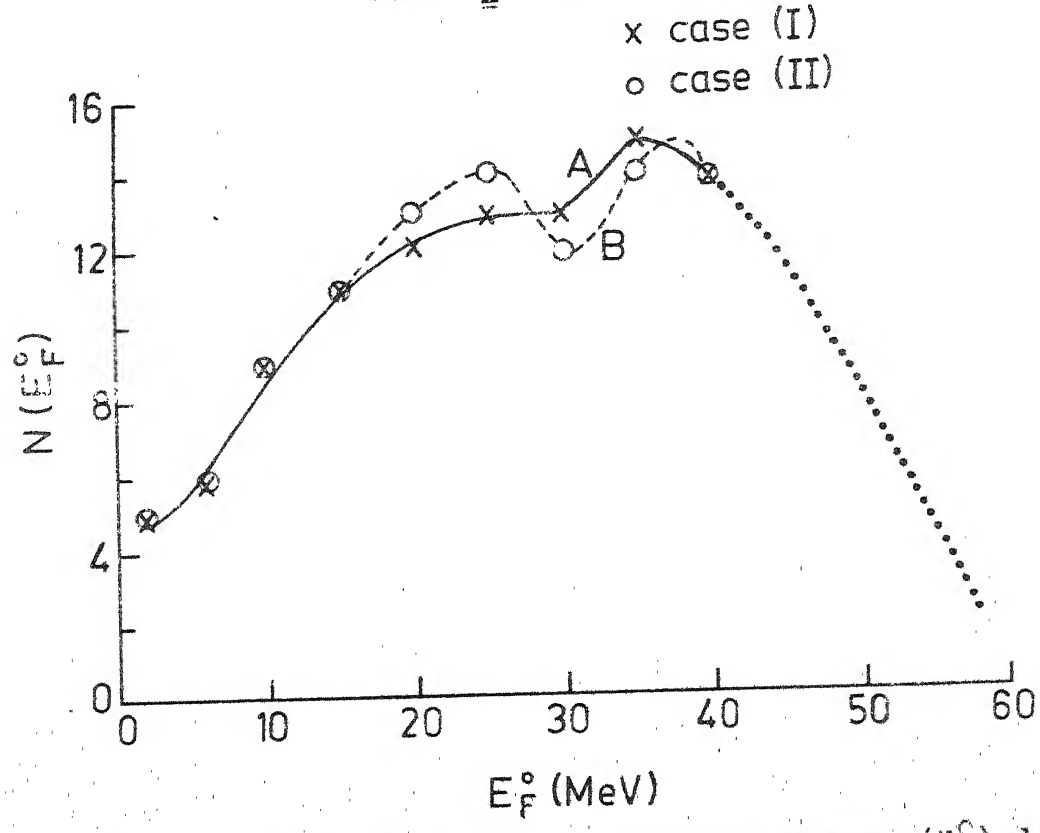

Fig. 5.8(b). The initial fragment energy (E°_{F}) distribution for R = 1.4.

The ordinates in (a) and (b) are in arbitrary units. Case I is when E_{α} and E_F distributions are used in assigning weights. Case II when the anticorrelation condition is also used in assigning

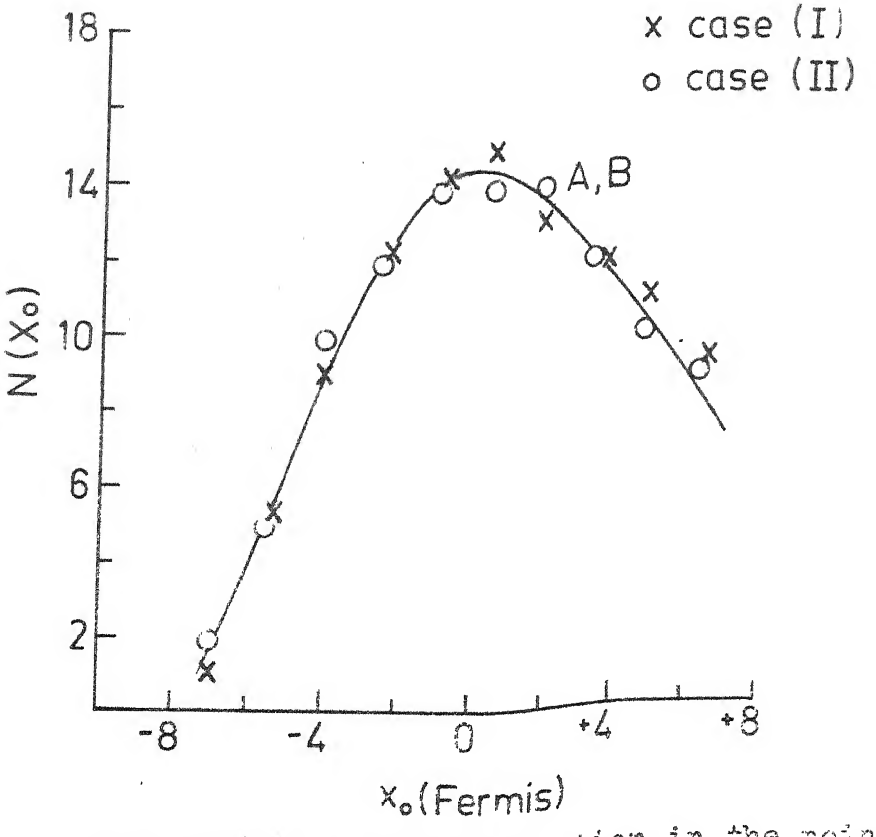

Fig. 5.8(c). The distribution in the point of emission of the alpha particle (X_0) for $\lambda = 1.4$.

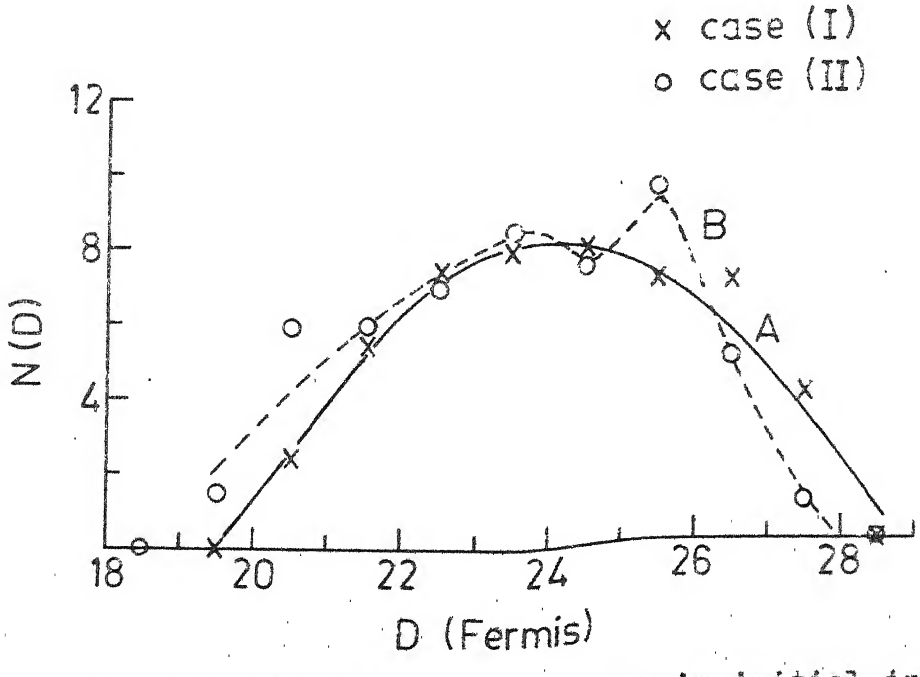

Fig. 5.8(d). The distribution in initial interfragment distance (D).

The ordinates in (c) and (d) are in arbitrary units. Case I and Case II same as in (a) and (b).

for different values for E_α^o between other calcuoations and his, is the choice of X_o. The zero field point, as the most probable emission point, corresponds to a position closer to the light fragment; Fong however, requires it to be nearer the heavy fragment.

The distribution in initial values of interfragment distance, D, shown in Fig. 5.8 (d) is broad with a mean value of ~24 f and a width of about 6 f. This value is quite close to the one obtained by Fong and others. Boneh et al., obtained 26 f while Raisbeck and Thomas obtained 21f.

These distributions were first checked to see whether they reproduced the final distributions in E_α and E_F; the ones used in assigning 'weights' to the trajectories (see Table 5.4). Then they were used to predict angular distributions and a few final correlations. The calculated distributions agreed quite well with experimental distributions as elaborated in section 5.7.2. However, the observed anticorrelation between $\bar{E}_F$ and E_α could not be reproduced by these distributions as explained in the last section.

In order to obtain the initial distributions which reproduce the observed anticorrelation it was thought fit to use the anticorrelation condition as a criterion in assigning 'weights' to the trajectories in addition to the E_α and E_F distributions. The values of the anticorrelation for different values of R were taken from the experimental

results of Mehta et al., (1973) and were used in the same manner as was done with the E_α and E_F distributions.

The initial distributions obtained when the anti-correlation condition was also used, are shown by curves B in Figs. 5.8 (a) to (d). Here again there is an indication of two peaks both in the E_α^o and E_F^o distributions with some changes in their positions and relative amplitudes. By and large there is no significant change in these distributions. The X_o distribution too does not change when the anticorrelation condition is used in assigning weights. This implies that the anticorrelation condition has no significant effect on these initial distributions.

The distribution in initial values of D when the anticorrelation condition is used is shown in curve B of Fig. 5.8 (d). The distribution is broad, however, there are indications of two peaks one around 23.5 f and the other around 25.5 f. It was seen that with fixed D it was possible to get the correct anticorrelation, however, using the anticorrelation condition the distribution in D is not narrow and single peaked as one might expect. The distribution in D for different values of R indicates that the (broad) peak shifts ($\sim$1 to 2 f) towards lower D values for mass ratios different from R = 1.4. Such a result could possibly imply that in symmetric fission the deformation (elongation of the neck) is relatively not large and the

increase in the total number of prompt neutrons for symmetric mass division (Terrel curve) is probably due to increased fragment excitation coming from viscous effects.

In order to throw more light on this apparent paradox (ei.e. D not being single peaked) the initial distributions, with fixed D, were studied. The values of D chosen for this purpose were 23.25±.25f and 25.5±.25 f, corresponding to the approximate peak positions referred to in the last paragraph. The distributions in E_α^o and X_o are shown in Figs. 5.9(a) and (b). The E_F^o distributions for these two cases were narrow and had mean values of 15 MeV for the lower D value and 35 MeV for the higher D value with corresponding mean alpha energies of 1.0 and 3 MeV respectively. The X_o distributions in both cases are broad with mean values corresponding to a position closer to the light fragment in the case of the lower D value and to a position closer to the heavy fragment for the higher D value. In the latter case, however, there is an indication of two peaks on either side of the zero-field point with the peak nearer the heavy fragment being more prominent. The θ_L distribution reflects this double peaking (Fig. 5.9(c)).

The significant aspect of the results shown in Figs. 5.9(a) and (b) is that they indicate that both classes of initial values i.e. those of Boneh et al., (1967) (adiabatic model) and of Fong (1970) (statistical model) can be obtained. Boneh et al., used initial alpha and

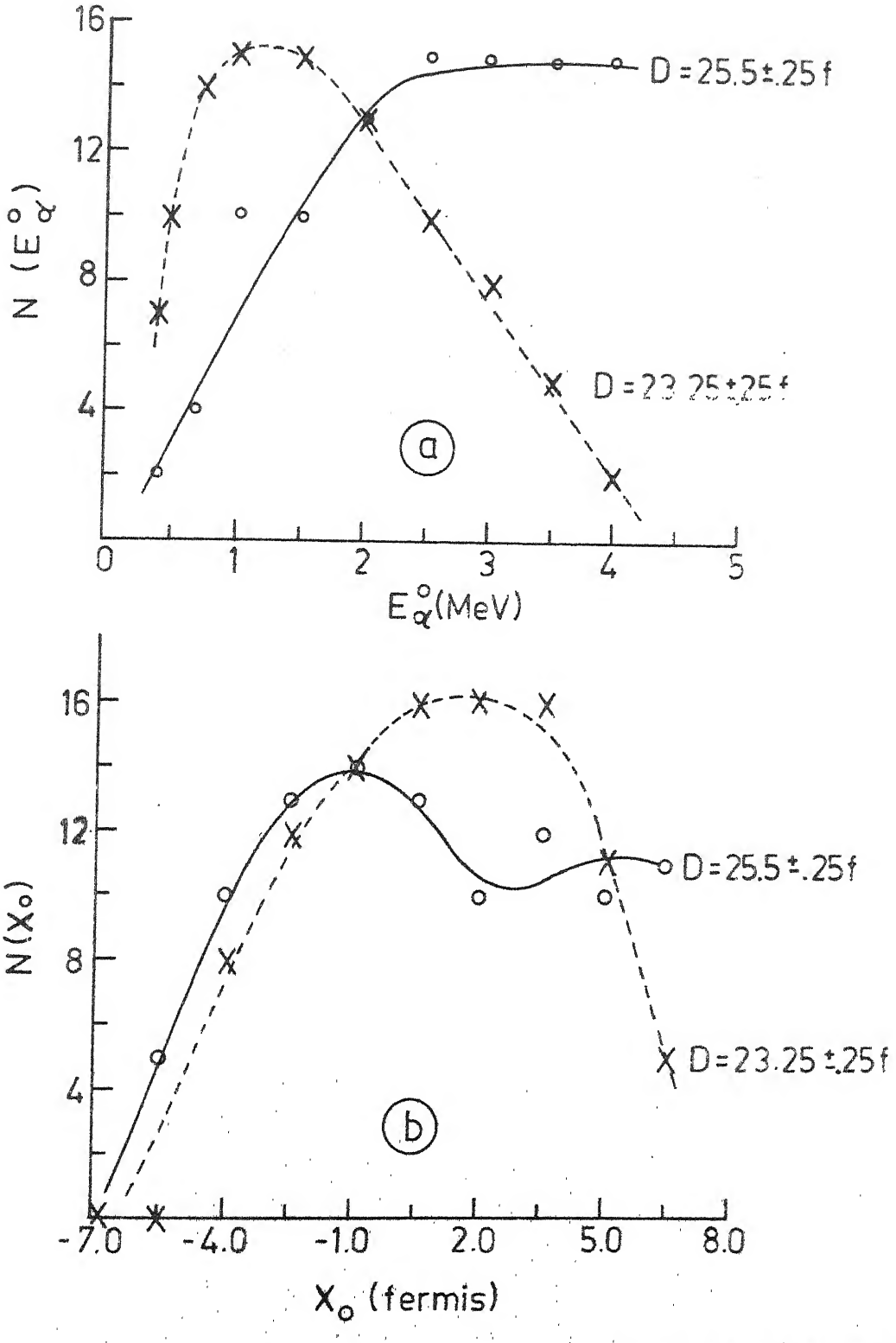

Fig. 5.9. Initial distribution in (a) initial alpha energy (E^{o}_{α}) and (b) point of emission of the alpha particle (X_o) for fixed values of D ($R = 1.4$). The ordinates are in arbitrary units.

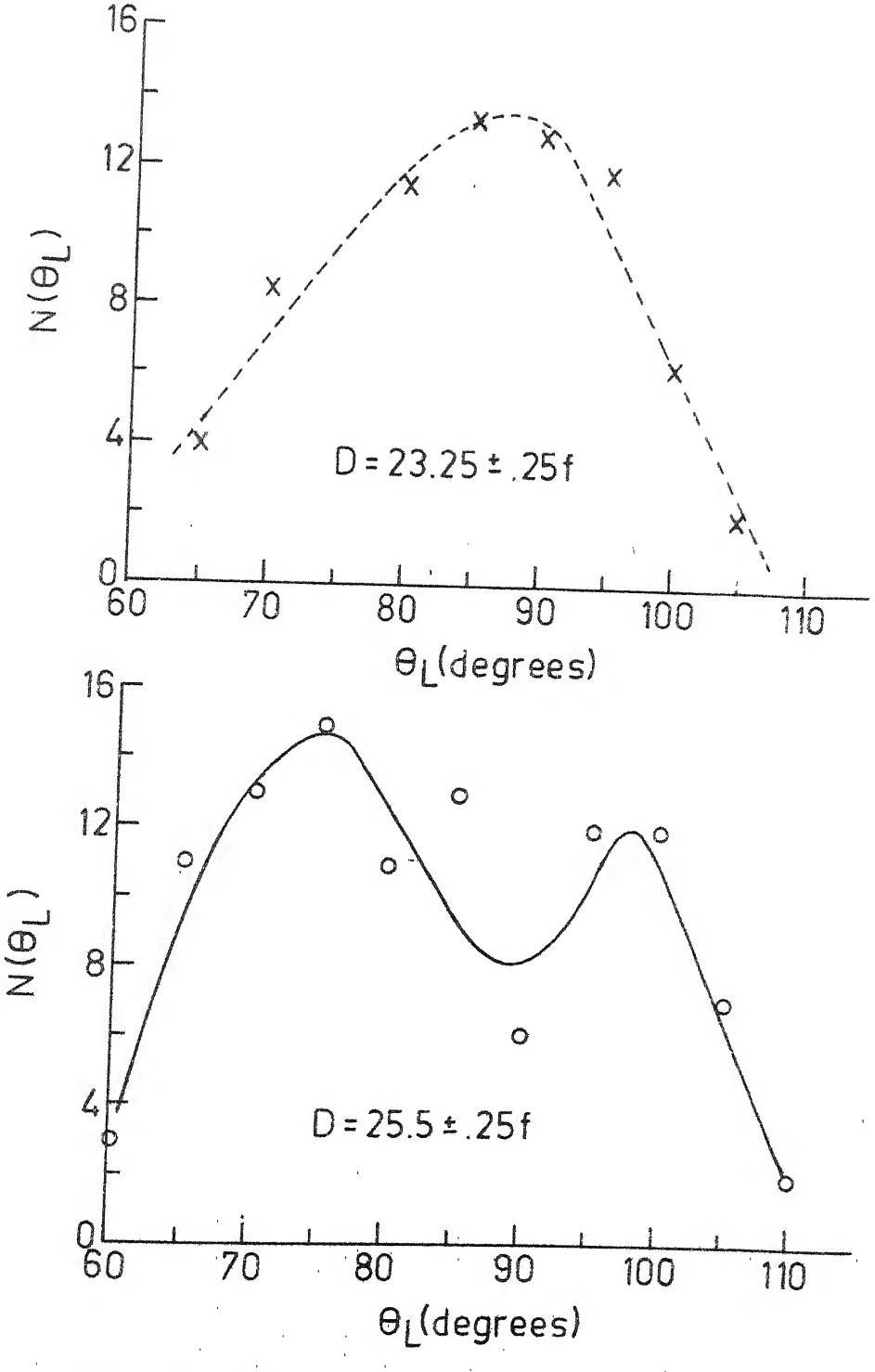

Fig. 5.9(c). The distribution in final angle of the alpha particle (θ_L) for fixed values of D. (R = 1.4). The ordinates are in arbitrary units.

fragment energies of 3 MeV and 35 MeV with D~26f and Fong had used initial energies ~0.5 and 1 MeV with D~24f. Boneh et al., had obtained the zero field point as the most probable emission point while Fong had required this point to be closer to the heavy fragment. This latter result does not agree with the most probable X_o obtained in the present calculations for D≃23.5f.

Cavallari et al., (1970) had also obtained distributions in the initial parameters and their average values (see section 5.5.1). They had however used three average final alpha energies of 9, 15 and 18 MeV in assigning weights to the trajectories. The other final values eg. for E_F and θ_L were just used to select those trajectories which gave the best approximation to the experimental values (E_F = 177.3 MeV $\theta_L = 92 \pm 30^o$). Hence, at best the initial distribution obtained are those which can reproduce any of the three final values of alpha energy and approximately the final fragment energy and final angle. Using the initial values they obtained (see Table 5.1) it would not be possible to obtain the correct anticorrelation, in fact the value of the anticorrelation obtained for very small initial energies would be≃ -1 as explained in section 5.7.3. They did not check their distributions against the final fragment distributions (except for the requirement that $E_L/E_H \approx 1.32$) or the anticorrelation condition as has been done in the present calculations.

To summarize the results on initial distributions one firstly notices that the initial distributions are broad, covering both the predictions of the adiabatic and statistical model as elaborated above. The noteworthy fact about them is that even when the anticorrelation condition was imposed as a criterion, these distributions remained unaltered. This fact suggests that the initial distributions are in fact broad and choosing either low or high initial energies within the distributions would not alter the final values substantially. It would therefore be incorrect to say either that the particles have attained an appreciable fraction of their final energy or that they are almost at rest at scission.

Most calculations including the present are support the result that the most probable emission point for the alpha particle is the zero-field point. However, there is some disagreement in the value of the interfragment distance at scission. The present calculations indicate that in order to reproduce the final anticorrelation a very narrow distribution of interfragment distance is required and its mean value is close to that obtained by some calculations eg. those of Boneh et al., (1967).

5.7.5 Correlations between initial parameters

One of the simplifying assumptions made in all trajectory calculations including the present one, is that

of treating the initial parameters as uncorrelated quantities within the constraints of the concervation laws. This assumption is made because of the lack of apriori knowledge about such correlations. One thus begins with uncorrelated initial parameters. However, in order to explain some of the final correlations, some qualitative conjectures about initial correlations have often been made (eg. Boneh et al., 1967). As yet, none of the calculations have succeeded in coming up with some definite information on initial correlations.

In the last section, the effect of distributions in initial parameters on the anticorrelation was examined. In order to get more information on the final anticorrelation it was thought worthwhile to examine the effect of some possible correlations in initial parameters. Intuitively, one would imagine thay an initial negative correlation between E_α^o and E_F^o would lead to the final anticorrelation. However, correlations between the other parameters could also influence the final anticorrelation.

In order to study the (possible) initial correlation between E_α^o and E_F^o the distribution in E_F^o when $E_\alpha^o \leq 1$ MeV and for $E_\alpha^o > 1$ MeV were obtained. These distributions, shown in Fig. 5.10, indicate a positive correlation between E_α^o and E_F^o. The distributions remain unchanged when the anticorrelation condition is also imposed. The mean values of

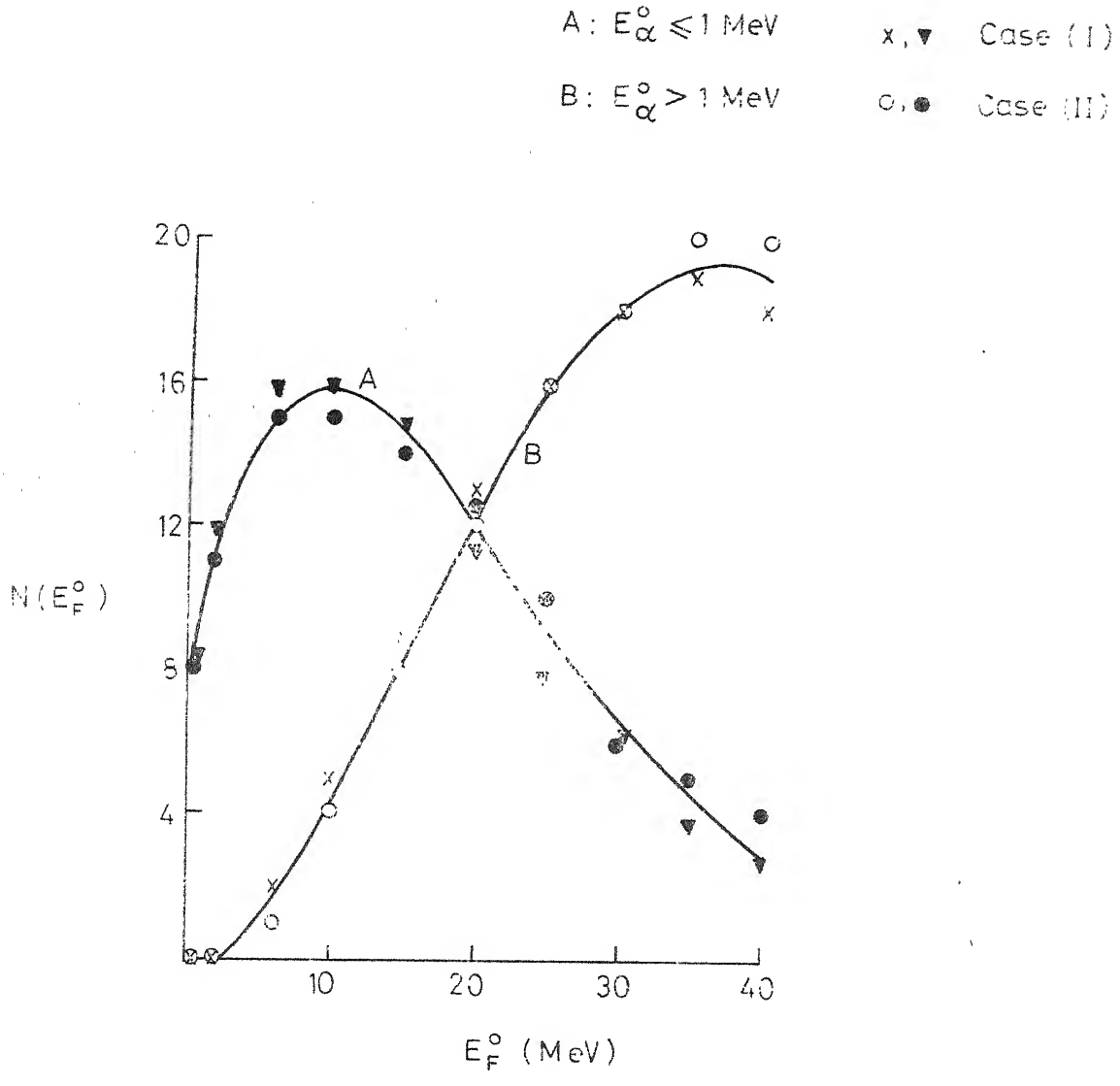

Fig. 5.10. The correlation between the initial alpha energy (E_α°) and the initial fragment energy (E_F°) for R = 1.4. The ordinate is in arbitrary units. Case (I) and case (II) as in Fig. 5.8.

E_F^o from these distributions are close to the ones obtained by Fong (1970) and others ($E_\alpha^o \leqslant 1$ MeV) and by Boneh et al., (1967) and Raisbeck and Thomas (1968) ($E_\alpha^o > 1$ MeV). This result indicates that although there is an initial positive correlation between E_α and E_F the final values are negatively correlated. This initial positive correlation is probably compensated for by some other correlation which is strongly negative. In terms of the energy transfer from deformation to kinetic energy, this result indicates that the extent to which this transfer takes place is either small, resulting in small E_α^o and E_F^o ; or is large resulting in large E_α^o and E_F^o. Both situations seem equally valid and lead to the final anticorrelation.

As mentioned in the previous section the initial positive correlation between E_α^o and E_F^o remains essentially unchanged when D is held fixed. For the two values of D studied, namely 23.5f and 25.5f, the average values of E_α^o and E_F^o were 1.0 and 15 MeV and 3.0 and 35 MeV respectively. These results may be pictured in the following manner: when the transfer from compound nucleus excitation/ deformation to kinetic energy is small the kinetic energy of the nascent fragments is small with a relatively small interfragment separation and when the energy transfer is large implying a larger kinetic energy of the nascent fragments the separation is relatively larger. The results of Fong (1970) and others indicated a lower value of D than that obtained by

Boneh et al., (1967).

The X_o distribution for these two regions of E_α^o is peaked around the zero field point to within 0.5f. The X_o distribution is therefore not affected by a choice of either low or high initial energies contrary to the suggestion by Boneh et al., (1967) that the initial alpha energy is dependent on X_o. These distributions did not change when the anticorrelation condition was imposed indicating their validity.

Another possible initial correlation is that between X_o and D. It was seen that in order to obtain the correct anticorrelation D had to be held fixed and the X_o distribution was broad with possibly two peaks (Fig. 5.9(b)). When the anticorrelation condition was used as a criterion in assigning weights, the X_o distribution was peaked around the zero-field point whereas the D distribution indicated the possibility of two peaks (Fig. 5.8(d)). A similar result i.e. two values for X_o for a fixed D, has been obtained by Choudhury (1976). Some empirical correlations between X_o and D were tried but they failed to produce the correct anticorrelation. The exact nature of this correlation is not clear but it does seem that in order to produce final energies satisfying the anticorrelation condition the potential energy configuration at the moment of alpha emission (determined by D and X_o) is important.

5.8 The effect of fragment deformation on initial distributions

In section 5.2 certain approximations used in trajectory calculations were explained. These approximations were necessary in order to simplify the problems in calculation by reducing the number of parameters. If the fragments are considered to be undeformed spheres, then their charge centres would coincide with their centres and hence could be considered as point charges. This means that higher order multipoles arising out of a non-spherical charge distribution are neglected. The non-inclusion of dipole and quadrupole interactions would reduce the potential by 1% and 4% respectively (see section 5.2). Since $\bar{E}_\alpha$ and $\bar{E}_F$ are about 16 MeV and 180 MeV respectively, the errors due to this approximation could amount to about 1 MeV in $\bar{E}_\alpha$ and about 8 MeV in $\bar{E}_F$. These figures are actually overestimates since after scission both D and the deformation of the fragments are rapidly changing and the potentials due to these multipoles would become insignificant after a small time interval i.e. a few iterations in the calculations. It was seen (Table 5.4) that the average final energies obtained from these calculations agreed very well with those of experiment. Hence, as was also pointed out by Halpern (1963), the mean final energies would not be significantly altered by the inclusion or non-inclusion of higher order multipoles in the interaction.

However, the inclusion of deformations could effect the distribution in D and X_0 since the charge centres and consequently the zero field point would shift depending upon the extent of deformation. Hence it would be instructive to compare the initial distributions obtained using deformed fragments with the earlier ones.

Geilikman and Khlebnikov (1964) had carried out trajectory calculations using deformed fragments. They had considered quadrupole and octupole deformations and had neglected the change of these deformations with time. Their results on energy and angular distributions compare very well with those of Halpern (1963) who used the point-charge approximation.

The aim of the present calculation was to determine the effect the inclusion of deformations had on the initial distributions. For a mass ratio R = 1.4 it was assumed that only the light fragment was deformed into a spheriod with $\varepsilon = 0.7$ and that the heavy fragment was spherical. This case is only representative and is meant to determine whether the inclusion of deformation had any effect at all on the initial disteibutions. It was further assumed that the deformation was independent of time i.e. the fragments retained their shapes.

The potential due to a spheroidal nucleus at (r,θ) is

$$V(r,\theta) = 3Ze \sum_{n=0}^{\infty} \frac{(a^2-b^2)\, P_{2n}\,(\mathrm{Cos}\,\theta)}{(2n+1)(2n+3)\, r^{2n+1}}$$

where Ze is the charge of the nucleus and 'a' and 'b' denote the semi-major and semi-minor axis respectively. By volume conservation we have

$$4/3\pi ab^2 = 4/3\pi R_o^3$$

where R_o is the radius of the undeformed nucleus

$$\therefore \quad ab^2 = R_o^3$$

using $$\frac{a^2-b^2}{R_o^2} = \varepsilon^2$$

we have

$$V(r,\theta) = \frac{3Ze}{R_o} \sum_{n=0}^{\infty} \frac{\varepsilon^{2n}\, P_{2n}\,(\mathrm{Cos}\,\theta)}{(2n+1)(2n+3)(r/R_o)^{2n+1}}$$

with $\varepsilon = 0.7$ and for $r \approx 2$ of the series falls off rapidly hence only terms till $P_4\,(\mathrm{Cos}\,\theta)$ are considered

$$\therefore \quad V(r,\theta) = \frac{3Ze}{R_o}\left[\frac{1}{3(r/R_o)} + \frac{\varepsilon^2}{15}\,\frac{P_2(\mathrm{Cos}\,\theta)}{(r/R_o)^3} + \frac{\varepsilon^4}{35}\,\frac{P_4(\mathrm{Cos}\,\theta)}{(r/R_o)^5}\right]$$

The field at (r,θ) is

$$\vec{E}(r,\theta) = -\nabla V(r,\theta)$$

$$= -\left[\hat{r}\,\frac{\delta V}{\delta r} + \frac{\hat{\theta}}{r}\,\frac{\delta V}{\delta \theta}\right]$$

$$\therefore \vec{E}(r,\theta) = -\frac{3Ze}{R_o}\left[\frac{1}{3}\frac{-1/R_o\,\hat{r}}{(r/R_o)^2} + \frac{\varepsilon^2}{15}\left(\frac{-3}{R_o}\frac{P_2(\cos\theta)\,r\,P_2'(\cos\theta)\hat{\theta}}{(r/R_o)^4} + \frac{}{(r/R_o)^3 r}\right)\right.$$

$$\left. + \frac{\varepsilon^4}{35}\left(-\frac{5}{R_o}\frac{P_4(\cos\theta)\,\hat{r}}{(r/R_o)^6} + \frac{P_4'(\cos\theta)\,\hat{\theta}}{r(r/R_o)^5}\right)\right]$$

$$\vec{E}(r,\theta) = \frac{3Ze}{r^2}\left[\frac{1}{3} + \frac{\varepsilon^2}{15(r/R_o)^2}\,3P_2(\cos\theta) + \frac{\varepsilon^4\,5\,P_4(\cos\theta)}{35(r/R_o)^4}\right]\hat{r}$$

$$- \frac{3Ze}{r^2}\left[\frac{\varepsilon^2}{15}\frac{P_2'(\cos\theta)}{(r/R_o)^2} + \frac{\varepsilon^4}{35}\frac{P_4'(\cos\theta)}{(r/R_o)^4}\right]\hat{\theta}$$

Since $P_2(\cos\theta) = 1/2\,(3\cos^2\theta-1)$; $P_2'(\cos\theta) = 3\sin\theta\cos\theta$

$P_4(\cos\theta) = 1/8\,(35\cos^4\theta-30\cos^2\theta+3)$;

$P_4'(\cos\theta) = -5/2\,\mathrm{Sinc}\,\theta\,(7\cos^3\theta-3\cos\theta)$

and $\hat{r} = \sin\theta\cos\phi\,\hat{i} + \sin\theta\sin\phi\,\hat{j} + \cos\theta\,\hat{k}$

$\hat{\theta} = \cos\theta\cos\phi\,\hat{i} + \cos\theta\sin\phi\,\hat{j} - \sin\theta\,\hat{k}$

where i,j and k are unit vectors along the x,y and z directions.

$$E_x = \frac{3Ze}{r^3}\,x\left[\frac{1}{3} + \frac{\varepsilon^2}{10(r/R_o)^2}\left(\frac{5z^2}{r^2}-1\right) + \frac{\varepsilon^4}{56(r/R_o)^4}\left(\frac{63z^4}{r^4} - \frac{42z^2}{r^2}+3\right)\right]$$

$$E_y = \frac{3Ze}{r^3}\,y\left[\frac{1}{3} + \frac{\varepsilon^2}{10(r/R_o)^2}\left(\frac{5z^2}{r^2}-1\right) + \frac{\varepsilon^4}{56(r/R_o)^4}\left(\frac{63z^4}{r^4} - \frac{42z^2}{r^2} + 3\right)\right]$$

$$E_z = \frac{3Ze}{r^3}\left[\frac{z}{3} + \frac{\varepsilon^2}{10(r/R_o)^2}\left(\frac{3z^3}{r^2} - \frac{2z}{r^2}(x^2+y^2) - z\right) + \frac{\varepsilon^4}{56(r/R_o)^4}\left(\frac{35z^2}{r^4}\right.\right.$$

$$\left.\left. - \frac{30z^3}{r^2} + 3z - \frac{4(x^2+y^2)}{r}\left(\frac{7z^3}{r^3} - \frac{3z}{r}\right)\right)\right]$$

These relations were used in the calculation of forces on the three particles.

The values of the initial parameters used were the same as those used earlier. Ten thousand trajectories were computed for R = 1.4 and each trajectory was assigned a 'weight' as before. The maximum percentage error in energy conservation was ~ 2%.

The initial distributions obtained are shown in Fig. 5.11(a) to (d). One can at once see that there is no significant change in the distributions as a result of including deformations. These distributions also remain unaltered when the anticorrelation condition is imposed. The initial positive correlation was also reproduced. The final θ distribution did not show any significant change though the mean value was slightly reduced from 86° to 84.6°.

The method adopted here to examine the effects of deformation of fragments has not produced any new result except to indicate perhaps that unless the effects of deformation are larger there would be no significant change in the initial distributions. The magnitude of the interaction

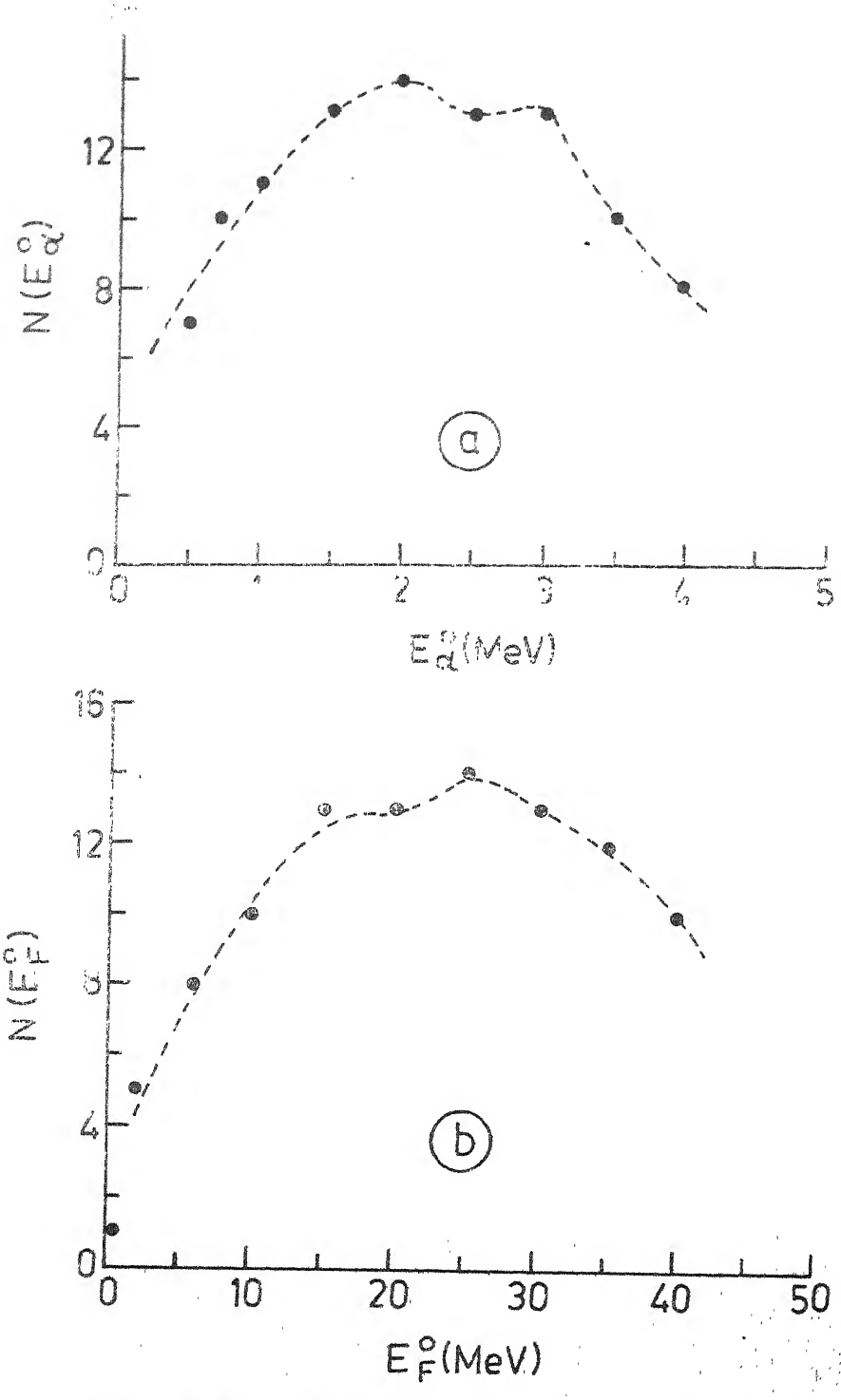

Fig. 5.11. Initial distribution in (a) alpha energy (E^{o}_{α}) and (b) fragment energy (E^{o}_{F}) when deformation effects are included. (R = 1.4). The ordinates are in arbitrary units.

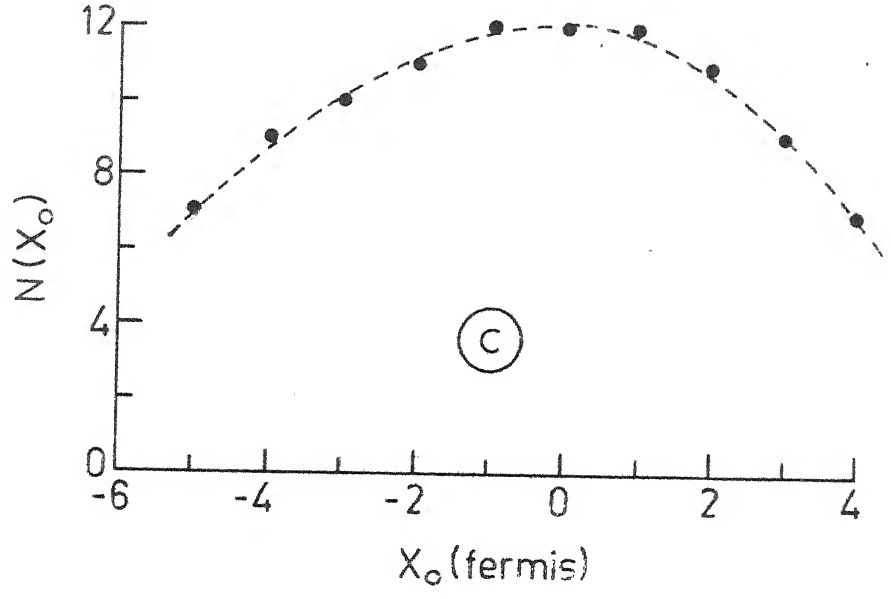

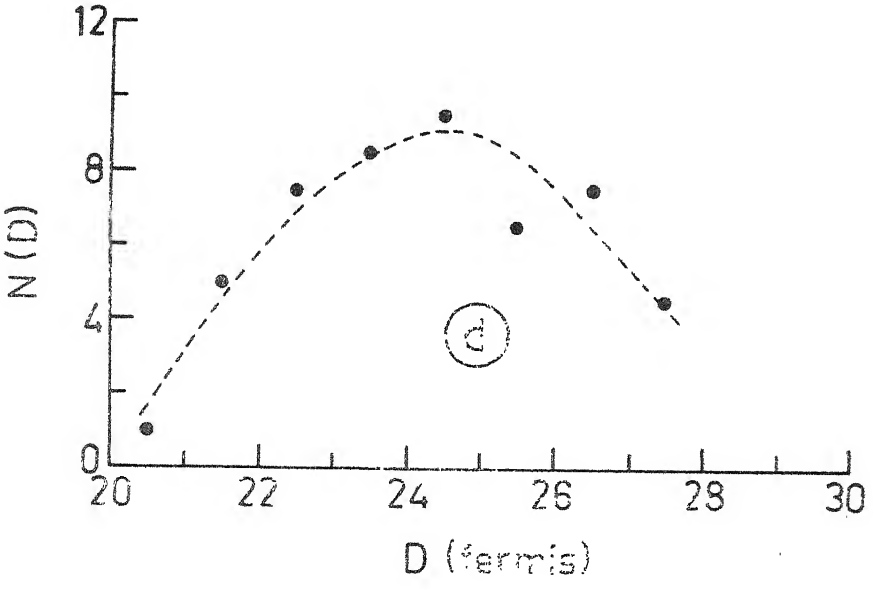

Fig. 5.11.(Cont'd.) Initial distribution in (c) point of emission of the alpha particle (X_o) and (d) interfragment distance (D) when deformation effects are included. (R = 1.4). The ordinates are in arbitrary units.

between the fragments has increased due to the inclusion of higher multipoles, however this increase does not alter the the results. In order to study the effects of deformations more thoroughly, time dependent deformations of both fragments should be included.

CHAPTER VI

SUMMARY OF RESULTS

Channel effects have been observed in prompt neutron emission, average kinetic energy of fission fragments etc., in slow neutron (thermal to 1 MeV) induced fission of ^{235}U. The aim of the present work was to determine whether such effects could be observed in the yield and average energy of light charged particles(LCP) emitted in the fission of ^{235}U and ^{239}Pu in this neutron energy region.

The LCP yield shows definite structure outside the limits of error for both the nuclei studied. The LRA yield shows distinct structure around 200 keV neutron energy - an increase of about 20% above the thermal yield in the case of ^{235}U and about 7% in the case of ^{239}Pu. The ^{239}Pu results also indicate increases around 600 keV and 1 MeV and a drop (~14%) between 250 and 300 keV. The variation of average LRA energy with neutron energy shows some structure (~0.6 MeV) around 200 keV. With better neutron energy resolution it would be possible to examine this structure more thoroughly and draw definite conclusions about variation of average energy. The width, on the other hand, seems to be insensitive to variation in neutron energy.

The increase in LRA yield around 200 keV for ^{235}U can be understood in terms of the increase in fission via

even parity states preferentially populated due to the p-wave interaction in this energy region. Since the positive parity states lie lower than the negative parity states the 'extra' energy made available goes to enhance the LRA emission probability. The drop in LRA yield between 250 and 300 keV in the case of ^{239}Pu can also be explained in terms of the relative predominance of the p-wave interaction. In this case fission takes place predominantly via negative parity states (eg. -1^-) which lie higher than the positive parity ground state (0^+), thus the 'decrement' in energy is reflected in the reduction in the LRA emission probability.

The extracted 'triton' yields also indicate structure in the neutron energy region investigated. The strucutre is more pronounced in ^{235}U fission as compared to ^{239}Pu fission. The increase (2 to 3 times) around 500 keV in ^{235}U fission probably reflects some characteristics of the emission mechanism of tritons which are different from those of LRA. The ^{239}Pu results have large errors due to poor statistics hence no definite conclusions can be drawn about the yield variation.

One may therefore conclude that channel effects manifest themselves in the LRA yield and that the use of the LRA to probe the properties of the fissioning nucleus at the saddle point have proved fruitful.

The method adoped in the present trajectory calculations differs from most other calculations in that the initial parameters took a distribution of values i.e. no restriction was imposed on their initial values. The initial values (trajectories) which produced correct final values were selected by the method of assigning 'weights' using experimental distributions and then selecting the relatively more 'weighted' trajectories. The initial distributions were obtained using these selected trajectories.

The significant aspect of the results obtained is that they have shown that by and large it is possible to obtain the correct final distributions and most of the final correlations without imposing any restrictions on the variation of the initial parameters. Previous calculations have used either only low or only high initial energies. The authors had concluded that in order to produce the correct final distributions it was necessary to restrict the variation of the initial parameters. The initial energy distributions obtained in the present calculations are broad and show possible peaking in the low and high energy regions indicating that there is no apriori reason for choosing either only low or only high initial energies - both of these can produce the correct final distributions.

Of the approximations used to simplify such calculations, the point-charge approximation has time and again been held responsible for the inability in explaining or

reproducing some experimental observations (Boneh et al., 1967; Katase, 1968). It has been suggested that the inclusion of deformation effects would resolve these questions. An attempt to include simple deformation effects in the present calculations has indicated that there is no significant change in the initial distributions.

The experimentally observed anticorrelation between $\bar{E}_F$ and E_α which is a unique characteristic of ternary fission, has been the crux of determining the validity of the choice of initial energies. Boneh et al. (1967) had concluded that in order to reproduce the correct anticorrelation it was necessary to use high initial energies whereas Choudhury (1976) has obtained the same result using low initial energies. The present results indicate that in order to obtain the correct anticorrelation it is necessary to restrict the variation in interfragment distance without regard to the initial energies being high or low. When the anticorrelation condition was used as a criterion in assiging 'weights' to the trajectories, the initial distributions remained unaltered indicating conclusively that the initial distributions are in fact broad.

The idea that correlations between initial parameters do exist and that they effect the final correlations has often been been mooted (eg. Boneh et al., 1967), however, the few atempts that have been made in this direction, notably by Boneh et al., have not resulted in any conclusive result on these correlations.

An attempt in this direction has been made in the present calculations and one result that has been obtained is that the initial alpha and fragment energies are positively correlated. The final negative correlation between these two quantities seemed to necessitate a correlation between the point of emission of the alpha particle and the inter-fragment distance, however, it was not possible to obtain any conclusive result on this correlation.

REFERENCES

Adamov, V.M., Drapchinskii, L.V. Kovalenko, S.S., Petrzhak, K.A., and Tyutyugin, I.I.(1967) Sov. J. Nucl. Phys. 5, 30

Ajitanand, N.N.(1969) Nucl. Phys. A133, 625

Allen, W.D.(1960) In "Fast Neutron Physics" ,(J.B. Marion and J.L. Fowler, eds) Vol I pg.361

Andreev, V.N. (1961) "Proc. Conf. on Nuclear Fission" , Leningrad, 1961.

Apalin, V.F., Gritsyuk, Yu.N., Kutikov, I.E., Lebedev, V.I., and Mikaelyan, L.A. (1964) Nucl. Phys. 55, 249

Apalin, V.F., Gritsyuk, Yu.N., Kutikov, I.E., Lebedev, V.I., and Mikaelyan, L.A. (1965) "Proc. IAEA. Symp.Phys. Chem. of Fission" , Salzburg, 1965, 1, 586. IAEA, Vienna.

Asghar, M., Chastel, R., and Doan, T.P. (1971) "Journees d'Etudes sur la Fission" , Cadarache, 1971.

Baerg, A.P., Bartholomew, R.M., Brown, F., Katz, L., and Kowalski, S.B. (1959) Can. J. Phys. 37, 1418

Bate, G.L., Chaudhury, R., and Huizenga, J.R. (1963) Phys. Rev. 131, 722

Bekhami, A.N., Roberts, J.H., Loveland, W.D., and Huizenga, J.R. (1968) Phys. Rev. 171, 1267

Bishop, C.J., Vandenbosch R., Aley, R., Shaw, R.W. Jr., and Halpern, I. (1970) Nucl. Phys. A150, 129

Blocki, J., and Krogulski, T. (1968) Nucl. Phys. A122, 417

Blons, J., Derrian, H., and Michaudon, A. (1970) "Nuclear Data for Reactors", 1, 513. IAEA, Vienna

Blons, J., Derrian, H., and Michaudon, A. (1971) "Proc. Third Conf. Neut. Cross Sections and Tech." , Knoxville, 2, 829

Blyumkina, Yu.A., Bondarenko, I.I., Kuznetsov, V.F., Nesterov, V.G., Okolovich, V.N., Smirenkin, G.N., and Usachev, L.N. (1964) Nucl. Phys. 52, 648

Bohr, A. (1956) "Proc. Int. Conf. Peaceful Uses of At. Energy", Geneva, 2, 151. Unitee Nations, New York

Bohr, N., and Wheeler, J.A. (1939) Phys. Rev. 56, 426

Boldeman, J.W., Bertram, W.K., and Walsh, E.L. (1976) Nucl. Phys. A265, 337

Bol'shov, V.I., Kuznetsov, V.F., Smirenkin, G.N., Ermagambetov, S.B., and Okolovich, V.N. (1968) LASL Translation No. LA-TR-68-19.

Boneh, Y., Fraenkel, Z., and Nebenzahl, I. (1967) Phys. Rev. 156, 1305

Brack, M., and Quentin, P. (1973) "Proc. IAEA Symp. Phys. Chem. of Fission" , Rochester, 1973, 1, 231. IAEA Vienna

Brolley, J.E., and Dickinson, W.C. (1954) Phys. Rev. 94, 640

Burgus, W.H. (1962) " Proc. Conf. Nucl. Chem. Fission and other Low Energy Nucl. Processes" , AERE, Harwell. (AEC Report No. IDO-16797)

Cavallari, F., Fossati, F., and Pinelli, T. (1971) Lett. Nuovo Cimento 2, 1217

Choudhury, R.K. (1976) MSc thesis, Bombay University (unpub.)

Cohen, S., and Swiatecki, W.J. (1962) Ann. Phys. 19, 67

Cohen, S., and Swiatecki, W.J. (1963) Ann. Phys. 22, 406

Coppola, M., and Knitter, H.H. (1967) Kern. Isotop. Chemie. 10, 459

Cosper, S.W., Cerny, J., and Gatti, R.C. (1967) Phys. Rev. 154, 1193

Cowan, G.A., Turkevich, A., Browne, C.I., and L.A.S.L. Radiochemistry Group (1961) Phys. Rev. 122, 1286

Cowan, G.A., Bayhurst, B.P., and Prestwood, R.J. (1963) Phys. Rev. 130, 2380

Cowan, G.A., Bayhurst, B.P., Prestwood, R.J., Gilmore, J.S., and Knobeloch, G.W. (1966) Phys. Rev. 144, 979

Cowan, G.A., Bayhurst, B.P., Prestwood, R.J., Gilmore, J.S., and Knobeloch, G.W. (1970) Phys. Rev. C2, 615

Cuninghame, J.G., Kitt, G.P., and Rae, E.R. (1961) Nucl. Phys. 27, 154

Cuninghame, J.G., Fritze, K., Lynn, J.E., and Webster, C.B. (1964) Nucl. Phys. 84, 49

Dakowski, M., Chwaszczewska, J., Krogulski, T., Piasecki, E., and Sowinski, M. (1967) Phys. Lett. 25N, 213

Deruytter, A.J., and Neve de Mevergnies, M. (1965) "Proc. IAEA Symp. Phys. Chem. of Fission", Salzburg 1965, 2, 429. IAEA, Vienna.

Drapchinskii, L.V., Kovalenkov, S.S., Petrzhak, K.A., and Tyutyugin, I.I. (1964) Sov. J. At. Energy 16, 164

Ertel, J.P. (1968) M.S. Thesis, Emory University also in "Statistical Theory of Nuclear Fission" by P. Fong (1969) pg. 191. Gordon and Breach, New York.

Farwell., G., Segre, E., and Wiegand, C. (1947) Phys. Rev. 71, 327

Feather, N. (1969) "Proc. IAEA Symp. Phys. Chem. of Fission", Vienna, 1969. pg. 83. IAEA Vienna

Flocard, H., Quentin, P., Vautherin, D., and Kermann, A.K. (1973) "Proc. IAEA Symp. Phys. Chem. of Fission," Rochester, 1973, 1, 221. IAEA Vienna.

Fluss, M.J., Dudey, N.D., and Malewicki, R.L. (1972) Phys. Rev. C6, 2252

Fluss, M.J., Kaufman, S.B., Steinberg, E.P., and Wilkins, B.D. (1973) Phys. Rev. C7, 353

Fong, P. (1969) "Statistical Theory of Nuclear Fission", Gordon and Breach, New York

Fong, P. (1970) Phys. Rev. C2, 735

Fraenkel, Z. (1967) Phys. Rev. 156, 1283

Frankel, S., and Metropolis, N. (1947) Phys. Rev. 72, 914

Fraser, J.S., and Milton, J.C.D. (1954) Phys. Rev. 93 818

Fréhaut, J., and Shackleton, D. (1973) " Proc. IAEA Symp. Phys. Chem. of Fission", Rochester, 1973, 2, 201 IAEA, Vienna

Frenkel, J. (1939) Phys. Rev. 55, 987

Frisch, O.R. (1939) Nature (London) 143, 276

Gadgil, A.J. (1973) MSc Project report, I.I.T. Kanpur (Unpub.)

Gazit, Y., Katase, A., Ben-David, G., and Moreh, R. (1971) Phys. Rev. C4, 223

Geilikman, B.T., and Khlebnikov, G.I. (1965) Atomnaya Energiia 18, 218

Gibbons, J.H., and Newson, H.W. (1960) In "Fast Neutron Physics" (J.B. Marion and J.L. Fowler, eds.) Vol I pg.133 Interscience Publishers, New York

Glendenin, L.E., Coryell, C.D., and Edwards, R. (1954) In "Radiochemical Studies: The Fission Products", (C.D. Coryell and N. Sugarman, eds.) McGraw Hill, New York

Gordon, G.E., Larsh, A.E., Sikkeland, T., and Seaborg, G.T. (1960) Phys. Rev. 120, 1341

Griffin, J.J. (1960) "Proc. Int. Conf. Nuc. Struc!', Kingston, 1960. North Holland, Amsterdam

Hahn, O., and Strassman, F. (1938) Naturwissenschaften 26, 755

Halpern, I. (1963) CERN Report 6812/P (unpublished)

Halpern, I. (1965) "Proc. IAEA Symp. Phys. Chem. of Fission", Salzburg, 1965 2, 369. IAEA, Vienna

Halpern, I. (1971) Ann. Rev. Nuc. Sci. 21, 245

Hanson, A.O., and Mckibben, J.L. (1947) Phys. Rev. 72, 673

Hill, D.L., and Wheeler, J.A. (1953) Phys. Rev. 89, 1102

Hill, D.L. (1958)"Proc. Int. Conf. Peaceful Uses At. Energy", 2nd, 15, 244. United Nations, Geneva

Hyde, E.K. (1964) "Nuclear Properties of the Heavy Elements", Vol III, Fissionphenomena, Prentice-Hall, New Jersey

Katase, A. (1968) J. Phys. Soc. Japan 25, 933

Krishnarajulu, B., Gadgil, A.J., and Mehta, G.K. (1973) "Proc. Nucl. Phys. Solid State Physics Symp." (India) 16B, 17

Krishnarajulu, B., and Mehta, G.K. (1974) "Proc. Nucl. Phys. Solid State Phys. Symp." (India) 17B, 144

Krishnarajulu, B. and Mehta, G.K. (1975) Pramana 4, 74

Krishnarajulu, B., and Mehta, G.K. (1975) "Proc. Nucl. Phys. Solid State Phys. Symp." (India) 18B, 134

Krishnarajulu, B., Sen, S., and Mehta, G.K. (1976) "Proc. Conf. Sci. Industr. Appl. of Small Accl." Texas pg. 394

Krishnarajulu, B., Mehta, G.K., Choudhury, R.K., Nadkarni, D.M., and Kapoor, S.S. (1977) Pramana 8, 315

Krogulski, T., Chwaszczewska, J., Dakowski, M., Piaseck, E., Sowinski, M., and Tys, J. (1969) Nucl. Phys. A128, 219

Krogulski, T., and Blocki, J. (1970) Nucl. Phys. A144, 617

Leachman, R.B. (1956) Phys. Rev. 101, 1005

Leachman, R.B. (1962) "Proc. Am . Nucl. Soc." Boston, 1962

Loveland, W.D., Fairhall, A.W., and Halpern, I. (1967) Phys. Rev. 163, 1315

Lynn, J.E. (1968) "The theory of Neutron Resonance Reactions", Clarendon Press, Oxford, pg. 351-459

Meadows, J.W., and Whalen, J.F. (1967) J. Nucl. Energy 21, 157

Mehta, G.K., Lebowitz, J.M., and Melkonian, E. (1967) "Proc. Nucl. Phys. Solid State Phys. Symp." (India) 10B, 327

Mehta, G.K., Poitou, J., Ribrag, M., and Signarbieux, C. (1973) Phys. Rev. C7, 373

Meitner, L., and Frisch, O.R. (1939) Nature (London) 143, 239

Melkonian, E., and Mehta, G.K. (1965) "Proc. IAEA Symp. Phys. Chem. of Fission", Salzburg, 1965 2, 355. IAEA, Vienna

Michaudon, A. (1973) In "Advances in Nucl. Phys." (M. Baranger and E. Vogt, eds.) Vol 6. Plenum Press, New York and London

Michaudon, A. (1976) "Proc. Int. Conf. Interac. Neut. with Nuclei", Lowell, Massachussetts 1976

Milton, J.C.D., and Fraser, J.S. (1961) Phys. Rev. Lett. 7, 67

Milton, J.C.D., and Fraser, J.S. (1965) "Proc. IAEA Symp. Phys. Chem. of Fission", Salzburg, 1965 2, 39. IAEA, Vienna

Moore, M.S., and Miller, L.G. (1965) "Proc. IAEA Symp. Phys. Chem. of Fission", Salzburg, 1965 1, 87. IAEA, Vienna

Muga, M.L., and Rice, C.R. (1969) "Proc. IAEA Symp. Phys. Chem. of Fission", Vienna, 1969 pg. 107. IAEA, Vienna

Mukherji, S. (1969) Nucl. Phys. A129, 297

Musgrove, A.R. de L. (1971) Austral. J. Phys. 24, 129

Myers, W.D., and Swiatecki, W.J. (1966) Nucl. Phys. 81, 1

Nadkarni, D.M. (1969) Ph.D. Thesis University of Bombay (unpub.)

Nadkarni, D.M. and Kapoor, S.S. (1970) "Proc. Nucl. Phys. Solid State Phys. Symp." (India) 13B, 73

Nadkarni, D.M., Choudhury, R.K., Rama Rao, P.N., and Kapoor, S.S. (1975) "Proc. Nucl. Phys. Solid State Phys. Symp." (India) 18B, 131

Nardi, E., Boneh, Y., and Fraenkel, Z. (1969) "Proc. IAEA Symp. Phys. Chem. of Fission", Vienna, 1969 pg. 143. IAEA, Vienna

Nardi, E., and Fraenkel, Z. (1970) Phys. Rev. C2, 1156

Nesterov, V.G., Smirenkin, G.N., and Shpak, D.L. (1967) Sov. J. Nucl. Phys. 4, 713

Nobles, R.A. (1962) Phys. Rev. 126, 1508

Northcliffe, L.C., and Schilling, R.F. (1970) Nucl. Data Tables A7, 233

Okolovich, V.N., and Smirenkin, G.N. (1963) Atomnaya Energiia 15, 250

Piasecki, E., Dakowski, M., Krogulski, T., Tys, J., and Chwaszczewska, J. (1970) Phys. Lett. B33, 568

Piekartz, H., Blocki, J., Krogulski, T., and Piasecki, E. (1970) Nucl. Phys. A146, 273

Rae, E.R., Margolis, B., and Troubetskoy, E.S. (1958) Phys. Rev. 112, 492

Raisbeck, G.M., and Thomas, T.D. (1968) Phys. Rev. 172, 1272

Rajagopalan, M., and Thomas, T.D. (1972) Phys. Rev. C5, 2064

Rajagopalan, M. (1972) Ph.D. Thesis, Princeton University (Diss. Abstr. 6899-B Vol 32 No. 12)

Regier, R.B., Burgus, W.H., Tromp, R.L., and Sorensen, B.H. (1960) Phys. Rev. 119, 2017

Reisdorf, W., Unik, J.P., Griffin, H.C., and Glendenin, L.E. (1971) Nucl. Phys. A177, 337

Ryabov, Y.V., So. Don Sik, Chikov, N., and Janeva, N. (1971) Sov. J. Nucl. Phys. 13, 255

Ryabov, Y.V., So. Don Sik, Chikov, N., and Janeva, N. (1972) Sov. J. Nucl. Phys. 14, 519

Schmitt, H.W., Neiler, J.H., Walter, F.J., and Chetham-Strode, A. (1962) Phys. Rev. Lett. 9, 427

Schröder, I.G., Deruytter, A.J., and Moore, J.A. (1965) Phys. Rev. 137B, 519

Shapiro, F.L. (1968) "Nuclear Structure" STI/Pub/189 pg. 283. IAEA, Vienna

Simmons, J.E., and Henkel, R.L. (1960) Phys. Rev. 120, 198

Simpson, F.B., Miller, L.G., Moore, M.S., Hockenbury, R.W., and Kind, T.J. (1971) Nucl. Phys. A164, 34

Stephens, F., Jr., Asaro, F., and Perlman, I. (1954) Phys. Rev. 96, 1568

Strutinsky, V.M. (1967) Nucl. Phys. A95, 420

Strutinsky, V.M. (1968) Nucl. Phys. A122, 1

Swiatecki, W.J. (1958) "Proc. Conf. Peaceful Uses of At. Energy" , Geneva, 1958 15, paper P/651

Terrell, J. (1962) Phys. Rev. 127, 880

Terrell, J. (1965) "Proc. IAEA Symp. Phys. Chem. of Fission", Salzburg, 1965 2, 3. IAEA, Vienna

Thomas, T.D., and Whetstone, S.L. (1966) Phys. Rev. 144, 1060

Tronchon, J., Lucas, B., Michaudon, A., and Ryabov, Y.V. (1973) J. Phys. 34, 131

Tsien, S.T. (1948) J. Phys. Radium 9, 6

Unik, J.P., Cuninghame, J.G., Croall, I.F. (1969) " Proc. IAEA Symp. Phys. Chem. of Fission'' , Vienna, 1969 pg. 717. IAEA, Vienna

Vandenbosch, R., Warhanek, H., and Huizenga, J.R. (1961) Phys. Rev. 124, 846

Vandenbosch, R., amd Huizenga, J.R. (1973) ''Nuclear Fission'' , Academic Press, New York and London

Vitta, P.B. (1970) Nucl. Phys. A170, 417

Vitta, P.B. (1971) Can. J. Phys. 49, 2778

Vorobiev, A.A., Grachev, V.T., Komar, A.P., Kondurov, I.A., Nikitin, A.M., and Seliverstov, D.M. (1969) Sov. J. At. Energy 27, 713

Wagemans, C., and Deruytter, A.J. (1972) Nucl. Phys. A194, 657

Wagemans, C., and Deruytter, A.J. (1973) Nucl. Phys. A212, 556

Wahl, A.C., Ferguson, R.L., Nethaway, D.R., Troutner, D.E., and Wolfsberg, K. (1962) Phys. Rev. 126, 1112

Weinstein, S., Reed, R., and Block, R.C. (1969) '' Proc. IAEA Symp. Phys. Chem. of Fission'' , Vienna, 1969 pg. 477. IAEA, Vienna

Weizsacker, C.F. (1935) Z. Phys. 96, 431

Wheeler, J.A. (1956) Physica 22, 1103

Wilets, L., and Chase, D.M. (1956) Phys. Rev. 103, 1296

Wilets, L. (1964) ''Theories of Nuclear Fission'' , Oxford Univ. Press (Clarendon), London and New York.